

# DISSERTATION

## **Investigations of the Growth Mechanism of Self-Assembled Alkylsiloxane Films by Atomic Force Microscopy, Ellipsometry, and Infrared Spectroscopy**

ausgeführt zum Zwecke der Erlangung des akademischen Grades eines Doktors der technischen Wissenschaften unter der Leitung von

Ao. Univ.-Prof. Dipl.-Ing. Dr. techn. Gernot Friedbacher  
Institut 164-AC  
Institut für Chemische Technologien und Analytik  
der  
Technischen Universität Wien

eingereicht an der Technischen Universität Wien  
Fakultät Technische Naturwissenschaften und Informatik

von

**Dipl.-Ing. Johann Foisner**  
Matrikelnummer 9525455  
Pernerstorfergasse 3/18  
1100 Wien

Wien, am 28.10.2003



# 1 Abstract / Kurzfassung

## 1.1 Abstract

The use of ultra thin organic films and increasing demands in science and technology for new functionalized materials and surfaces have experienced rapid progress in recent years. Self-assembly is an essential example of the so called bottom-up fabrication principle in nanotechnology. A particularly attractive feature of self-assembled monolayers (SAMs) is the modification of inorganic-organic interfaces and surfaces on the molecular level. In the fabrication of SAMs, various deposition parameters have been found to show a huge impact in case of the growth of organosilane monolayers. In this work atomic force microscopy, infrared spectroscopy, and ellipsometry have been used to ascertain the influence of the experimental parameters on growth mechanism and kinetics of alkylsiloxane monolayers on silicon.

In the first part of this thesis the influence of the precursor concentration on the growth of alkylsiloxanes with different chain lengths has been investigated. 1 mmol/L is a typical concentration used for film formation. The growth behavior at high precursor concentrations strongly differs from the behavior observed at low concentrations. At high concentrations, a substantial amount of material can be adsorbed at the surface, even after short maturation times of the precursor solution. However, it has been found that for long chain molecules such as octadecyltrichlorosilane prearrangement of the molecules in solution is necessary to achieve ordered flat films. Obviously, rearrangement of OTS molecules on the surface is hindered due to formation of covalent siloxane bonds. For alkylsilanes of shorter chain length flat films have been observed even after short maturation times indicating that the ordering kinetics in solution depends on the chain length.

The number of active sites and the presence of a water film on the substrate surface strongly affect growth kinetics and structure of submonolayer siloxane films. Chemical modification of our substrates, namely hydrophobization with short chain silanes was accomplished to study the influence of these parameters. We found that the growth behavior of self-assembled monolayers of alkylsiloxanes changes dramatically by a stepwise deactivation of surface silanol groups. The island shape changes from a fractal to a nearly circular geometry. This can be explained by an increased mobility of the organic molecules due to the reduced number of active OH-groups for chemisorption. On the other hand, hydrophobization of the substrate by TMCS adsorption disturbs the contiguity of the adsorbed

water film leading to hindered long-range transport of the adsorbed OTS molecules. This in turn reduces the growth rate of the initially formed ODS islands. Furthermore, it has been concluded that TMCS leads to a blockage of further island growth due to reaction with terminal OTS molecules at the edge of the islands. Moreover, it has been found that the deactivation is reversible in case a monovalent silane precursor like TMCS is used, which is not able to form a crosslinked siloxane network.

Summarizing, it has been shown that the growth of alkylsiloxane monolayers is governed by a complex interplay of ordering of the precursor in solution, chemisorption to active OH-groups on the surface, as well as surface mobility influenced by the hydrophilic/hydrophobic properties of substrate determining the formation/ suppression of a water film on the surface. These parameters and their interplay influence SAM formation both qualitatively (morphology of sub-monolayer films) and quantitatively (adsorption kinetics).

## 1.2 Kurzfassung

Die Herstellung neuer funktionalisierter Materialien und Oberflächen unter Verwendung von ultradünnen organischen Schichten hat in den letzten Jahren zunehmend an Bedeutung gewonnen. Das Prinzip der Selbstorganisation nimmt auf dem Gebiet der Nanotechnologien einen wichtigen Stellenwert ein, wobei vor allem die vielfältigen Gestaltungsmöglichkeiten am anorganisch-organischen Interface großes Interesse erwecken. In der Literatur sind verschiedenste Prozessparameter angeführt, die die Selbstorganisation von Organosilanen auf Siliziumoberflächen beeinflussen. In der vorliegenden Arbeit wurden die Einflüsse mehrerer experimenteller Parameter auf den Mechanismus und die Kinetik des Wachstums untersucht. Zur Charakterisierung der Schichten wurden die Rasterkraftmikroskopie, die Infrarot Spektroskopie, sowie die Ellipsometrie verwendet.

Der erste Teil der Arbeit beschäftigt sich mit dem Einfluss der Prekursorkonzentration auf das Wachstum von Alkylsiloxanen. Die zur Bildung von selbstorganisierten Filmen verwendeten Konzentrationen liegen üblicherweise in einem Bereich um 1 mmol/L. Eine Erhöhung der Konzentration bis auf 50 mmol/L bewirkt eine deutliche Veränderung im Wachstumsprozess der Schichten. Durch die hohe Konzentration kann innerhalb kürzester Zeit viel Material an der Oberfläche adsorbieren. Langkettige Moleküle wie Octadecyltrichlorsilan benötigen eine Reifungszeit, um bereits in Lösung geordnete Aggregate bilden zu können. Nach kurzen Reifungszeiten wurden hochgeordnete Filme nur von kurzkettigen Silanen erhalten, was darauf hindeutet, dass die Ordnungskinetik in der Lösung von der Kettenlänge abhängt.

Die Wachstumskinetik und die Struktur von Siloxaninseln hängen sehr stark von der Anzahl der reaktiven Zentren an der Oberfläche und von der Existenz eines Wasserfilms ab. Zum Studium dieser Parameter wurde die hydrophile Siliziumoberfläche mit kurzkettigen Silanen hydrophobisiert und damit die aktiven Bindungsstellen blockiert. Dies führte in erster Linie zu einer signifikanten Abnahme der Wachstumsgeschwindigkeit. Die Form der ODS-Inseln ging von einer fraktalen Struktur in eine nahezu kreisrunde Geometrie über. Das kann durch eine erhöhte Mobilität der organischen Moleküle aufgrund der niedrigeren Anzahl aktiver OH-Gruppen für die Chemisorption erklärt werden. Weiters stört die Hydrophobisierung des Substrats durch TMCS Adsorption den zusammenhängenden adsorbierten Wasserfilm, wodurch der Transport von OTS Molekülen über längere Strecken eingeschränkt wird. Dies bedingt eine niedrigere Wachstumsgeschwindigkeit für die anfänglich abgeschiedenen ODS Inseln. Weiters wurde darauf geschlossen, dass TMCS durch

Reaktion mit OTS Molekülen am Rand der Inseln zu einer Blockierung des weiteren Inselwachstums führen kann. Bei der Verwendung von Prekursormolekülen, die nicht in der Lage waren vernetzte Siloxanfilme zu bilden, war die Deaktivierung reversibel.

Zusammenfassend kann gesagt werden, dass das Wachstum von Alkylsiloxan Monoschichten durch ein komplexes Wechselspiel von Ordnung des Prekursors in der Lösung, Chemisorption an aktiven OH-Gruppen an der Oberfläche und der Oberflächenmobilität kontrolliert wird. Die zuletzt angesprochene Oberflächenmobilität wird auch durch die hydrophilen/ hydrophoben Eigenschaften des Substrates und die damit verbundene Ausbildung/ Unterdrückung eines Wasserfilms auf der Oberfläche bestimmt. Diese Parameter und deren Wechselspiel beeinflussen die Bildung von Selbst-organisierten Monoschichten sowohl in qualitativer (Morphologie von Sub-Monolagenfilmen) als auch in quantitativer (Adsorptionskinetik) Hinsicht.

## 2 Acknowledgement

I would like to thank **A.o. Prof. Dipl.-Ing. Dr. techn. Gernot Friedbacher** for the possibility to perform my dissertation in his research group. His support and his guidance, but also his ability to delve himself into unconventional discussions about inexplicable results let him become an archetype of a consistent and determined researcher. Thanks for the insights in scanning probe microscopy as well as for the essays about viniculture and the serious attempts to familiarize us with the most important grades of Austrian wine.

Very special thanks go to **A.o. Prof. Dipl.-Ing. Dr. techn. Helmuth Hoffmann** for explaining me all the details of IR measurements. Many years of experience let him become a source of wordly wisdoms and technical advice. I've learned from him that a careful study of literature often helps to achieve the investigation aims and to explain unexpected results. Thanks for "extremely interesting discussions of supremely complex topics".

I also want to thank the other members of both groups, especially **Dipl.-Ing. Andreas Glaser** for his friendship and his two years lasting lesson in precision, styling, and persistence. **Dipl.-Ing. Clemens Müllner** has to be thanked for the development of an extremely useful software package and for memorable lessons in "Burgenländisch". Above all, **Dipl.-Ing. Dr. techn. Jürgen Kattner** has to be mentioned as my supervisor at the beginning of this work. Thank you for acquainting me with most of the experimental procedures. Furthermore, **Dipl.-Ing. Thomas Leitner**, **Dipl.-Ing. Thomas Lummerstorfer**, and **Christoph Rill** have to be mentioned for always being helpful and reliable colleagues.

Special thanks go to all students, who have supported this work by their laboratory courses in our group.

Last but not least I want to thank my family, especially my brothers for their understanding and support all through school and my vicissitudinous life. Thanks for all, and that's for you, Mama and Papa.

### 3 Table of contents

<b>1</b>	<b>Abstract / Kurzfassung.....</b>	<b>1</b>
1.1	Abstract .....	1
1.2	Kurzfassung.....	3
<b>2</b>	<b>Acknowledgement .....</b>	<b>5</b>
<b>3</b>	<b>Table of contents.....</b>	<b>6</b>
<b>4</b>	<b>Introduction .....</b>	<b>8</b>
4.1	Self-Assembly .....	9
4.2	Octadecylsiloxane (ODS) on silicon .....	12
4.3	State of the art and motivation of this work .....	19
4.3.1	Concentration profile/ adsorption from highly concentrated solutions.....	19
4.3.2	Surface modification .....	19
4.3.3	Nanostructured surfaces .....	20
<b>5</b>	<b>Experimental.....</b>	<b>21</b>
5.1	AFM .....	21
5.2	Ellipsometry .....	23
5.3	IR spectroscopy .....	23
5.4	Karl-Fischer measurements.....	24
5.5	Sample preparation.....	24
5.5.1	Wafer preparation.....	24
5.5.2	Preparation of the adsorption solutions.....	26
5.5.3	Adsorption experiments .....	26
5.5.4	Multilayer adsorption .....	28
5.5.5	Temperature control .....	29
<b>6</b>	<b>Results .....</b>	<b>31</b>
6.1	Concentration profile experiment – “glass tube experiment” .....	31
6.2	Adsorption from highly concentrated solutions .....	36
6.3	Influence of the chemical surface composition on film growth.....	43
6.3.1	Preliminary experiments with various deactivation reagents.....	43
6.3.1.1	Butyltrichlorosilane (BuTCS)/ Phenyltrichlorosilane (PhTCS).....	43
6.3.1.2	Trimethoxysilane (TMeOS) .....	45

6.3.1.3	Methyltrichlorosilane (MTCS).....	46
6.3.2	Hydrophobization of silicon surfaces with TMCS.....	46
6.3.3	TMCS hydrophobization of silicon substrates partially covered with ODS islands .....	59
6.3.4	Simultaneous adsorption of TMCS and OTS.....	61
6.4	Adsorption of TSHME.....	63
6.4.1	Adsorption of pure TSHME.....	63
6.4.2	Mixed films of ODS and TSHME.....	67
6.4.3	Nanostructured surfaces .....	69
<b>7</b>	<b>Conclusion .....</b>	<b>71</b>
<b>8</b>	<b>Index of Figures .....</b>	<b>74</b>
<b>9</b>	<b>References.....</b>	<b>80</b>



## 4 Introduction

Thin organic films have aroused widespread interest over the last decades. Their potential use in several technical applications and the possibility to configure an inorganic-organic interface on a molecular level let them get interesting for research and development. Possible applications reach from boundary lubricants<sup>1</sup> in information storage devices<sup>2</sup> and micromechanical systems<sup>3</sup> to surface modification and passivation<sup>4</sup>, protective coatings<sup>5</sup>, fabrication of small scale structures, sensors, modelling of biomembrane functions, and molecular electronic devices [e.g. <sup>6, 7</sup> and references cited therein]. Besides applications in "classical" areas of technology, organic thin films can play an important role in interfacing biomolecular electronics<sup>8</sup> and biosensor applications<sup>9</sup>.

The most crucial reason why organic materials are attractive in such diverse fields is probably the tunability of the properties of these "hybrid" materials by selectively modifying specific functional groups while leaving the rest of the molecule unchanged. The change from a hydrophobic to a hydrophilic surface by changing just the endgroup of monolayers from CH<sub>3</sub>- to OH-termination shows the potential of such films. Considering the several million organic compounds known and a correspondingly wide variety of molecular properties, it is not surprising that there are different routes for the preparation of organic thin films. Examples for various production pathways are spincoating, organic molecular beam deposition (OMBD) or organic molecular beam epitaxy (OMBE)<sup>10</sup>, Langmuir-Blodgett deposition (Figure 1), and several techniques of selective self-assembly (see chapter 4.1).

Langmuir films consist of amphiphilic molecules spread on a liquid surface like water. The hydrophilic headgroup has an affinity to the water while the hydrophobic endgroup sticks out on the other side. Langmuir-Blodgett (LB) films are prepared by transferring Langmuir films onto a solid substrate. Multilayers are prepared by repeated (periodic) dipping of the substrate in appropriate solutions.

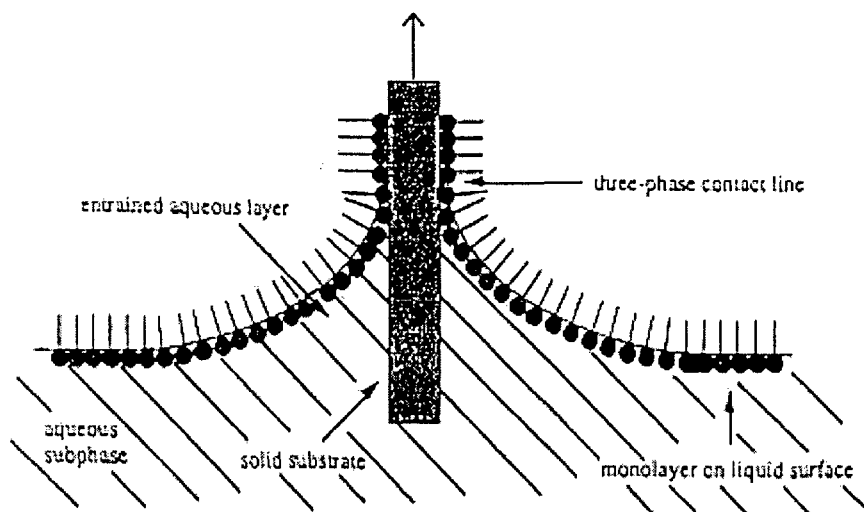


**Figure 1:** Langmuir-Blodgett transfer of amphiphilic molecules from a liquid/gaseous interface to a solid substrate<sup>11</sup>.

## 4.1 Self-Assembly

Molecular self-assembly is an important phenomenon in nature. For instance DNA replication, the build-up of living cells and biomembranes satisfy the criteria of self-assembly. Self-assembly is a process in which atoms, molecules and aggregates of molecules and components arrange themselves in ordered functioning entities without the aid of human manipulation. These assemblies often show new functions and properties that cannot be exhibited by the isolated monomer. Figure 2 shows an example for a self-assembly system. Phospholipids are able to arrange themselves into various macromolecular structures. In solution micelles, vesicles, both uni- and multilamellar can be formed depending on the experimental parameters (e.g. lipid concentration, temperature). On solid substrates mainly bilayers are formed by phospholipids which can be used for the modelling of biomembrane functions. Other amphiphilic molecules with a specific affinity of their headgroup to a substrate are able to build-up highly ordered self-assembled monolayers (SAMs).

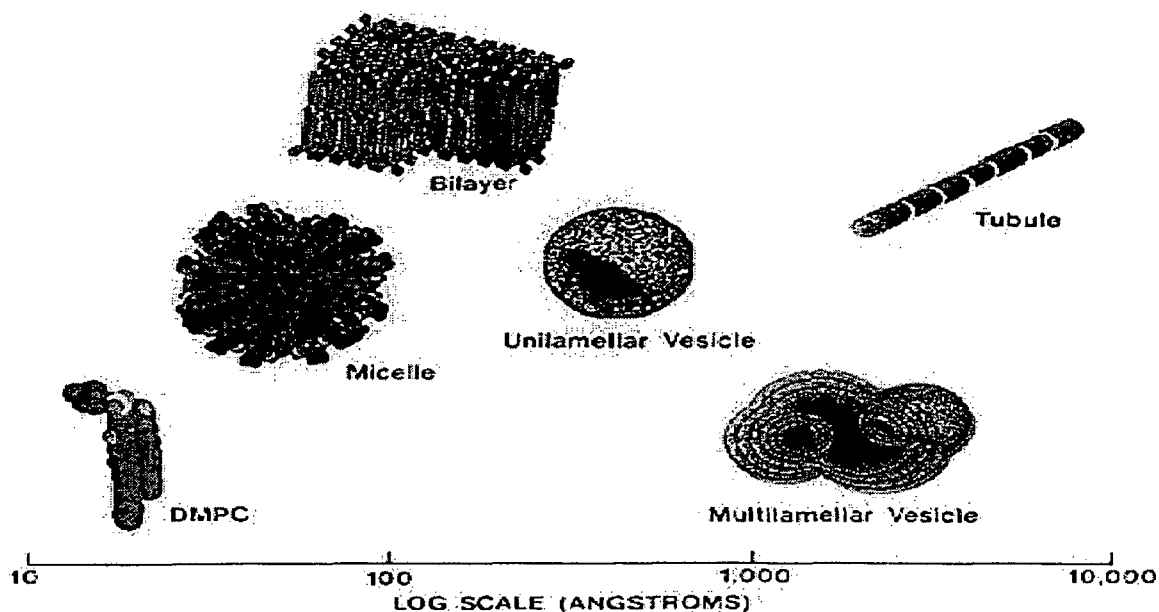


**Figure 2:** Various self-assembled structures of phospholipids for dimyristoyl phosphatidyl choline, DMPC<sup>12</sup>.

In history the concept of self-assembly was first established by Zisman and co-workers<sup>13</sup> in 1946. In the last two decades a revival took place in this field of research. One reason was the development of new analytical methods like scanning probe techniques which allowed a direct view on the molecular interface of such adsorbed films. A second cause was the demand of new materials leading to so called “smart materials” where the well-known properties of existing basic materials were improved. A second trend was the upcoming of nanomaterials, which exhibit unique, novel, and sometimes tunable properties and functionalities nonexistent in their bulk counterparts, caused by their limited dimensions. Progressive developments in synthesis and processing techniques allow almost unprecedented control in the nanostructure formation and manipulation. The enhanced possibilities for analysis lead to knowledge about many different systems and mechanisms of self-assembly. Mechanistic interactions for mediating self-assembly are hydration forces (hydrophilic and hydrophobic interactions), van der Waals forces, capillary forces, electrostatic interactions, surface forces, and chemical bonding<sup>14</sup>.

Self-assembled monolayers (SAMs), are formed by spontaneous physisorption or chemisorption of molecules with a specific affinity of their headgroup to a substrate onto a surface. SAMs are one or two nanometer thick films of organic molecules that form a two dimensional crystal on an adsorbing substrate (Figure 3).

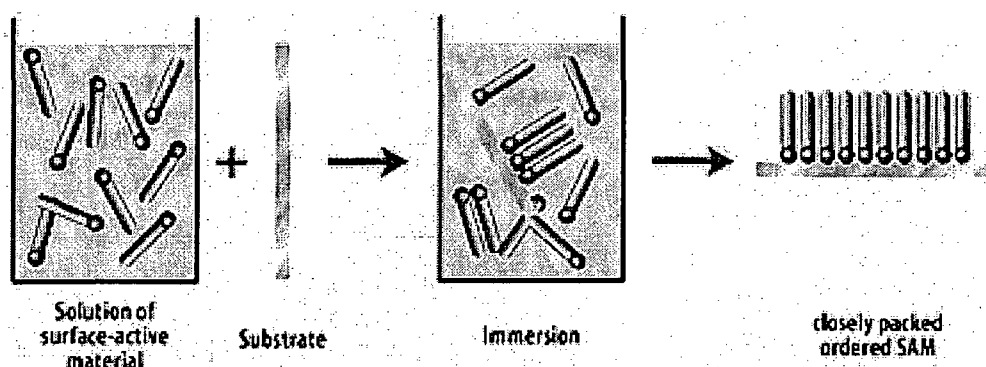


Figure 3: Scheme of self-assembly process<sup>15</sup>

Self-assembled monolayers are monomolecular layers which are spontaneously formed upon immersing a solid substrate into a solution containing amphifunctional molecules. The two dominating systems in this field of research are organosulfur compounds on noble metal substrates and organosilicon compounds on oxidic surfaces. For the sake of completeness a few other systems have to be mentioned. Fatty acids on metals and metal oxides have been studied first by Allara and Nuzzo<sup>16</sup>. Alkylphosphonic acids (like octadecylphosphonic acid, OPA) on metal and non-metal surfaces have been studied by Schwartz et al.<sup>17</sup>. Starting with hydrogen terminated silicon, Linford and Chidsey<sup>18</sup> demonstrated the attachment of alkenes onto the silicon substrate by forming direct Si-C bonds. Finally, the work of van Alsten<sup>19</sup> has to be noted, who has investigated the formation and stability of SAMs on engineering metals such as steel, copper, aluminium, brass, and stainless steel using  $\alpha,\omega$ -metal bisphosphonates. Several more compounds have been found to belong to the widespread topic of self-assembly<sup>6,7</sup>, and new systems are still being developed and investigated. Above all the best known and most studied system are thiols on gold.

For the sake of completeness, several other techniques based on self-assembly have to be mentioned. In order to achieve lateral control of SAMs a variety of patterning techniques have been used. "Classical" applications such as e-beam writing<sup>20</sup> and UV-lithography<sup>21</sup> have been adapted for surface modification and engineering. New methods like micromachining (using an SPM tip  $\Rightarrow$  scanning probe lithography)<sup>22</sup> and microcontact printing ( $\mu$ CP)<sup>23,24</sup> have been developed, motivated by the potential applications of nanopatterned surfaces with engineered chemical and biological properties. Reported applications include the use of patterned SAMs to direct selective deposition of metal thin films by CVD<sup>25</sup> and ceramic thin films by sol-gel methods<sup>26</sup>. Another very active area is targeted towards producing sensors for

biological molecules, which typically implies capturing and binding of the molecule of interest by the SAM<sup>27</sup>.

## 4.2 Octadecylsiloxane (ODS) on silicon

### General

Self-assembled monolayers (SAMs) of organosilane compounds, namely alkyltrichlorosilanes, have firstly been investigated by Maoz and Sagiv<sup>28</sup> in the early eighties. Although the reproducibility of alkyltrichlorosilane monolayer formation was and still is a great problem, organosilanes became one of the most popular SAM systems. Among the desirable properties of organosilanes, their chemical and mechanical robustness on a widespread variety of substrate materials are of outstanding importance. Considering the attractiveness of SAMs, it is not surprising that several experimental techniques have been used to gain insight into the structural characteristics of such films. Various groups have determined the degree of order of the films depending on deposition parameters like temperature or solution age using infrared spectroscopy<sup>6,29,30,31</sup>, XPS<sup>6,32</sup>, GI-XRD<sup>31,33</sup>, ellipsometry<sup>32,34</sup>, NMR<sup>6,31</sup>, scanning probe techniques<sup>17,30,35,36</sup>, raman spectroscopy<sup>31,37</sup>, HREELS<sup>38,39</sup>, TOF-SIMS<sup>40,41</sup>, sum frequency generation (SFG)<sup>42</sup>, and contact-angle measurements<sup>6,43</sup>. Moreover, many more techniques have been used<sup>44</sup> to ascertain the influence of the experimental parameters on growth mechanism and kinetics. Thus, it is not astonishing that the results of various groups sometimes lead to contradictory interpretations.

Even the question whether island growth takes place<sup>36, Fehler! Textmarke nicht definiert., 45</sup>, and which parameters lead to a change in the growth mechanism is not fully understood yet. In contradiction to these reports claiming an island growth mechanism, Wassermann<sup>32</sup> has established a growth model for octadecyltrichlorosilane explaining a uniform layer growth. This model was based on experimental data from ellipsometry and x-ray reflectivity (XR). Furthermore, it was claimed that partial monolayers do not reach the same thickness as closed films, although they show the same density. On the other hand, an in-situ IR study<sup>46</sup> shows that the hydrocarbon chains change from an initially random configuration to a more ordered film with increasing coverage. However, such a gradual alignment does not fit into the expected island growth mechanism.

### *Influence of temperature, chain length, and terminal group*

One of the first parameters found to show a huge impact on the growth of organosilane monolayers was the deposition temperature. Parikh et al.<sup>47</sup> found a critical temperature  $T_C$  for alkylsilane deposition depending on the chain length of the precursor, above which ordered monolayer growth cannot be obtained. They observed an increase of  $3.5^\circ \text{C}$  per  $\text{CH}_2$  unit resulting in  $T_C = 28 \pm 4^\circ \text{C}$  for octadecyltrichlorosilane (OTS). In a later study Kato<sup>48</sup> confirmed the trend of increasing critical temperature with increasing chain length. Below this temperature highly ordered films or densely packed islands have been obtained. Above the transition temperature only disordered films have been observed. With increasing temperature the measured coverage decreases. This was explained by Rye<sup>49</sup> as a consequence of the thermal budget of the silane chains. At elevated temperatures low energy rotations of the C-C bonds can occur, leading to a larger space requirement of the alkane chains compared to a proposed all-trans conformation of the chains in ordered films. In both studies the critical temperature  $T_C$  has been associated with the triple point of a Langmuir-Blodgett (LB) phase diagram like Silberzan et al.<sup>50</sup> have interpreted their results in 1998.

Carraro et al.<sup>35</sup> have found three different growth regimes depending on the temperature. Below  $16^\circ \text{C}$  island growth has been observed. Such a growth pattern is expected for Langmuir nucleation of liquid-condensed domains coexisting with the gas phase. Above  $40^\circ \text{C}$  homogenous growth was found according to the exclusive occurrence of the liquid expanded phase. In the intermediate temperature range they speak of a mixed regime, i.e. a coexistence of a liquid expanded and a liquid condensed phase similar to the formation mechanism described for LB films. The discrepancy between results from different authors shows the complexity of this matter.

Bierbaum and Grunze<sup>51</sup> have reported that for longer chain lengths both ordering and deposition takes longer, due to blocking of reactive sites and a decreased diffusion rate of the precursor molecules to the surface, respectively. They observed island growth only for OTS but not for short-chained alkylsilanes ( $< \text{C}_4$ ). The same observation has been reported by Kluth et al.<sup>38</sup>, who have determined that for  $< \text{C}_6$  the layers are less densely packed. Vallant et al.<sup>52</sup> have observed an increase of film quality with increasing chain length from  $\text{C}_{11}$  to  $\text{C}_{18}$ . They have found a slightly lower adsorption rate and less ordered films for shorter chain lengths. These results were based on in-situ internal reflection IR spectroscopy indicating an increasing tilt angle of the chains through a slight shift in the wavenumbers of the  $\nu(\text{CH}_2)$  bands. Similar results have been reported by Hoffmann et al.<sup>53</sup>. Lower order for

shorter chain length has been explained by reduced van der Waals interaction energies between adjacent hydrocarbon chains. Salmeron and co-workers<sup>54</sup> used AFM to study the frictional behavior of self-assembled monolayers of alkanethiols and alkylsilanes on gold and mica, respectively. They found that for molecules with more than 8-10 carbon atoms in their chain the frictional behavior is very similar, whereas a strong dependence on chain length is observed for lengths below eight carbon atoms. These observations have been ascribed to the increased formation of defects and distortions in the alkyl chains, which occur preferentially in the less densely packed films of shorter chain molecules. Bernasek<sup>41</sup> studied alkanethiols on gold with different chain lengths using TOF-SIMS. Varying the chain length has influenced the thin films in both packing and stability. The stability was observed by measuring the extent of oxidation in the SAMs, which showed a direct correlation with the relative coverage, caused by increased gauche defects in the shorter chain films, leading to less densely packed monolayers. The results of the paragraph above have been proven by Jennings et al.<sup>55</sup>. They studied the effect of chain length on the protection of copper by n-alkanethiols. Due to the many attractive features of SAMs (densely packed films with controlled thickness and composition by a simple chemisorption process), applications as films for inhibiting corrosion on metals<sup>56</sup> has gained great interest. Both groups<sup>55,56</sup> found that SAMs formed from longer chain molecules ( $\geq C_{16}$ ) provide substantially greater coating resistance than thinner films. However, the results concerning the effect of different endgroups are contradictory. Jennings et al.<sup>55</sup> found that by introduction of an ethereal or alcoholic endgroup the quality of the films decreases. Therefore, the efficiency of the barrier coatings decreases caused by a decrease in van der Waals interactions between the chains through a greater distance. Zamborini<sup>56</sup> have observed that for similar thicknesses of the layers OH- and COOH- endgroups are superior to hydrophobic surfaces for corrosion protection. They suggest that the ability to build up hydrogen bonds let them get more stable and passivating than methyl terminated monolayers.

#### *Influence of substrate, precursor concentration, and solvent*

Self-assembled monolayers of n-alkyltrichlorosilanes are robust, organized films, chemisorbed on solid substrate surfaces. Their stability and resistance against mechanical, thermal, and chemical attacks result from strong covalent bonds to the substrate surface and cross-polymerization through condensation between adjacent OTS molecules. The covalent bonds to the substrate are formed by siloxane linkages (Si-O-Si) of OTS to the surface silanol

groups. In the past, various groups have investigated the relationship between the hydration state of silicon and the formation of alkylsiloxanes. Angst and Simmons<sup>57</sup> found closed packed monolayers of OTS on fully hydrated surfaces of silicon, as well as lower coverage on dry silicon wafers. Similarly, Allara et al.<sup>29</sup> found that proper substrate hydration is a fundamental prerequisite for the deposition of densely packed, highly organized alkylsiloxane monolayers of reproducible structure. The presence of a water layer acting as a lubricant layer between the monolayer and the substrate leads to the fact that the film organization is decoupled from the substrate chemistry. In this manner monolayers of similar structure can be obtained on substrates of widely different chemical characteristics. In contrast to Allara et al.<sup>29</sup>, Markham and LeGrange<sup>58</sup> reported that a completely hydrated surface is not necessary for obtaining full monolayer coverage.

In an early AFM study Bierbaum et al.<sup>51</sup> found that the characteristics of island growth are influenced by the state of the silicon substrate. They suggested that changes in binding groups on the substrate affect the surface diffusion of OTS molecules, and therefore may also influence shape and size of the developing islands. In a comparative study of two widely different substrate materials, silicon and mica, Brunner et al.<sup>46</sup> found two types of substrate effects influencing the growth of OTS. The total number of OH-groups of a fully activated silicon wafer, which is the most used substrate for the investigation of self-assembly processes of alkylsiloxanes, has been assumed to be  $5 \times 10^{14}$  per  $\text{cm}^2$ <sup>32,58</sup>. These silanol groups act as binding sites, and therefore restrict the diffusion of OTS molecules on the surface. This results in a large number of smaller islands, which show sharp edges. On mica the number of OH-groups is negligible. Therefore, large ordered islands with rather rounded edges have been observed. By depositing full monolayers of ODS on mica and subsequent oxidation of the hydrocarbon chains well-defined silicon oxide layers were formed. The deposition of only one monolayer of silicon oxide on mica led to an abrupt change of the morphology of subsequently deposited sub-monolayer islands of ODS. The authors concluded that island morphology and structure are controlled by the chemical composition (number of reactive sites) of the outermost substrate surface and are not influenced by the nature of the underlying bulk material. In contrast to that, a continuous decrease of adsorption rates has been observed for an increasing number of silicon oxide layers. The different rates between mica and silicon have been discussed to arise from the negative surface charge of freshly cleaved mica. Long-range interactions with the polar head group of the OTS molecules might enhance adsorption compared to an uncharged substrate like silicon. Upon increasing the oxide layer thickness this enhancement of the adsorption is reduced due to increasing shielding of the surface charge. The findings described above lead to the conclusion that two parameters, on the one



hand, the number of active sites on the surface, and on the other hand, the presence of a water film on the substrate surface, dominate the self-assembly process. The hydration film, consisting of a few monolayers of water is suggested to develop preferentially on hydrophilic surfaces like mica or silicon oxide.

Furthermore, the surface structure of the substrate plays an important role for the self-assembly process. Bohn and co-workers<sup>59</sup> have found a significant increase in adsorption rate and surface coverage by decreasing the roughness of their gold substrates. Another observation was that an increase of the thiol concentration from  $10^{-3}$  to 10 mmol/L lead to an increase of the adsorption rate, converging to the same final value in film thickness and order. Equal results have been reported by Larsen et al.<sup>60</sup>, but they emphasized their study by an investigation of the effect of different solvents on the growth of self-assembled monolayers. They found a pronounced effect of solvents on the formation of ODS films on silicon, whereby, solvents with intermediate solubility of water (e.g. heptane) lead to closely packed monolayers. In contrast, the use of a solvents (e.g. dodecane) with lower water contents resulted in the formation of ODS multilayers. The use of various solvents is one of the reasons leading to widely controversial results. Solvent mixtures of bicyclohexyl/ THF<sup>48</sup>, CCl<sub>4</sub>/ isobar G<sup>57</sup>, hexadecane/ CCl<sub>4</sub>, several n-alkanes<sup>29</sup>, toluene (in this work), and many more systems have been described. Unfortunately, not all of the reports include an exact description of water contents and mixing ratio of the solvents. Thus a comparison of results from many authors with the own work is often very difficult or even impossible. It can be expected that the solvatization of the surfactants by the solvent is a competitive reaction to the formation of monolayers by covalent bonding between the precursor molecules and the surface silanol groups.

The water content of the deposition solution is a further parameter which is hinted above to have a great influence on self-assembly formation. Apart from the discussed water film on the substrate surface, water in the solvent is required for initial hydrolysis of the alkylchlorosilanes. Previous work from Leitner et al.<sup>45</sup> has shown that the water content strongly influences growth kinetics, size, and shape of the deposited ODS structures. Larger islands were found for higher water concentrations, indicating a prearrangement of the OTS molecules already in solution. In order to shed more light on this aspect and on the influence of the water content on the critical temperature Glaser and co-workers<sup>61</sup> have performed dynamic light scattering (DLS) measurements of the precursor solutions at different temperatures. Surprisingly, only one size (diameter~200 nm) of aggregates has been found for all experiments. The parameters (water concentration and solution temperature) which have

been varied have shown to influence only the formation rate of the aggregates. These results indicate that also the age of the adsorption solution influences both the structure of SAMs, as well as the adsorption kinetics, which has already been described by Leitner and co-workers<sup>45</sup>. They found an optimum maturation time of their deposition solutions (OTS in toluene) of ten minutes for a given deposition time.

### *Mixed monolayers and multilayers*

In contrast to the well defined adsorption of self-assembled monolayers, multilayers were suggested to degrade in film quality with increasing layer thickness. In first reports of silane multilayers Pomerantz et al.<sup>62</sup> used methyl 23-trichlorosilyl-tricosanoate (MTST) to build up multilayers. Later on Tillmann<sup>63</sup>, and Wassermann and coworkers<sup>32</sup> described a simple method for multilayer adsorption. Both groups used MTST to form densely packed monolayers in a first step. The completed monolayers were then immersed into a solution of  $\text{LiAlH}_4$  in THF in order to reduce the ester group, followed by rinsing with HCl and Millipore water. The formation of multilayers has been achieved by a repeated application of the steps described above. The progress of multilayer formation was investigated by ellipsometry, infrared spectroscopy and contact angle measurements. Summarizing, a linear relationship between the number of layers and the measured layer thickness has been observed. IR measurements showed small impurity peaks resulting either from incomplete reductions or from polysiloxane contaminations containing ester groups. Other reaction pathways to obtain multilayers included hydroboration and oxidation of a terminal vinyl group<sup>64</sup>.

Mixed monolayers provide abundant possibilities for surface engineering at a molecular level. Thus, many respective systems have been published in the last decade. Unfortunately, the reported results are contradictory in many cases. For example Offord et al.<sup>65</sup> observed ideal mixing of two silanes in the monolayer prepared by competitive adsorption. They found that the monolayer composition (primarily determined by layer thickness measurements) varied with the concentration ratio of the shorter and longer chain adsorbates in the deposition solution. Surface free energies of the mixed monolayers did not indicate a macroscopic phase separation of the different precursor molecules and were found to be higher than for single component SAMs. Lagutchev and co-workers<sup>66</sup> reported that simultaneous adsorption of chlorosilanes and their partially fluorinated analogs results in preferential adsorption of the fluorinated species. SFG measurements provided a strong evidence for a close co-adsorption of both compounds arguing against a phase separation.

Mathauer and Frank<sup>67</sup> take the biscuit in these series of results. They reported ideal mixing of two trichlorosilanes in all cases and for all concentration ratios, even for backfilling of partial monolayers of a single component. In contrast to that Kropman et al.<sup>68</sup> found evidence for phase separation for the adsorption of a mixture of dodecyltrichlorosilane (DoTS) and octadecyltrichlorosilane (OTS). Above all, phase separation is mostly reported for thiols. Stranick and co-workers<sup>69</sup> reported that mixed compositions of even very similar alkanethiols on gold phase-separate into nanometer scale domains of each component. In a further study Atre et al.<sup>70</sup> investigated the chain length dependence of wetting properties in binary mixtures of OH- and CH<sub>3</sub> terminated alkanethiols. They observed that for shorter chain lengths randomly mixed monolayers were obtained. The longer the CH<sub>3</sub>-terminated chains, the more the trend goes to a phase separation of the two compounds. Folkers et al.<sup>71</sup> described an order of stabilities of pairs of alkyl groups in the SAMs: long-long > short-short > long-short. Their results indicate phase separation into microscopic islands.

Well known applications of mixed self-assembled monolayers are the modification of chromatographic silica surfaces in chemical separations<sup>72</sup> or the selective adsorption of proteins on phase-separated two component organosilane monolayers<sup>73</sup>.

Despite all the possible stumbling blocks on the way to reproducible and fully controllable SAMs, they are particularly attractive for the following reasons<sup>7</sup>:

- the ease of preparation
- the tunability of surface properties via modification of molecular structures and functionalities
- the use as building blocks in more complex structures, e.g., for “docking” additional layers to a surface or acting as reactive sites for surface reactions
- the possibility of lateral structuring in the nanometer regime

### **4.3 State of the art and motivation of this work**

This work has been accomplished within a research project of the Austrian “Fonds zur Förderung der wissenschaftlichen Forschung” (FWF – project number P14763). Above all, the project aims have been to shed more light on the growth of self-assembled monolayers of alkylsiloxanes on various substrates by variation of several deposition parameters.

#### **4.3.1 Concentration profile/ adsorption from highly concentrated solutions**

In order to perform in-situ ellipsometry of the growth of self-assembled monolayers on silicon J. Kattner<sup>74</sup> has designed a so called “glass tube experiment” (Figure 6). A 4x1-cm<sup>2</sup> silicon wafer was placed into a glass tube filled with toluene. Then OTS was added through a hole in the tube and position-dependent adsorption of OTS was monitored by scanning along the length of the silicon substrate. Surprisingly, strong lateral inhomogeneities in film thickness have been found. Moreover it turned out that at the drop-in position full monolayer coverage could not be achieved. For a clarification of this phenomenon AFM has been involved. The first results achieved indicated that under the given conditions disordered growth of ODS takes place. This was the motivation for further experiments with highly concentrated solutions and various precursor molecules.

#### **4.3.2 Surface modification**

The findings concerning the substrate surface for adsorption experiments described above (see chapter 4.2) lead to the conclusion that two parameters, on the one hand, the number of active sites on the surface, and on the other hand, the presence of a water film on the substrate surface, dominate the self-assembly process. The hydration film, consisting of a few monolayers of water, preferentially develops on hydrophilic surfaces like mica or silicon oxide. In order to study the influence of this parameter, we have considered hydrophobization of our silicon substrates. Moreover, chemical modification of our substrates was aimed at control of the number of reactive hydroxyl groups through blockage with a small molecule.

Tripp and Hair<sup>75,76</sup> have investigated the reaction of different chloromethylsilanes on silica by infrared spectroscopy. They proposed an order of reactivity with the surface silanol groups of  $(\text{CH}_3)_3\text{SiOH} > (\text{CH}_3)_2\text{Si}(\text{OH})_2 > \text{CH}_3\text{Si}(\text{OH})_3$  (after hydrolysis). They observed that trimethylchlorosilane (TMCS) reacts with all kinds of surface silanols blocking about 80 % of the accessible OH-groups. A later study using XPS, DRIFT, and Si-MAS NMR confirms this reactivity scale<sup>77</sup>.

Concerning the hydrophobicity of the surface, Lu and Zhao<sup>78</sup> have shown that the surface chemistry of MCM-41 molecular sieves can be effectively modified towards higher hydrophobicity by chemical attachment of trimethylchlorosilane. They demonstrated that a silylated surface is very hydrophobic without significant adsorption of water. Fuji et al.<sup>79</sup> investigated the relationship between coverage of hydrophobic groups on glass bead surfaces and macroscopic properties such as wettability. They observed a drastic increase in contact angle at surface coverages of about 50 %, which means that the sample surface changes significantly from a hydrophilic to a hydrophobic surface. These results as well as the fact that TMCS is a monofunctional reagent with a simple reaction pathway compared to multifunctional silanes<sup>75,76</sup> encouraged us to utilize TMCS for our hydrophobization experiments. Above all, several other short chain reagents (see Table 1) have been used to verify the arguments given above.

#### 4.3.3 Nanostructured surfaces

In a previous work, Vallant et al.<sup>52</sup> have studied the formation of monolayers using alkylsiloxanes with different chain lengths and various terminal groups (e.g. -CN, -Br, -CH<sub>3</sub>, -COOH). They observed a well ordered densely packed film only for long chain molecules. The monolayer quality decreases by decreasing the chain length and by introducing other functional groups than -CH<sub>3</sub>. Basnar et al.<sup>80</sup> have performed first experiments to build up multilayers of self-assembled alkylsiloxanes using trisilylheptadecanoic acid methyl ester (TSHME). Partial multilayers were formed by repeated deposition of TSHME and subsequent reduction to yield a hydrophilic surface for the next adsorption step. The remaining areas of the originally silicon/ silicon oxide surface were inhibited from multilayer growth by deposition of ODS islands. In this manner 3d-structures have been fabricated for both the organic multilayer systems and the subsequently oxidised silicon oxide features. Recapitulations of these results and further investigations on the growth behavior of mixed self-assembled films of OTS and TSHME have been performed in this thesis.

## 5 Experimental

### 5.1 AFM

Atomic force microscopy (AFM) probes the surface of a sample with a sharp tip, a couple of microns long and often less than 10 nm in diameter. The tip is located at the free end of a cantilever that is 100 to 200  $\mu\text{m}$  long. Forces between the tip and the sample surface cause the cantilever to bend, or deflect. A detector measures the cantilever deflection as the tip is scanned over the sample, or the sample is scanned under the tip. The measured cantilever deflections allow a computer to generate a map of surface topography. AFMs can be used to study insulators and semiconductors as well as electrical conductors.

The AFM measurements were accomplished with a Nanoscope III Multimode SPM from Digital Instruments, Veeco Metrology Group, Santa Barbara, CA. They were performed in tapping mode (TM-AFM) using silicon cantilevers with integrated silicon tips (spring constant 28 - 52 N/m, resonance frequency  $\sim 330$  kHz) under ambient conditions. The principle set-up of the AFM is shown in Figure 4. A laser-beam is focussed onto a cantilever oscillating near its resonance frequency ( $\sim 330$  kHz). The reflected beam is directed towards a photodiode via a moveable mirror. The photodiode consists of two halves, and changes in the oscillation behavior of the cantilever, induced by changes in the interaction of the tip with the sample surface are detected by comparison of the received intensities. The difference signal of the two halves is used to control the vertical distance of the piezo-scanner in order to keep the deflection of the cantilever constant. A computer records both the piezo signal as well as the phase shift in the oscillations of the cantilever. The measured cantilever deflections allow a computer to generate a map of surface topography. Phase detection refers to the monitoring of the phase lag between the signal that drives the cantilever to oscillate and the cantilever oscillation output signal. Changes in the phase lag reflect changes in the mechanical and chemical properties of the sample surface like elasticity, adhesion, and friction leading to changes in the tip-sample interaction through variations of long and short range forces.

The cantilevers used were Pointprobe cantilevers (Nanosensors, Germany) for tapping mode application. They are made of silicon and their characteristics are listed below.

- |                        |                             |
|------------------------|-----------------------------|
| • manufacturer:        | Nanosensors, Germany        |
| • resistivity:         | 0.01-0.02 $\Omega\text{cm}$ |
| • resonance frequency: | 290-340 kHz                 |
| • force constant:      | 28-52 N/m                   |
| • material:            | n <sup>+</sup> - silicon    |

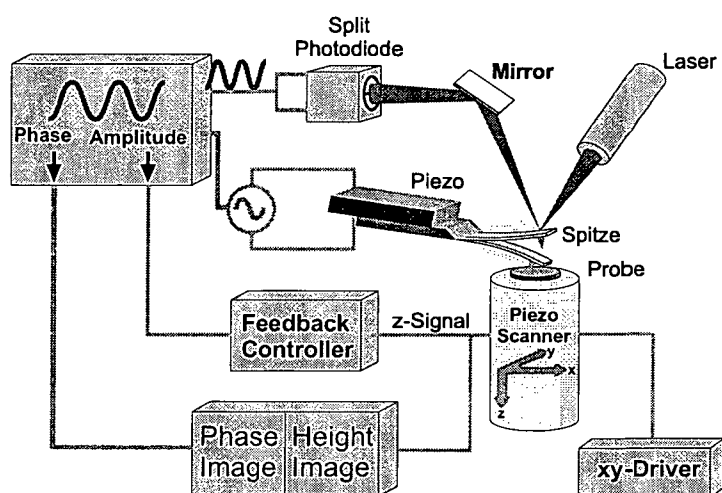


**Figure 4:** Scheme of tapping mode atomic force microscopy<sup>81</sup>

All images were recorded in constant amplitude mode with a resolution of 512 x 512 pixels at scanning rates from 1,0 to 4,0 Hz. In this work two different piezo scanners were used. For the larger images a J-scanner (maximum scan range: 120 x 120  $\mu\text{m}^2$ ) was utilized. The other measurements were performed with an E-scanner (10 x 10  $\mu\text{m}^2$  scan range). Data analysis was performed with the NanoScope III software. The height distributions of the submonolayer islands were determined from cross-sectional profiles at several random locations of each AFM image. For images with only a few islands all islands have been gaged. It should also be mentioned that the absolute height value for sub-monolayer islands in the AFM images can be effected by the chemical surface termination of the respective layers due to the varying force interaction of the tip with hydrophilic and hydrophobic substrates. For our hydrophobic ODS islands on a hydrophilic silicon substrate this led to experimental height values which were significantly smaller than the heights of the islands (~1,5 nm instead of 2,6 nm). This is a well knowm artefact which has to be considered when interpreting the AFM images on a quantitative basis.

## 5.2 Ellipsometry

The ellipsometric measurements were performed with a PLASMOS SD 2300 instrument with a rotating analyzer. A He-Ne laser ( $\lambda = 632,8 \text{ nm}$ ) was used as light source at  $68^\circ$  incidence. A scheme of the basic parts of the system is shown in Figure 5. Determination of the silicon oxide film thickness and the organic film thickness is based on a model of three layers (Si / SiO<sub>x</sub> / air) and a four-phase model (Si / SiO<sub>x</sub> / adsorbate / air), respectively. This means, that for the determination of the organic film thickness the silicon oxide layer thickness has to be known. A commercial software based on the McCrackin algorithm<sup>82</sup> was used to calculate the film thickness from the measured ellipsometric angles (relative phase shift  $\Delta$  and amplitude ratio  $\Psi$ ). Changes of the polarisation of elliptically polarised light when passing through a medium with different refractive index than its surroundings makes it possible to determine a layer thickness for given refractive indices and absorption coefficients. Literature values were used for the optical constants of the layers<sup>83</sup>. For each sample 5 different spots were measured and the average value was determined. In this manner typical standard deviations between 0,1 and 0,5 Å have been obtained.

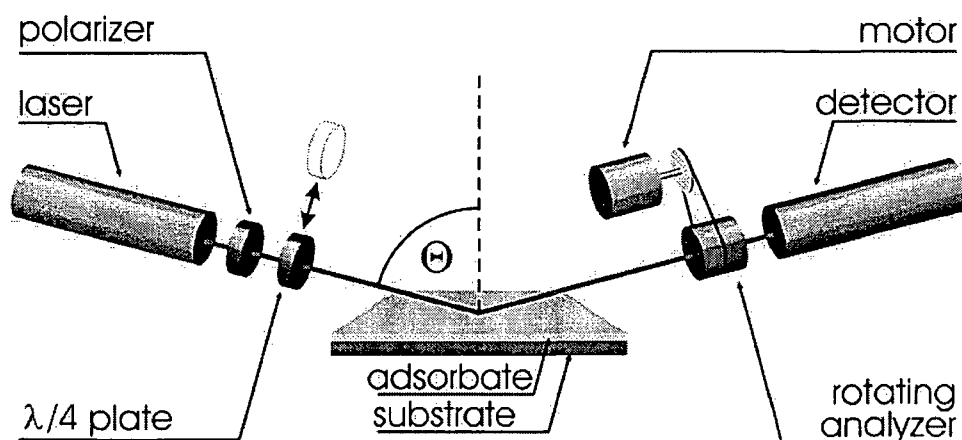


Figure 5: Scheme of rotating angle ellipsometer<sup>15</sup>

## 5.3 IR spectroscopy

External reflection infrared spectra were measured by using a custom-made external reflection optical system connected to a Mattson RS1 FT-IR spectrometer equipped with a narrow-band MCT detector, as described elsewhere. P-polarized light at an incidence angle of



$\sim 80^\circ$  was used. For each spectrum 1024 scans at  $4\text{ cm}^{-1}$  resolution were accumulated both from the film-covered sample and the clean silicon dioxide reference.

## **5.4 Karl-Fischer measurements**

The water concentration of the solvent was measured with a commercial Karl-Fischer-setup, a Metrohm Karl-Fischer Automat E547 using Hydranal Composite 1 from Riedel-de Haën. Each solution was measured at least three times and the average values were determined. The water concentrations for the experiments were adjusted by doping commercial toluene (water concentration  $\sim 4\text{-}6\text{ mmol/L}$ ) with a calculated amount of distilled water (see chapter 5.5.2).

## **5.5 Sample preparation**

As described in the introduction, the self-assembly process is strongly influenced by various deposition parameters. In order to prevent perturbing effects on the deposition experiment, all samples were prepared as described in the following chapters. However, it has to be mentioned that the preparation and cleaning procedure has been further enhanced during this work.

### **5.5.1 Wafer preparation**

For all experiments silicon-wafers from Wacker Siltronic AG were used. The wafers were prime grade, single side polished CZ-Si discs with a diameter of 100 mm and a thickness of 500 - 550  $\mu\text{m}$ . P-type wafers (boron was implanted) with a crystallographic orientation of  $\langle 100 \rangle$  and a resistivity of 7-21  $\Omega\text{cm}$  have been used.

The wafers were cut into pieces of  $1 \times 1\text{ cm}^2$  in size, except for the infrared experiments, where slices of  $2 \times 2,5\text{ cm}^2$  were used. Subsequently, the wafers were cleaned in toluene in an ultrasonic bath for 5 minutes, followed by rinsing with toluene, acetone, and ethanol. Afterwards the pieces were put in a UV-chamber (UV-CLEAN, BOEDEL, Germany) for 15 minutes in order to activate the surface for the adsorption process leading to formation

of silicon oxide and silanol-groups. The resulting oxide layer thicknesses were measured by ellipsometry and immediately after the measurements, the pieces were transferred into a glove-box with nitrogen atmosphere. The samples were prepared by deposition of the precursor compounds from toluene solutions with defined water content.

After the adsorption process the samples were sonicated in toluene for 5 minutes, wiped off with a tissue, and cleaned by rinsing with toluene, acetone, and ethanol. In a last step the samples were blown dry with nitrogen. The ellipsometric measurements were performed immediately after the cleaning procedure. In some cases a further treatment of the wafers was necessary, in order to obtain AFM images of clean surfaces or to prepare the samples for further adsorption experiments. The chemicals used for the deposition and cleaning procedures are listed in Table 1.

*Table 1: List of Chemicals*

Usage	Chemical	Purity	Manufacturer
monolayer adsorption	octadecyltrichlorosilane, OTS	95+ %	Sigma Aldrich
monolayer adsorption	hexadecyltrichlorosilane, HTS	97 %	ABCR
monolayer adsorption	dodecyltrichlorosilane, DoTS	97 %	ABCR
monolayer adsorption	n-decyltrichlorosilane, DTS	100 %	ABCR
monolayer adsorption	trichlorosilyl heptadecanoic acid methyl ester, TSHME	96 %	home made
substrate deactivation	phenyltrichlorosilane, PhTS	97 %	Sigma Aldrich
substrate deactivation	trimethylchlorosilane, TMCS	> 99 %	Merck
substrate deactivation	butyltrichlorosilane, BuTS	99 %	Sigma Aldrich
substrate deactivation	methyltrichlorosilane, MTS	99 %	Sigma Aldrich
substrate deactivation	trimethoxysilane, TMeOS	95 %	Sigma Aldrich
adsorption solvent	toluene	99,8 %	Sigma Aldrich
cleaning solvent	acetone	99,8 %	Sigma Aldrich
cleaning solvent	ethanol	99,9 %	Austria Hefe AG
reducing agent	lithium aluminium hydride, $\text{LiAlH}_4$	1M in THF	Sigma Aldrich

### 5.5.2 Preparation of the adsorption solutions

For the adsorption of OTS from toluene, the water concentration is a crucial parameter. It has been found that growth kinetics, size, and shape of the obtained structures strongly depend on the residual water concentration of the solvent. Thus, an exact adjustment of the water concentration is very important for investigation of deposition mechanisms. Although in principal the water content of solvents can be determined with the Karl-Fischer method with an accuracy of 2.5 %, reproducible preparation of solvents with concentrations in the lower mmol/L-range is tedious. Due to azeotrop formation of toluene and water, stable stock solutions of water-saturated toluene cannot be prepared and therefore repeated water determination of the solvent is necessary. Thus, the water content has been adjusted by direct doping with pure water. The water concentrations achieved in this manner have been cross-checked with the Karl-Fischer method. Typical deviations of 3 % from the nominal water concentration have been observed.

The adsorption solutions were prepared by addition of the precursor to toluene with an adjusted water concentration in order to obtain 10 ml of the final deposition solution. The exact deposition parameters like temperature and maturation time of the solutions are given in the chapters of the different experiments.

### 5.5.3 Adsorption experiments

A first deposition experiment was performed in a glass tube (Figure 6), where a sample of 1x4 cm<sup>2</sup> in size was immersed into toluene. Using a Hamilton syringe, OTS was injected approximately 0,5 cm above the sample through a hole in the glass tube. After ten minutes the solution was discarded and the sample was removed from the glass tube. The wafers were then processed according to chapter 5.5.1. For the AFM measurements the wafers were cut into 1x1 cm<sup>2</sup> pieces.

In order to shed more light on the results of the “glass tube” experiment monolayers of alkylsiloxanes were prepared from solutions of various precursors (specified in Table 1) in HPLC-grade toluene. Experiments have been performed within a concentration range of 0,5-50 mmol/L. The deposition experiments were performed under nitrogen atmosphere in a glove box at room temperature. Toluene with the adjusted water content was pipetted into a glass jar. In these experiments the water content was fixed to  $11 \pm 1$  mmol/L. Then the desired precursor volume was added using an Eppendorf-pipette. Afterwards, the wafers were immersed in the solutions for certain periods of time followed by rinsing with toluene.

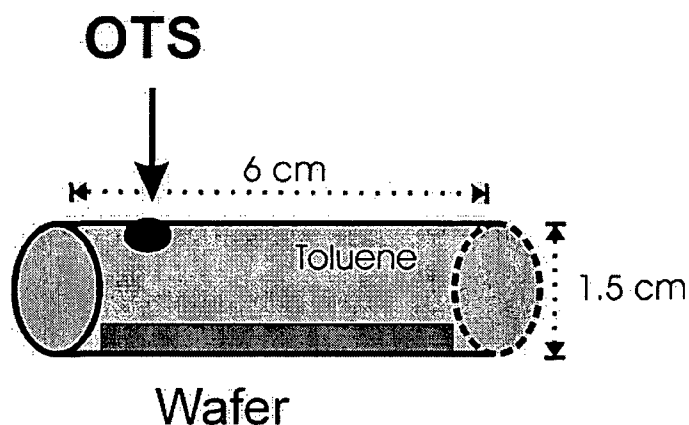


*Figure 6: Scheme of “glass tube experiment”*

In the case of deactivated substrates, the wafers were first immersed into TMCS solutions, rinsed with toluene, and subsequently immersed into OTS solutions. Finally, they were deposited in a beaker with toluene. These experiments were performed with an adjusted water content of the solvent toluene of  $15 \pm 0,3$  mmol/L and at a controlled temperature of  $20 \pm 1$  °C (see description of temperature control unit in 5.5.5).

#### 5.5.4 Multilayer adsorption

Further preparation steps were necessary in the case of multilayer growth using trichlorosilyl heptadecanoic acid methyl ester (TSHME). The sample treatment was done as follows:

- OTS was deposited by immersion of the wafers into a  $1 \cdot 10^{-3}$  mmol/L solution ( $\text{conc}_{\text{water}} = 12$  mmol/L) to yield a coverage of about 50 % on the native silicon.
- Then a complete monolayer was produced by immersion of the sample into a  $1 \cdot 10^{-3}$  mmol/L solution of TSHME in toluene ( $\text{conc}_{\text{water}} = 12$  mmol/L) for 30 minutes.
- The ester was reduced to yield hydroxyl groups on the surface for subsequent adsorption experiments by reducing the samples in a 0.1 mol/L solution of  $\text{LiAlH}_4$  in absolute toluene for 15 minutes. After that, hydrolysis for another 15 minutes in 1 mmol/L hydrochloric acid was carried out. The samples were sonicated in diluted hydrochloric acid and rinsed with bidistilled water, followed by sonication with toluene and ethanol for five minutes.
- Partial multilayers were obtained by repetition of the steps described above.

All experiments were performed with solutions with an adjusted water content of  $12 \pm 0,5$  mmol/L. The temperature was kept constant at 15 °C. After each deposition step the completeness of the deposition was investigated by ellipsometry and in this way the progress of the multilayer formation was monitored. After the application of the final layer the samples were characterised by TM-AFM.

### 5.5.5 Temperature control

In order to increase the reproducibility of our experiments, a temperature control unit for the adsorption experiments was developed. For this purpose an aluminium block with 10 recesses for deposition vessels was manufactured (Figure 7). The temperature is measured by a sensor in the metal block and a control unit compares the observed values with the desired values. Cooling and heating is done by a thermoelectric peltier device. The heat produced by peltier-cooling of the metal block is discharged by a cooling water circuit.

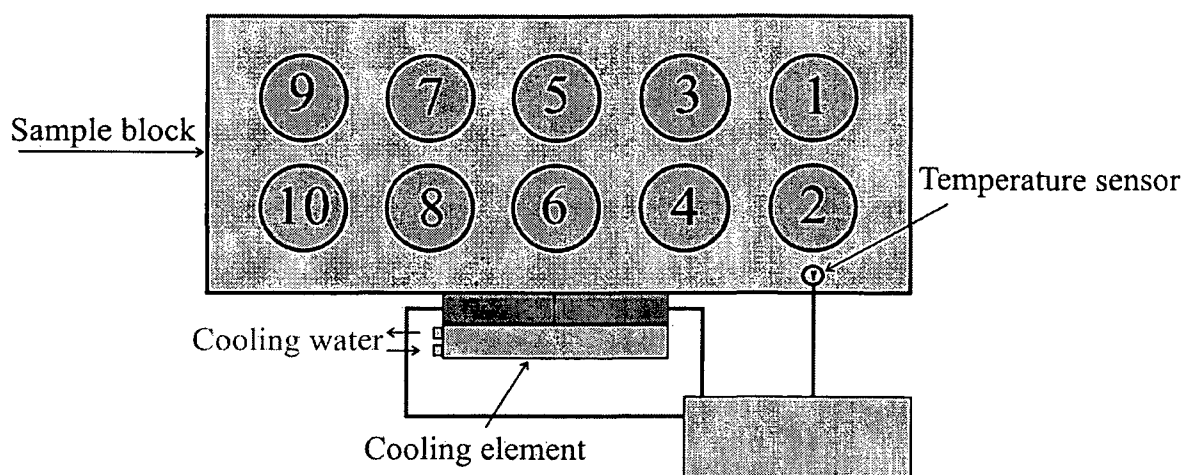


**Figure 7:** Scheme of temperature control unit with numbered positions for the reaction vessels.

In order to investigate the cooling/ heating rates at the different positions a series of measurements has been performed. Vessels with 10 mL of adsorption solution were positioned in each recess (as shown in Figure 8). Figure 9 shows how the measured temperature responds upon switching the setpoint temperature from 25 °C to 20 °C (marked with arrow I in Figure 9) and from 20 °C to 25 °C (marked with arrow II in Figure 9). It can be seen that the setpoint temperature is reached faster at positions 2, 4, 6, 8, and 10 adjacent to the peltier element. However, all positions reach the nominal temperature  $\pm 1$  °C within 5 minutes.

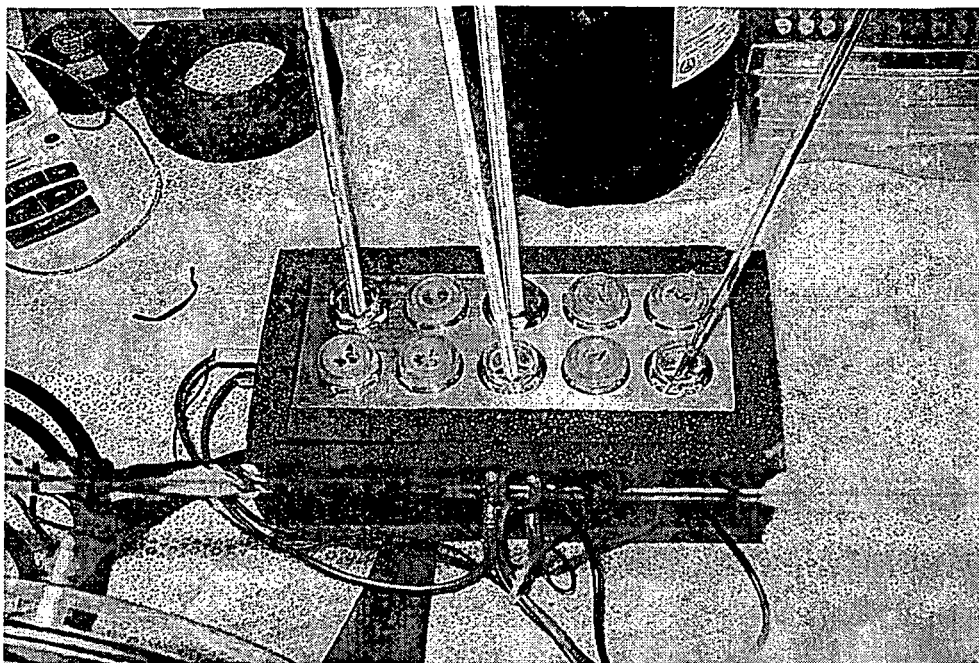


Figure 8: Photo of temperature control unit

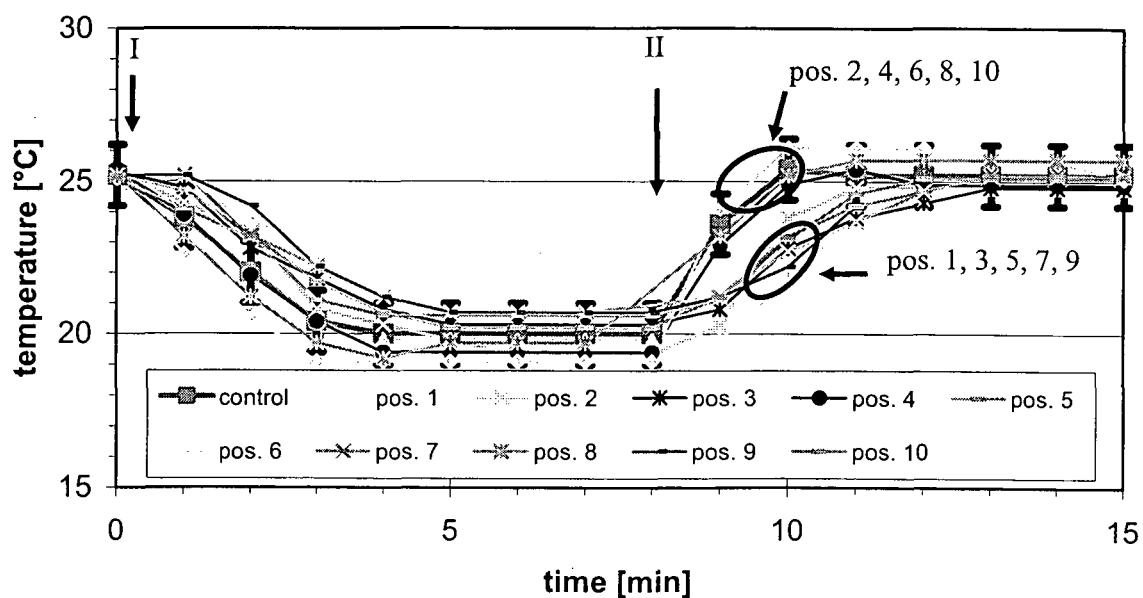
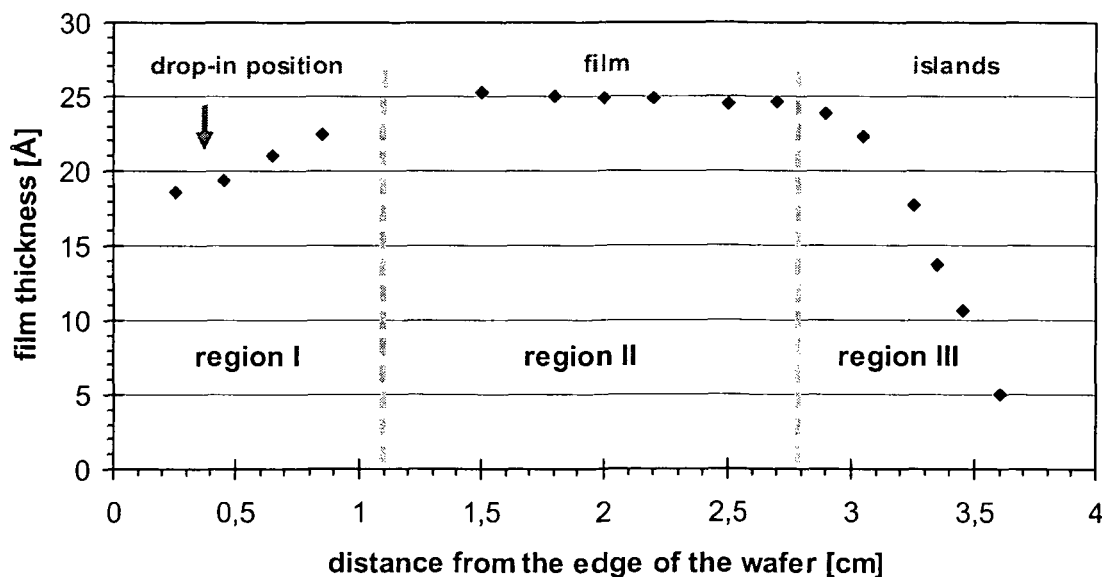


Figure 9: Temperature versus time for positions 1-10 of the aluminum block. At arrow I and II the setpoint temperature has been switched from 25 °C to 20 °C and from 20 °C to 25 °C, respectively. The line denoted with "control" represents the value displayed on the control unit of the instrument.

## 6 Results

### 6.1 Concentration profile experiment – “glass tube experiment”

In the first experiment, which was originally designed for in-situ ellipsometric measurements (in detail see chapter 4.3.1), the sample was immersed in toluene in a glass tube (Figure 6). Using a Hamilton syringe, the calculated volume of OTS corresponding to a final concentration of 0,5 mmol/L was injected into the glass tube. This led to a high local concentration at the drop-in position. After ten minutes the solution was discarded and the sample was removed from the glass tube. Surprisingly, in this experiment full monolayer coverage of the silicon surface could not be obtained at the drop-in position. Thus, additional AFM and ellipsometric measurements were performed in order to shed more light on this phenomenon.



**Figure 10:** Ellipsometric layer thickness of ODS films on silicon versus distance from the drop-in position obtained in the “glass tube experiment”

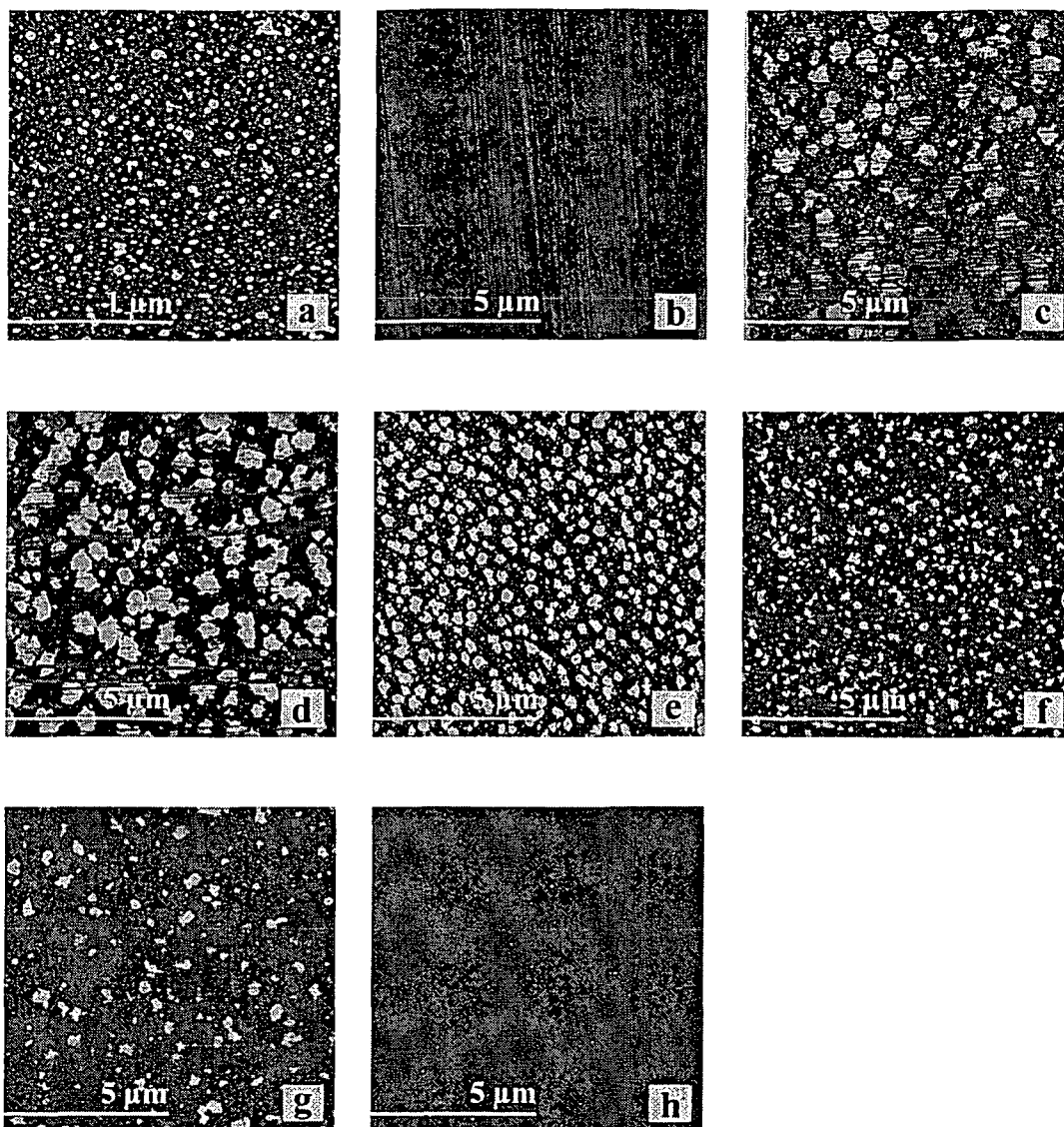
Figure 10 shows the film thickness versus the distance from the drop-in position. Three regions showing different growth behavior can be identified. At the drop-in position a layer thickness of  $1,9 \pm 0,1$  nm has been found, which increases to  $2,2 \pm 0,1$  nm within a distance of about 0.5 cm from the drop-in position (region I). This corresponds to only about



70 % of a full monolayer. In region II (1.1 to 2.3 cm from the wafer edge) a film thickness of  $2,5 \pm 0,05$  nm can be observed indicating full monolayer coverage. Finally, in region III (2.3 cm to the end of the wafer substrate) the film thickness starts to gradually decrease again down to almost zero near the end of the substrate.

Figure 11 shows AFM images corresponding to the data shown in Figure 10. At the drop-in position (Figure 11a) a rough surface (rms-roughness  $\sim 0,6$  nm) showing dots of typically 2 - 4 nm in height and 30 - 60 nm in diameter can be observed. In the regions between these spots a regular flat surface cannot be found either. This clearly shows that in this case self-assembly leading to flat ordered films cannot be achieved at high local concentrations.

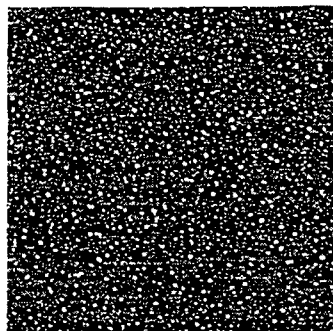
In contrast, it seems that at the drop-in position a high concentration of OTS leads to fast deposition of material, whereby the OTS molecules do not have sufficient time for ordering in solution prior to adsorption. Thus, a variety of oligomeric species with different degree of condensation can adsorb onto the surface in a disordered manner. This is both in agreement with the irregular surface observed in the AFM images and with the surface coverage of only 70 % revealed by ellipsometry. Full surface coverage cannot be achieved due to the irregular attachment of organic molecules blocking the surface for adsorption of further material. In region II, AFM images (Figure 11b) show a flat surface with an rms-roughness of 0,14 nm indicating the formation of an ordered monolayer film which is also in agreement with the ellipsometric film thickness of 2,5 nm. This change in the growth mechanism can be explained both by dilution of the organic species upon diffusion from the drop-in position and/or ordering of molecules in solution during the time of migration. In region III (Figure 11c - h) ordered film deposition takes place as well, however, due to further dilution of OTS and shorter net adsorption times, full monolayer coverage is not achieved anymore. Instead, flat ordered islands are observed, whose surface concentration decreases with increasing distance from the drop-in position. This is in good agreement with the thicknesses obtained by ellipsometry.



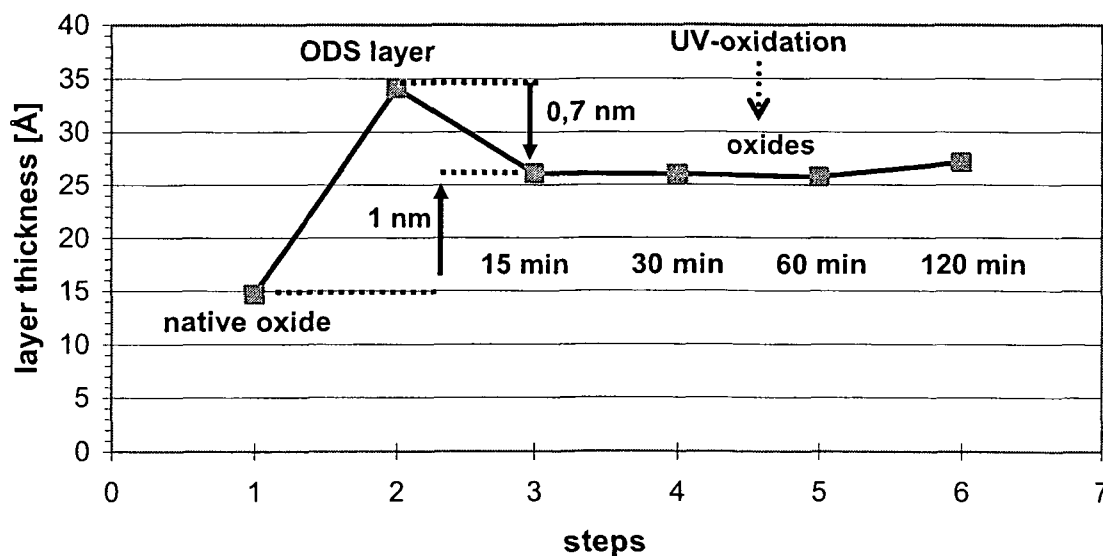
**Figure 11:** AFM images of ODS films obtained in the “glass tube” experiment *a)* Drop-in position corresponding to region I in Figure 10. *b)* Closed ODS film observed in region II of Figure 10. The vertical stripes originate from cleaning the wafer with a tissue after the deposition experiment. *c) – h)* Island formation in region III of Figure 10.

Figure 12 shows an AFM image of the drop-in position (see also Figure 11a) after 15 min of oxidation in a UV-chamber. It can be seen that the surface does not change qualitatively compared to the organic film in Figure 11a. Figure 13 shows that the layer thickness drops by 0,7 nm upon oxidation corresponding to a net increase of the oxide thickness (compared to the native oxide) of 1 nm. This corresponds to 3 monolayers of SiO<sub>2</sub>. Figure 13 shows that further oxidation up to 120 min did not lead to a decrease of this value indicating that oxidation is complete. This result is very surprising since only 70 % of a monolayer of ODS seem to form 3 monolayers of SiO<sub>2</sub> upon oxidation. In order to shed more light on this unexpected phenomenon the correct performance of our ellipsometer has been

verified by monitoring repeated deposition/ oxidation cycles with different alkylsilanes as previously described by Vallant et al.<sup>84</sup>. Figure 14 shows a linear increase of the organic layer thickness and the oxide layer thickness of 0,32 nm/ cycle for OTS and 0,30 nm/ cycle for UTS. These values are in full agreement with expectation indicating that our ellipsometer works properly. The slightly lower growth rate in case of UTS can be explained by the lower degree of order for the shorter molecule leading to slightly lower maximum coverages.



**Figure 12:** AFM image of drop-in position after 45 min of oxidation. The size of the image is  $5 \times 5 \mu\text{m}^2$ . The surface does not change qualitatively compared to the organic film shown in Figure 11a.



**Figure 13:** UV-oxidation of ODS film formed at the drop-in position. For explanation see text.

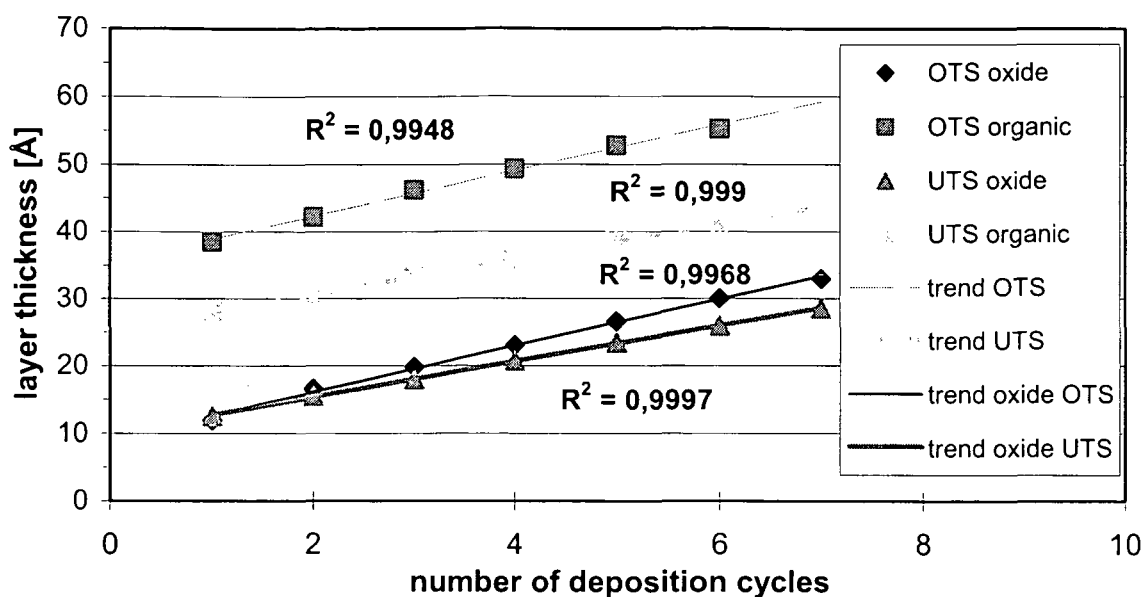


**Figure 14:** Results of adsorption- oxidation cycles with UTS and OTS (see text for details). The increase of the silicon oxide layer agrees well with the literature value of 0,3 nm per cycle.

Since the experiment described above could not explain the unexpectedly high oxide layer thickness of the “glass tube experiment”, further experiments with various precursor concentrations and chain length have been performed. These experiments are described in chapter 6.2.

It should already be mentioned at this point that these experiments could not clarify the contradictory thickness values of organic film and corresponding oxide layer observed in the “glass tube experiment”. Moreover, also XPS measurements were not conclusive either.

## 6.2 Adsorption from highly concentrated solutions

In order to directly investigate the influence of the precursor concentration and the time available for ordering in solution, 2 series of experiments with homogeneous solutions have been performed. OTS concentrations of 0.5, 5, 10, 20, and 50 mmol/L and a deposition time of 20 s have been chosen. Figure 15 shows AFM images for the first series performed with solutions matured for only 20 s (i.e. the substrate was dipped into the solution 20 s after OTS was added). For the lowest concentration of 0.5 mmol/L, which is commonly used in deposition experiments, a uniform surface with an rms-roughness of 0,09 nm can be observed (Figure 15a). With increasing OTS concentration an increasing number of bright dots (typically 40 - 60 nm in diameter and 2 - 4 nm in height) can be observed (Figure 15b-e) and the overall rms-roughness of the surface rises from 0,9 to 3,4 nm. The surface roughness between the bright spots is similar for all samples (approximately 0,9 nm) except for the highest concentration of 50 mmol/L (approximately 1,3 nm). From the described observations it can be concluded that at higher concentrations the adsorption is too fast to allow the formation of an ordered densely packed film. For example, a layer thickness of only  $1,37 \pm 0,03$  nm was measured for an OTS concentration of 50 mmol/L which is about half the thickness of a complete monolayer.

It should also be stressed that such incomplete layers cannot be converted into full monolayers even after a prolonged period of exposure up to several hours, further confirming that the surface is blocked due to irregular chemisorption of adsorbate molecules during the initial phase of the growth process. This observation is in agreement with the situation at the drop-in position of the "glass tube experiment".

Figure 16 shows the second series of experiments performed with solutions aged for 10 minutes. In this case island growth can be observed for all concentrations. With increasing concentration both the number of islands and the amount of deposited material between the islands increase up to an almost complete monolayer film for the highest concentration of 50 mmol/L (Figure 16e). This is supported by the ellipsometric film thickness reaching a value of  $2,3 \pm 0,03$  nm for the highest concentration which corresponds to a surface coverage of 88 %. The stripes visible in some of the images originate from cleaning of the samples by wiping with a tissue.

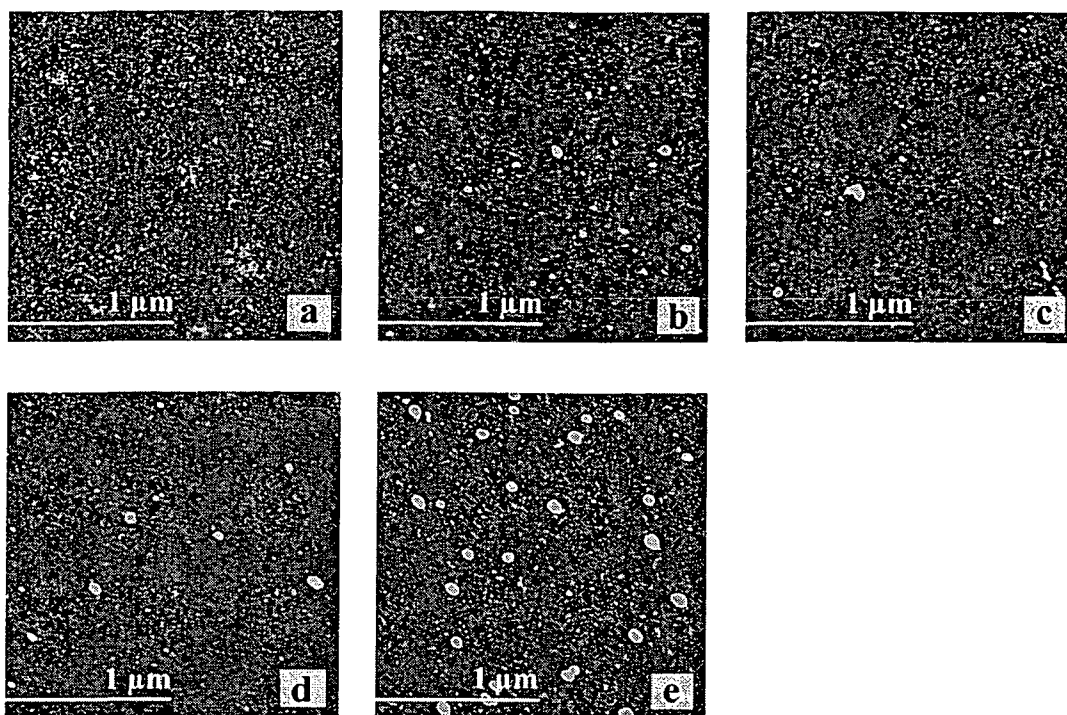


*Figure 15: AFM-images of ODS films on silicon obtained for OTS concentrations of a) 0.5, b) 5, c) 10, d) 20, and e) 50 mmol/L. Both adsorption time and maturation time of the OTS solution was 20 s.*

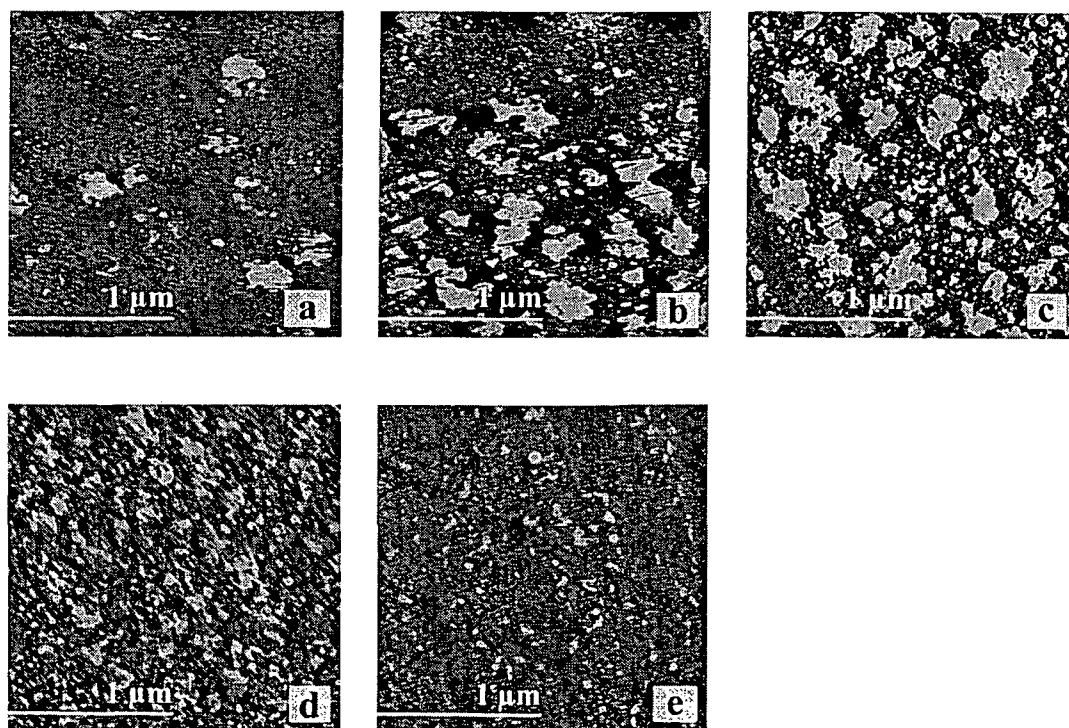


*Figure 16: AFM-images of ODS films on silicon obtained for OTS concentrations of a) 0.5, b) 5, c) 10, d) 20, and e) 50 mmol/L. The maturation time of the OTS solution was 10 minutes. The adsorption time was 20 s.*

In order to investigate the influence of the precursor chain length on the ordering process, deposition experiments with C<sub>10</sub>-, C<sub>12</sub>-, C<sub>16</sub>-, and C<sub>18</sub>-alkylsilanes at a concentration of 50 mmol/L and maturation times of 20 s and 10 minutes have been performed. The deposition time was 20 s in all cases.

Figure 17 shows the thickness of the films both for the matured (10 minutes) and the fresh (20 s) deposition solution. For the matured solution a linear increase of the thickness with increasing chain length can be observed and full monolayer coverage is achieved as indicated by the film thickness which is in good agreement with the chain length of the adsorbed molecules. Such a linear increase has also been observed for other concentrations of the precursors. This result indicates that, regardless of the chain length, ten minutes of aging is sufficient for ordering of the molecules prior to deposition, thus leading to flat films in which the thickness is only determined by the length of the adsorbed molecules. This conclusion is also confirmed by AFM images showing flat surfaces – apart from some scratches due to the cleaning process – with an rms-roughness of less than 0,1 nm (Figure 18).

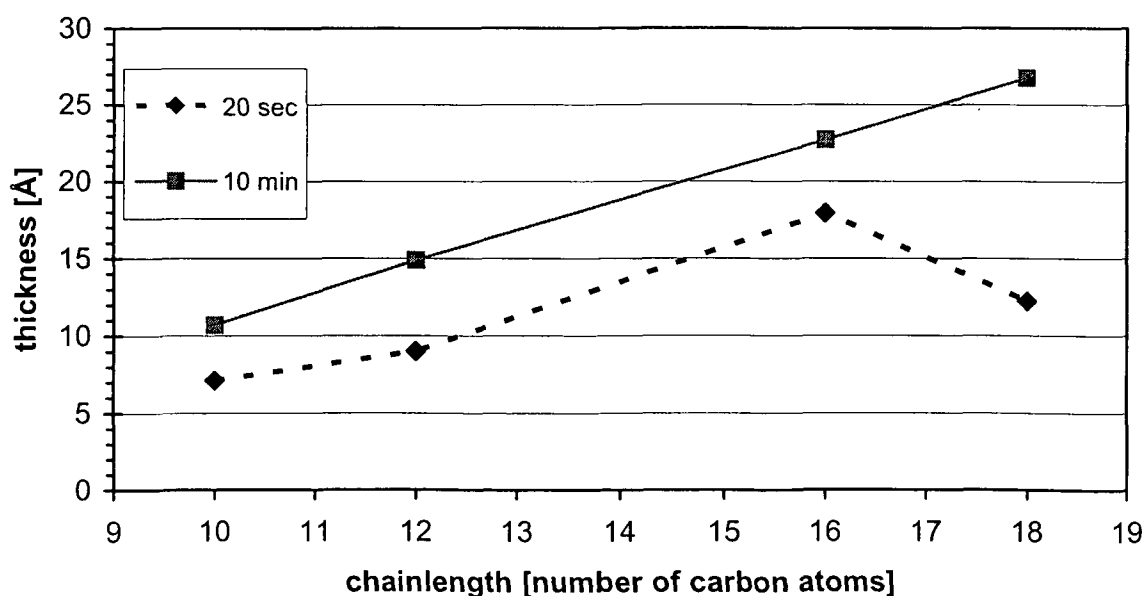


**Figure 17:** Layer thickness of alkylsiloxane films on silicon versus length of the alkylchain. The maturation time was 10 minutes (full line) and 20 s (dashed line), respectively. Deposition has been performed from a solution with an OTS concentration of 50 mmol/L. The adsorption time was 20 s in all cases.

In contrast to that, the growth behavior for the fresh solutions looks completely different. First of all, full monolayer coverage is never obtained. The ellipsometric thickness

for the siloxane layers derived from C<sub>10</sub>-, C<sub>12</sub>-, and C<sub>16</sub>-alkylsilanes is about 0,4 to 0,5 nm lower than expected for a complete film. This could be explained by the fact that the maturation time was not sufficient in order to obtain densely packed films. This is also supported by the corresponding AFM images (Figure 19) showing an rms-roughness of 0,15 to 0,3 nm which is significantly higher than the values obtained after maturing for 10 minutes. The images show only a few bright dots. By repeated rinsing and wiping with a tissue it could be verified that these dots do not originate from loosely bound impurities. Thus, the observed features could be interpreted as agglomerates of silanol molecules formed in solution and chemically stabilized at the surface by a certain degree of condensation. The increasing roughness of the films from C<sub>10</sub>- to C<sub>16</sub> suggests that further ordering leading to flat films is slower for longer chain lengths.

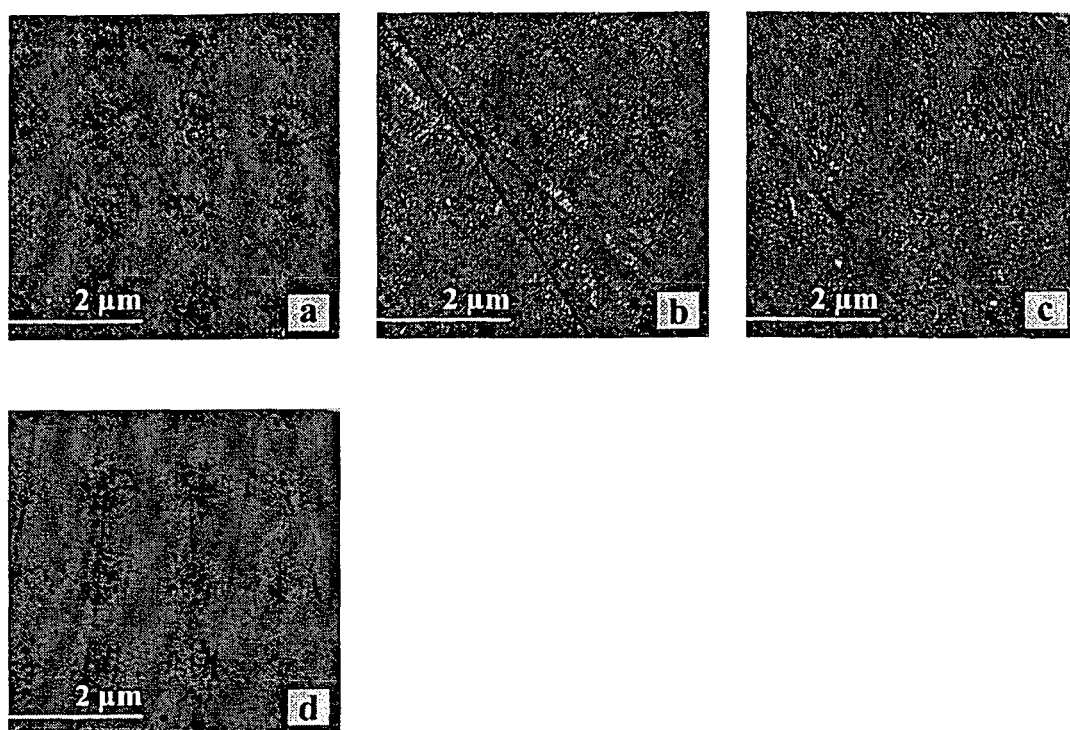


**Figure 18:** AFM images of alkylsiloxane films on silicon with an alkylchain length of a) 10, b) 12, c) 16, and d) 18 carbon atoms. Deposition has been performed for 20 s from a solution with an OTS concentration of 50 mmol/L. The maturation time of the deposition solution was 10 minutes. The stripes originate from cleaning of the wafer with a tissue.



In contrast to the growth of C<sub>10</sub>-, C<sub>12</sub>-, and C<sub>16</sub>-alkylsilanes, OTS shows a completely different behavior. The ellipsometric film thickness (Figure 17) shows a sharp drop from linearity down to a value of only 1,3 nm indicating a surface coverage of about 50 %. The corresponding AFM image (Figure 19) is also significantly different from the preceding images of the shorter-chain analogues. The whole sample area is dotted with bright spots of different size, height, and shape leading to a comparatively high rms-roughness of  $0,73 \pm 0,1$  nm.

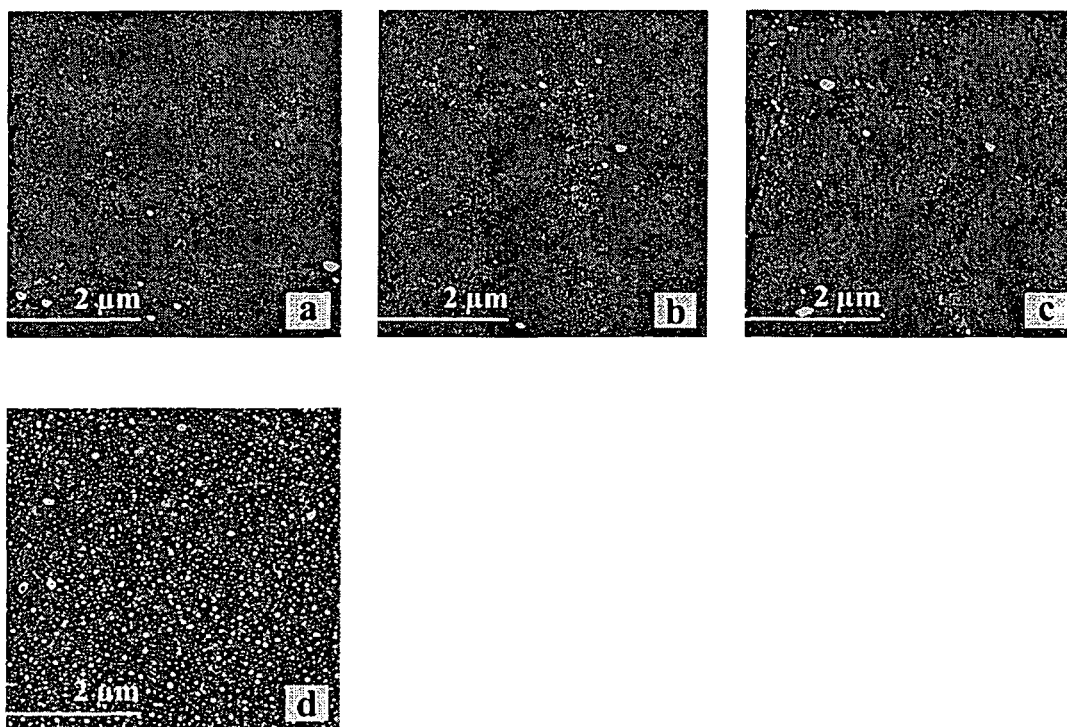


**Figure 19:** AFM images of alkylsiloxane films on silicon with an alkylchain length of *a)* 10, *b)* 12, *c)* 16, and *d)* 18 carbon atoms. Deposition has been performed for 20 s from a solution with an OTS concentration of 50 mmol/L. The maturation time of the deposition solution was 20 s.

There is no indication for an ordered layer growth. Even prolonged adsorption of up to 1 hour does neither increase the film thickness nor change the surface structure observed by AFM. This indicates that for a long-chain molecule like OTS, at high concentrations fast adsorption of heavily disordered species takes place leading to a passivation of the surface for further adsorption. Thus, full monolayer coverage cannot be achieved. Obviously rearrangement of organic molecules on the surface is hindered due to formation of covalent siloxane bonds. Bunker et al.<sup>85</sup> claim that monolayer formation is favoured with increasing chain length, because self-assembly in solution is driven by van der Waals interactions

between hydrocarbon groups. However, this does not explain the sharply different behavior of OTS in our experiments. In fact, according to this assumption OTS should rather form smooth films.

It has also been tried to judge the possibility for vesicle or micelle formation. Bunker et al.<sup>85</sup> have found that agglomerates can form above a critical aggregation concentration. For 1H, 1H, 2H, 2H-perfluorodecyltrichlorosilane (FDTS) in isooctane at a concentration above 52 mmol/L, they have observed the formation of aggregates with typical diameters of 130 nm by light scattering. After deposition circular objects with diameters of 300 nm and heights of typically 25 nm were visible in the AFM images. The authors speculated that the observed aggregates might be either inverse micelles or inverse vesicles, whereby vesicles are more likely due to a better match in size and shape. In principle this suggests that the features observed in our work might be micelles or vesicles, as well. However, due to the largely different experimental parameters in our study, the properties of our system with respect to vesicle formation might be different. Israelachvili<sup>86</sup> has proposed a model, in which the possibility for formation of micelles and vesicles from amphiphilic molecules can be estimated from a packing parameter based on geometric considerations. In our case this packing parameter suggests that micelle and vesicle formation is possible for all of our precursors from C<sub>10</sub> to C<sub>18</sub>, however, the different behavior of these compounds, particularly OTS, cannot be explained. Thus, we have also considered a potential effect of the deposition temperature. Parikh et al.<sup>47</sup> have found a critical temperature  $T_C$  for the deposition of ordered films which depends on the chain length. According to their findings for OTS, this temperature should be  $28 \pm 4^\circ \text{C}$ . With increasing deposition temperature they have observed decreasing film thicknesses. At temperatures above  $60^\circ \text{C}$  a surface coverage of only 70 % could be reached. Since we have observed such a low surface coverage already at room temperature, a temperature effect is not likely to explain the prominent behavior of OTS. Moreover, Carraro et al.<sup>35</sup> have observed the formation of homogenous films at temperatures above  $40^\circ \text{C}$ . Thus, the temperature neither explains the dot-like features in our AFM images, indicating agglomeration, nor the different growth behavior of the different precursors, which changes abruptly from C<sub>16</sub> to C<sub>18</sub>.

## *Conclusion*

The growth behavior of self-assembled monolayers of alkylsiloxanes at high precursor concentrations up to 50 mmol/L differs strongly from the behavior observed at low concentrations on the order of 1 mmol/L usually applied for film formation. At high concentrations, a substantial amount of material can be adsorbed at the surface, even after short maturation times of the precursor solution. However, for OTS it has been found that irregular rough films with lower density are obtained under these conditions and that full monolayer coverage cannot be achieved due to passivation of the surface with disordered organic molecules. At longer maturation times of the precursor solution, flat films are observed and full monolayer coverage can be achieved. For alkylsilanes of shorter chain length between ( $C_{10}$  and  $C_{16}$ ) a completely different behavior has been found. In this case flat films have been observed even after short maturation times.

### 6.3 Influence of the chemical surface composition on film growth

In order to study the influence of surface chemistry on film growth the number of reactive sites (OH-groups) has been controlled through blockage with a deactivation reagent. In order to find a well suited reagent preliminary experiments with various compounds have been performed as described in the following chapter.

#### 6.3.1 Preliminary experiments with various deactivation reagents

##### 6.3.1.1 Butyltrichlorosilane (BuTCS)/ Phenyltrichlorosilane (PhTCS)

The results shown in Figure 20 indicate that BuTCS is a very effective reagent for inhibition of ODS growth on silicon oxide. Deactivation of the active sites of the surface with BuTCS led to a dramatical decrease of the subsequent OTS adsorption. The adsorption time for OTS was 20 s in all cases.

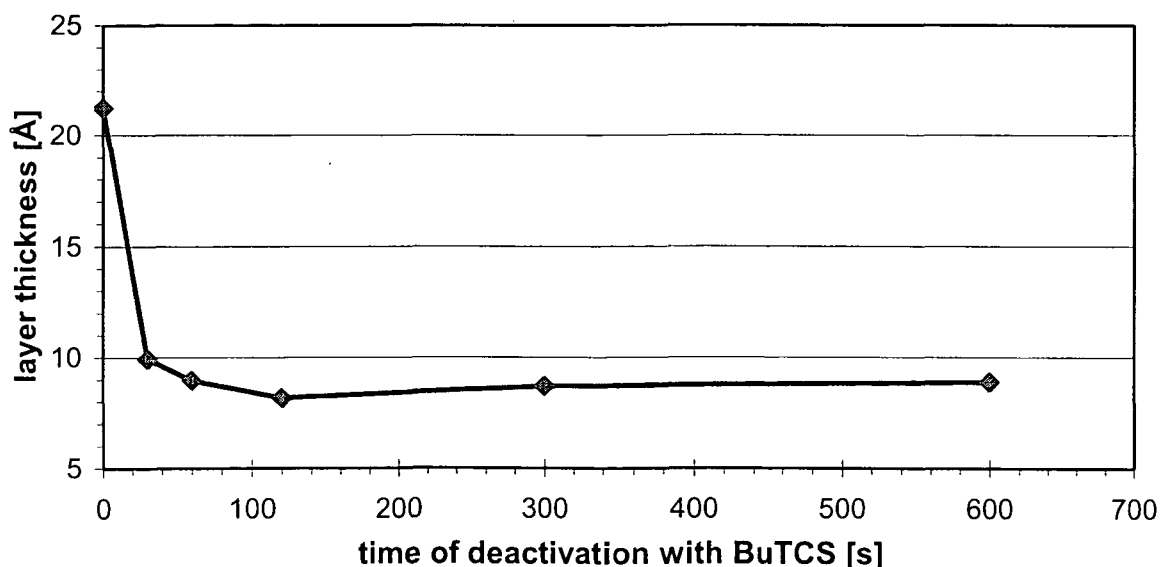


**Figure 20:** Layer thickness of ODS layers versus deactivation time of the silicon substrate in BuTCS. The adsorption time for OTS was 20 s in all cases. After 1 min of deactivation the film thickness corresponds to a full monolayer of BuTCS (see Figure 22).

After about 100 s of deactivation with a 5 mmol/L-BuTCS solution further changes in film thickness are not observed. Prolongation of the OTS treatment did not change this behavior, which indicates that a full deactivation of the surface has been achieved already after 100 s. Furthermore, this shows a high persistence of deactivation which means that the deactivation reagent cannot be replaced by OTS. Similar observations have been made for PhTCS which is shown in Figure 21. This behavior is different from deactivation with TMCS (described later) which can be explained by the higher stability of BuTCS and PhTCS films due to the possibility of crosslinking within the film molecules (see also chapter 6.3.2).

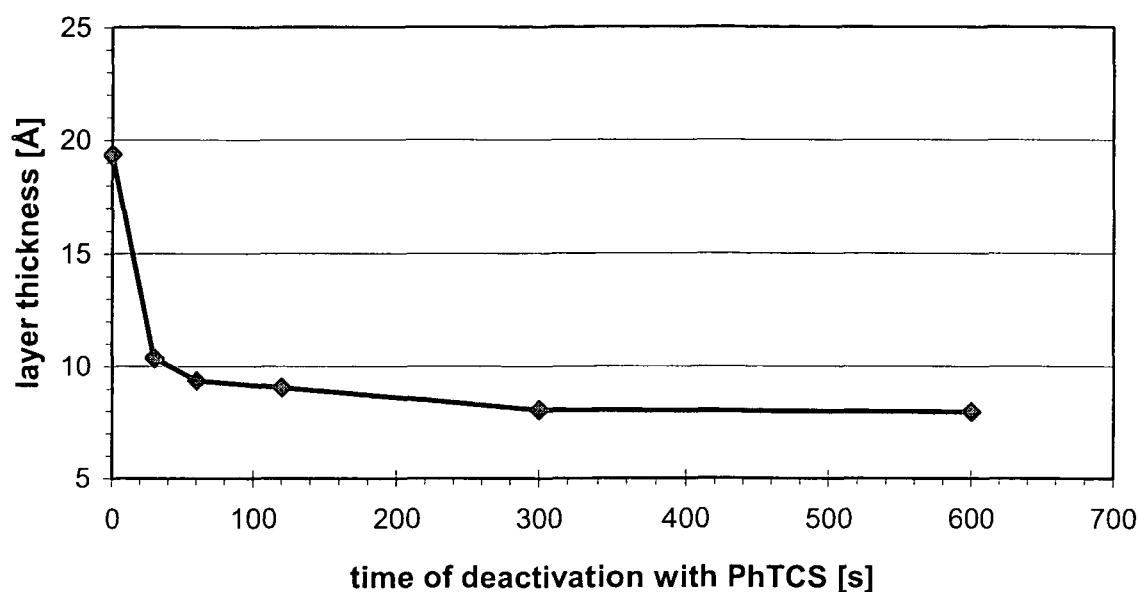


**Figure 21:** Layer thickness of ODS layers versus deactivation time of the silicon substrate in PhTCS. The adsorption time for OTS was 20 s in all cases. A dramatic decrease of the coverage can be observed even for short deactivation times.

Figure 23 shows AFM images corresponding to the data shown in Figure 20. In contrast to the active silicon substrate (Figure 23a) only a few small round ODS islands can be observed on an otherwise flat substrate. These islands slightly increase in number with adsorption time, which however does not contribute to the total layer thickness significantly. Since the formation of very stable films is too fast in case of BuTCS and PhTCS, fine control of the number of active sites is not possible with these reagents. Thus, they are not suited for our deactivation experiments.

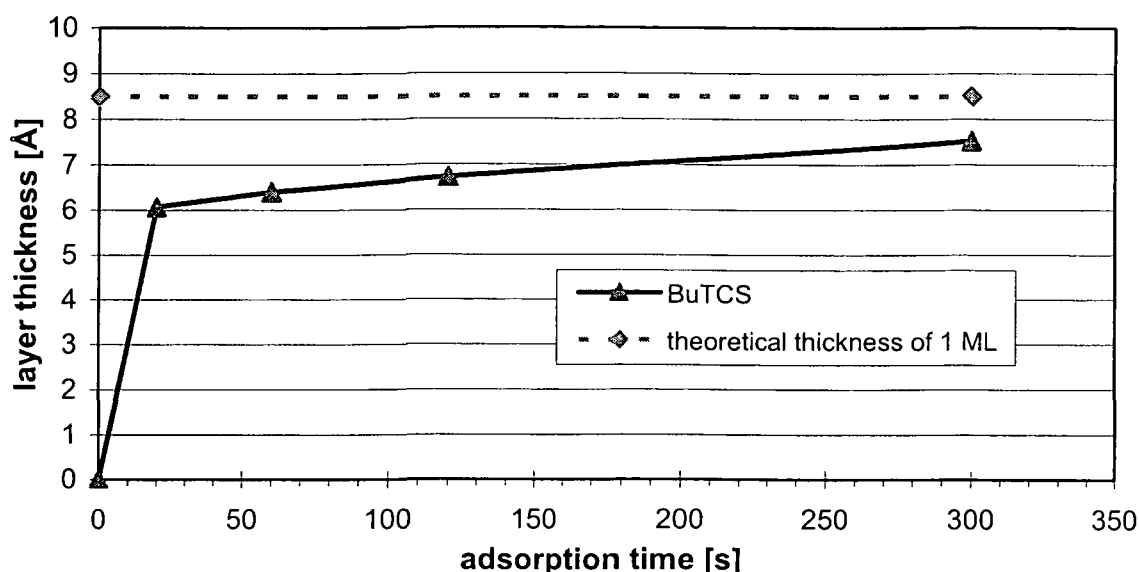


**Figure 22:** Layer thickness of BuTCS on silicon versus adsorption time. The dashed line marks the theoretical maximum layer thickness<sup>32</sup> for BuTCS for an all-trans conformation of the chains.

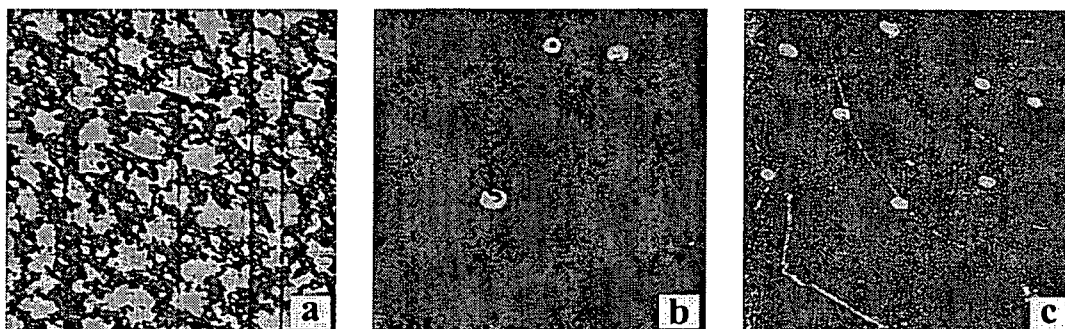


**Figure 23:** AFM images of ODS films on a) active silicon, and silicon modified through increasing deactivation times of b) 30 and c) 300 s in BuTCS ( $c = 5 \text{ mmol/L}$ ). The films were deposited through immersion in OTS ( $c = 1 \text{ mmol/L}$ ) for 20 s.

#### 6.3.1.2 Trimethoxysilane (TMeOS)

A further experiment was performed with TMeOS as deactivation reagent. OTS adsorption after deactivation with TMeOS led to a significant increase in film thickness indicating that deactivation with TMeOS is not effective. This may be explained by incomplete hydrolysis of TMeOS and by lack of crosslinking between TMeOS molecules on the surface leading to incomplete TMeOS layers. Thus, sufficient active sites for incorporation of OTS molecules are still available.

### 6.3.1.3 Methyltrichlorosilane (MTCS)

Adsorption of MTCS led to rough irregular surfaces (Figure 24) showing increasing roughness and film thickness with increasing adsorption time. Furthermore, a bad reproducibility has been observed. This can be explained by the 3 reactive silanol groups of MTCS leading to crosslinking (polymerization) in all spatial directions. Thus, adsorption of MTCS is not self-terminating. Clearly, MTCS is not suited as deactivation reagent.

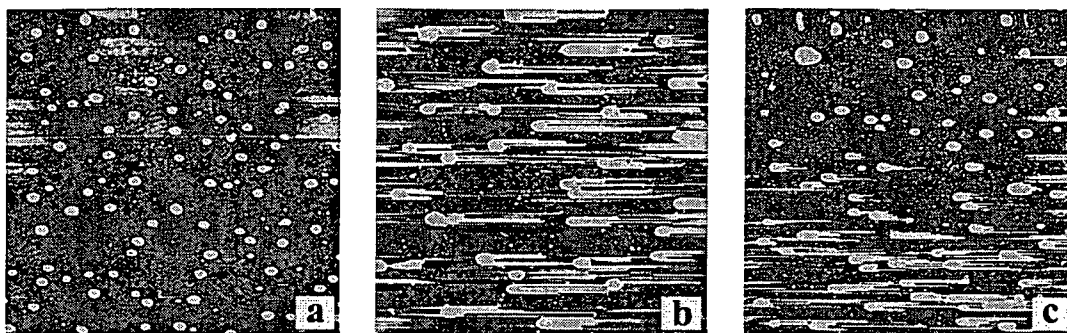
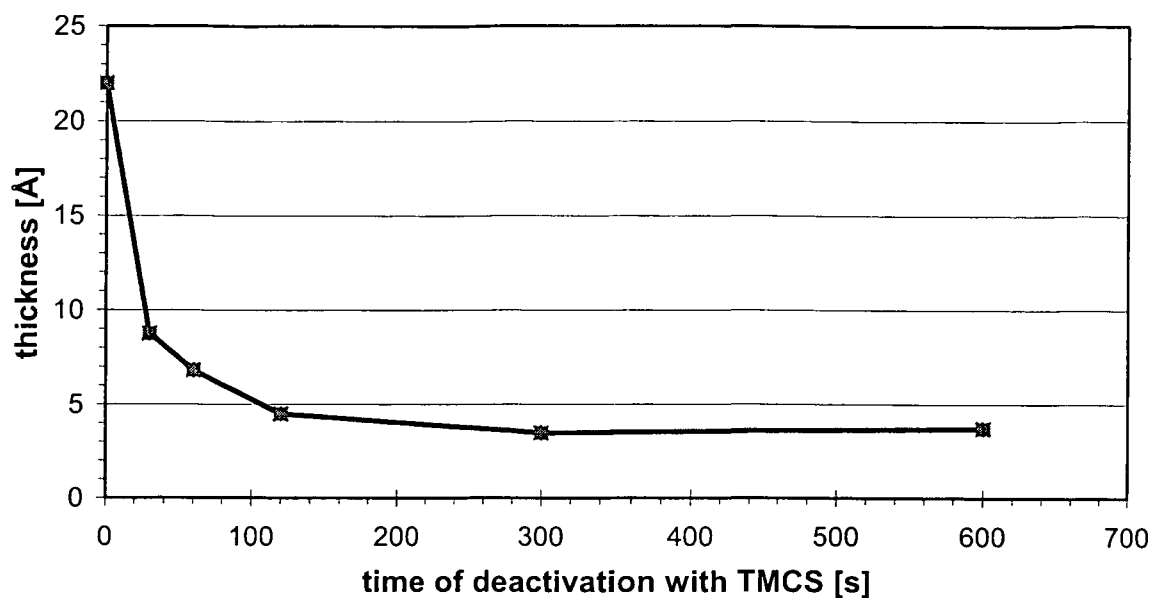


*Figure 24: AFM images obtained after deactivation of the silicon substrate with MTCS for a) 30 s, b) 300 s, and c) 600 s. Strong surface roughening due to three dimensional polymerization can be observed.*

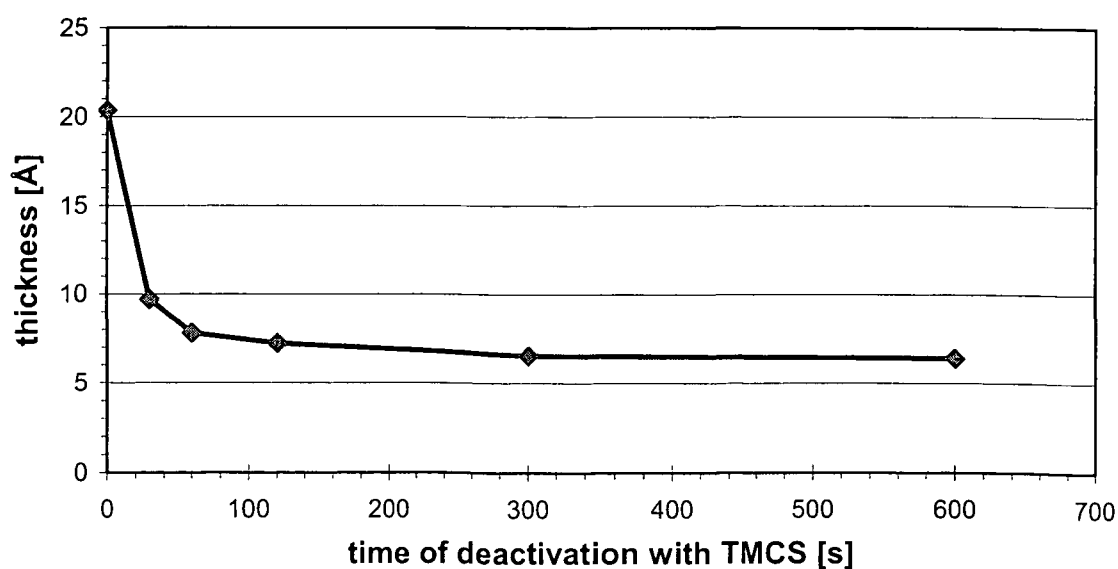
### 6.3.2 Hydrophobization of silicon surfaces with TMCS

Immersion of silicon wafers in a 5-mmol/L TMCS solution resulted in a maximum layer thickness of about 0,2 nm as determined by ellipsometry. Deactivation of the silicon oxide surface with TMCS led to a dramatic decrease of the subsequent OTS adsorption. Figure 25 shows the effect of deactivation in TMCS for immersion times from 0 (no deactivation, reference wafer for the OTS adsorption) up to 10 minutes. The immersion time of OTS was 20 s in all cases. The surface coverage decreases from about  $2,2 \pm 0,1$  nm to around  $0,9 \pm 0,1$  nm for a deactivation time of only 30 s. A sharp decrease in adsorption within one minute of deactivation can clearly be seen. Then the layer thickness slowly decreases until a practically constant value is reached after 5 min. The layer thickness after 5 minutes of deactivation, followed by depositing the wafer into a 1-mmol/L OTS solution for 20 s, is about 0,2 nm higher than that of a sole TMCS layer. Prolongation of the TMCS treatment up to 6 hours did not change this behavior, which indicates that a full deactivation

of the surface cannot be achieved. The same deactivation behavior has also been found for subsequent adsorption of HTS (Figure 26).



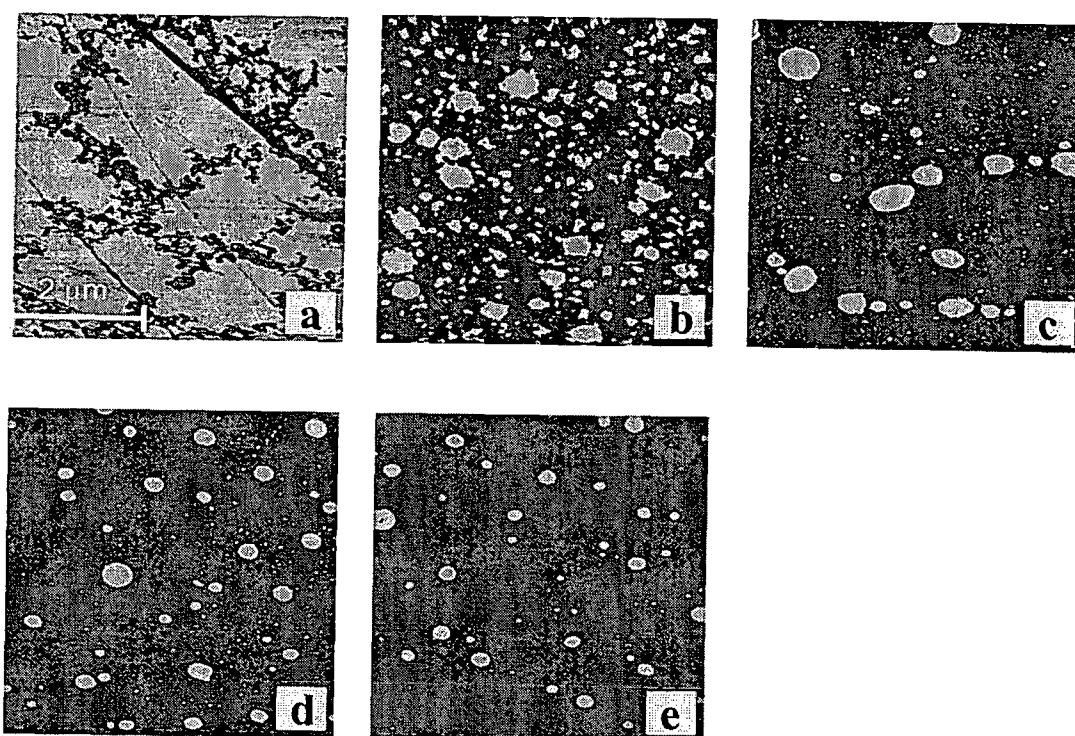
**Figure 25:** Layer thickness of ODS layers versus deactivation time of the silicon substrate in TMCS. The adsorption time for OTS was 20 s in all cases. A dramatic decrease of the coverage can be observed even for short deactivation times.



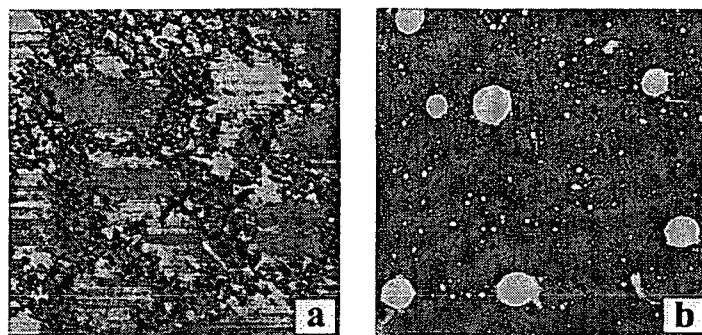
**Figure 26:** Layer thickness of HDS layers versus deactivation time of the silicon substrate in TMCS. The adsorption time for HTS was 20 s in all cases.



Figure 27 shows AFM images corresponding to the data shown in Figure 25. Figure 27a shows fractal islands which are typically achieved for OTS adsorption onto a fully activated silicon substrate. Surface coverages of about 85 % are usually attained for an adsorption time of 20 s of OTS under the given conditions (toluene solution containing 15 mmol/L  $\text{H}_2\text{O}$ ). In Figure 27b the situation after 30 s of immersion in TMCS and 20 s deposition in OTS is illustrated. The island size decreases from over 2 microns to around 400 nm for the larger islands, and they exhibit a spiky, circular shape. Many smaller islands with an average size of about 100 nm are observed as well. The height of the islands corresponds to totally aligned OTS molecules perpendicularly resting on the surface. Similar observations have been made for HTS adsorption on deactivated silicon surface (see Figure 28).



**Figure 27:** AFM images of ODS films on silicon modified through increasing deactivation times of a) 0, b) 30, c) 60, d) 120, and e) 300 s in TMCS ( $c = 5 \text{ mmol/L}$ ). The films were deposited through immersion in OTS ( $c = 1 \text{ mmol/L}$ ) for 20 s. Circular islands appear after about 60 s of TMCS deactivation.



**Figure 28:** AFM images of HDS films on silicon **a)** without deactivation, and **b)** after 120 s of deactivation in TMCS ( $c = 5 \text{ mmol/L}$ ).

A further increase of the deactivation time leads to a decrease in size and number of the smaller islands until they almost disappear after ten minutes of deactivation, whereas the larger islands seem to be constant in both size and number. The shape of the resulting islands gets more and more circular upon increasing deactivation. This transition in shape from a fractal form for the fully activated wafer surface (Figure 27a) to an almost perfect circular shape for the deactivated surfaces (Figure 27c-e) corresponds to a decrease of active sites on the surface. In the case of full activation, a maximum number of OH-groups is available on the silicon surface. Thus, there is a high probability for the approaching OTS molecules to be caught by building up a covalent bond (through condensation) with the substrate. The less active sites are accessible on the surface, the longer the OTS molecules are able to diffuse on the substrate. Thus, they are able to migrate to the energetically most favorable adsorption sites, leading to more and more circular islands. In the AFM images spiky circular islands have been observed up to a deactivation time of 2 minutes. For longer immersion times in TMCS visible fringes at the periphery of the islands have not been detected anymore.

Besides the number of active silanol groups, however, a further parameter influencing the mobility of OTS molecules is the water film on the surface. With higher hydrophobicity of the surface the contiguity of the water film decreases restricting diffusion of OTS molecules to smaller areas. Thus, smaller islands are observed.

Next, the persistence of the deactivation was investigated by increasing the adsorption times of OTS. For this purpose the silicon wafers were immersed into a 5-mmol/L TMCS solution for 30 minutes. Afterwards, they were deposited into a 1-mmol/L OTS solution for different times up to 20 hours. Ellipsometric data of the corresponding experiments (Figure 29) have shown that the layer thickness doubles from 0,4 nm for 20 s of adsorption to 0,8 nm after 5 minutes of adsorption. A prolongation of the deposition time in the OTS

solution leads to a further increase in layer thickness up to 2 nm after 4 hours and 2,3 nm after 20 hours.

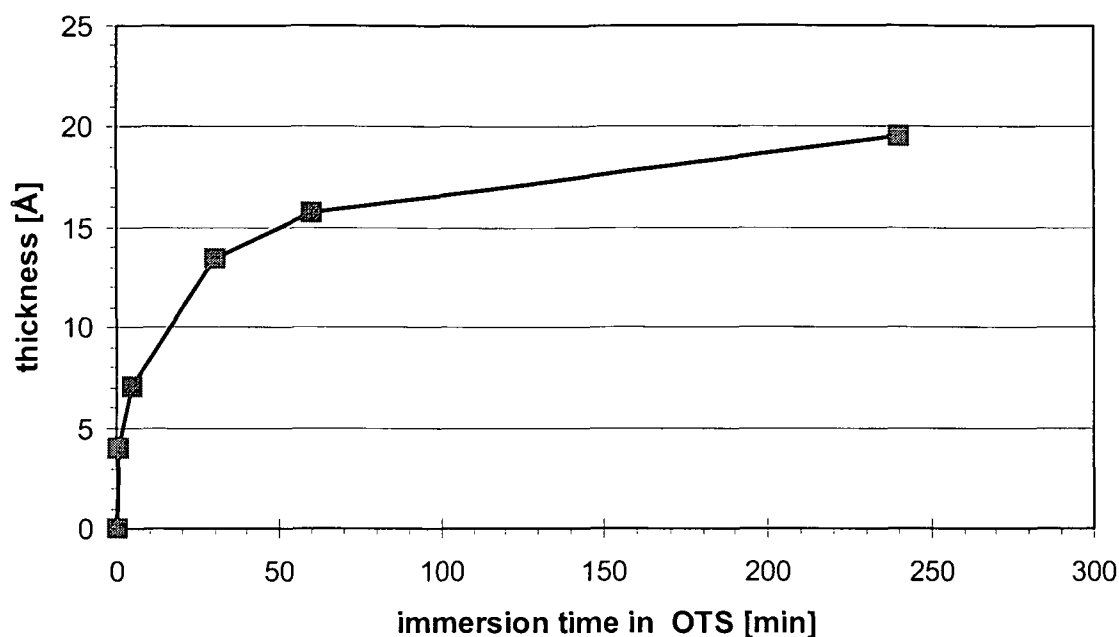


**Figure 29:** Ellipsometric layer thickness of ODS films on silicon versus immersion time in a 1 mmol/L OTS solution. The wafers were immersed for 1, 5, 30, 60, and 240 minutes after a deactivation period of 30 min in a 5 mmol/L TMCS solution.

It must be mentioned, however, that the growth is about 30 times lower than in case of active silicon substrates. Extended sonication in ethanol and intensive wiping of the wafers did not affect the layer thickness significantly. Therefore, a corruption of the data by physisorbed species can be excluded. It should also be stressed that even after a prolonged period of exposure for 20 hours the thickness of a highly ordered, densely packed film could not be obtained on such deactivated wafers. The results described above indicate that the deactivation is either not complete or reversible. In the case of an incomplete deactivation only a small percentage of the surface should be covered by TMCS. Since the achieved layer thicknesses were about 80 % of full monolayer coverage, this would mean that only the remaining 20 % should have been covered by TMCS. However, Tripp and Hair<sup>76</sup> have reported, that TMCS reacts with all kinds of surface silanols blocking about 80 % of the accessible OH-groups. Therefore, our results cannot be solely explained by incomplete deactivation of the silicon substrate.

In the case of a reversible deactivation, an exchange reaction between TMCS and OTS would need to take place. This could explain the obvious decelerated growth of the

monolayers after deactivation. Such exchange reactions have been reported for self-assembled monolayers of thiols on gold<sup>87,88,89</sup>, but not for alkyltrichlorosilanes. However, Wang et al.<sup>90</sup> found that chemisorbed siloxanes are able to migrate a few nanometer. They proposed a mechanism where slow hydrolysis of the siloxane bonds in presence of water occurs. The hydrolysis leads to physisorbed species, which are able to either migrate on the surface or to rebind to the surface at adjacent silanol sites (see Figure 30).

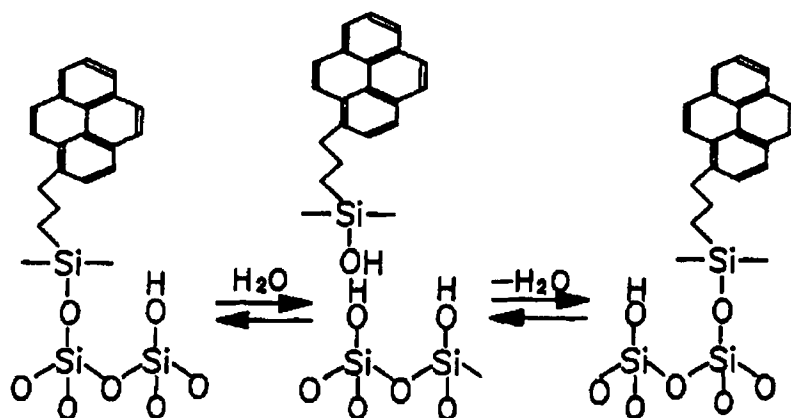


**Figure 30:** Mechanism for migration of chemisorbed siloxanes proposed by Wang et al.<sup>90</sup>

At the first glance, on a surface hydrophobized with TMCS, a surface water layer involved in this reaction should not exist. However, Uosaki et al.<sup>42</sup> have found interfacial water between a fused quartz surface and an ODS monolayer on top of it by in-situ SFG (sum frequency generation spectroscopy). The existence of such a water film has also been proposed by other groups. The existence of interfacial water can be explained by the fact that not every single OTS molecule in the film is bond to the surface. Thus, enough space between organic film and substrate surface is available for the water molecules. From that we conclude that water plays an important role in this exchange reaction (Figure 31) and a similar mechanism as reported by Wang et al.<sup>90</sup> can be expected.

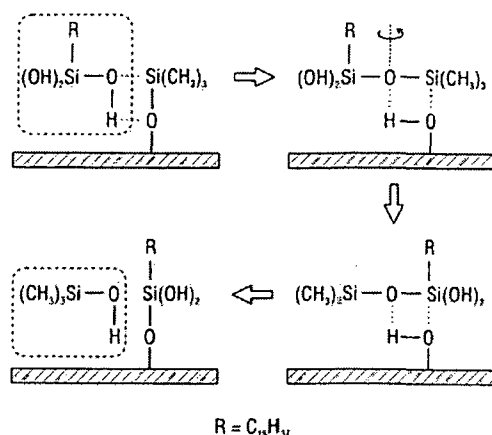


**Figure 31:** Proposed mechanism for exchange reaction of TMCS by OTS

AFM images corresponding to this experiment are shown in Figure 32. The stripes visible in the images originate from cleaning the wafer with a tissue after the deposition experiment in order to remove physisorbed OTS molecules and aggregates which are always present after long time deposition experiments. Circular islands can be found in all images. By increasing the immersion time of OTS up to 20 hours, number and size of the islands does not change significantly. The size of the islands varies in a range between 100 to 500 nm.

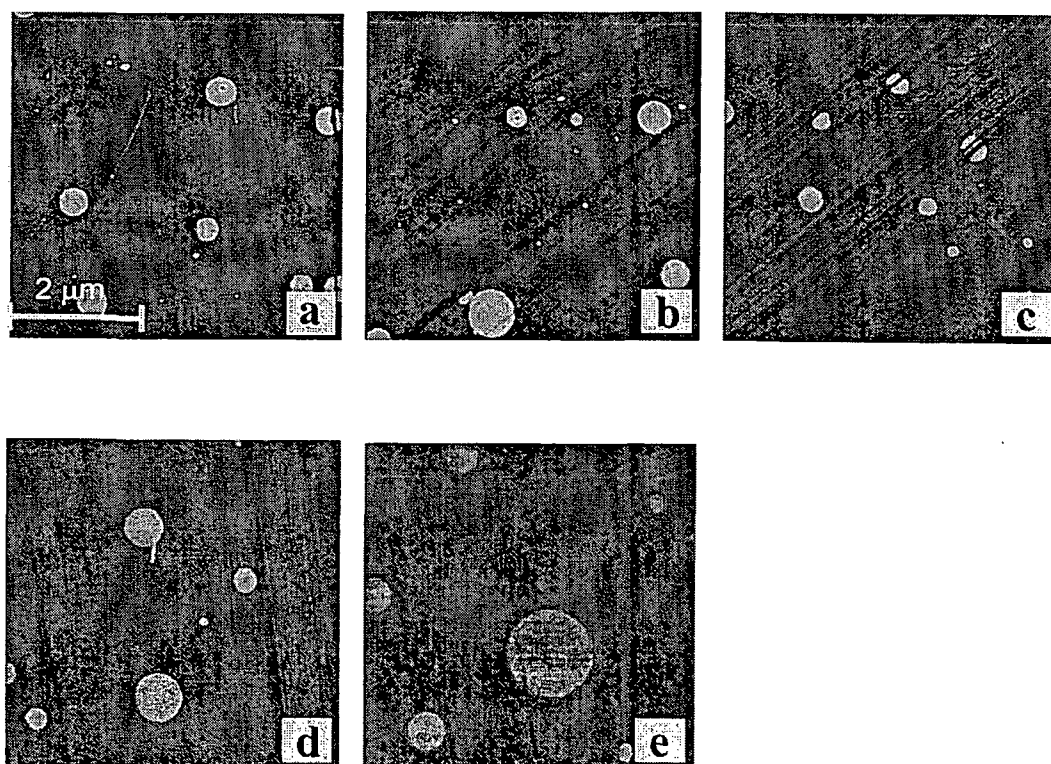


**Figure 32:** AFM images of ODS films on silicon obtained after deactivation with TMCS for 30 minutes. The wafers were deposited into an 1-mmol/L OTS solution for a) 5 min, b) 30 min, c) 60 min, d) 4 hours, and e) 20 hours. Circular islands can be observed in all cases.

Regarding the height of the islands (shown in Figure 33), a decreasing height contrast from 2.2 to 1.8, 1.3, 0.7, and 0.3 nm can be observed. This further supports an exchange reaction of the small TMCS molecule by OTS. The fact that further island growth is not observed could be explained by local replacement of individual TMCS molecules. Thus, the OTS molecules are not able to align to each other by Van der Waals interactions leading to disordered films in that region.

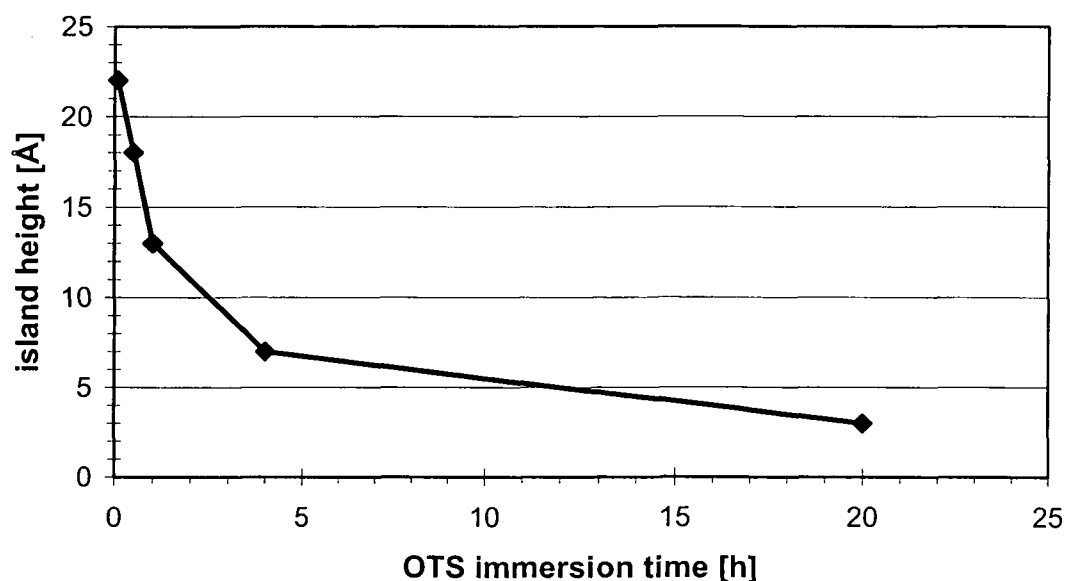


**Figure 33:** Height of ODS islands versus immersion time of the wafers shown in Figure 32. The wafers were immersed for 5, 30, 60, and 240 minutes after a deactivation period of 30 min in a 5-mmol/L TMCS solution.

In order to obtain information on the state of ordering of the adsorbed OTS molecules, infrared spectra of the deposited monolayers were recorded. The figures 35-38 show the CH-stretch region of IR spectra for four different states of order. In the case of a densely packed and ordered ODS film (Figure 34), obtained after an immersion time of 30 minutes in a 1-mmol/L OTS solution, two bands are visible, corresponding to the symmetric methylene stretch  $\nu_s$  ( $\text{CH}_2$ ), at about  $2850\text{ cm}^{-1}$  and the asymmetric methylene stretch  $\nu_{as}$  ( $\text{CH}_2$ ), at about  $2920\text{ cm}^{-1}$ . At about  $2966\text{ cm}^{-1}$  a small down pointing band for the terminal methyl group can be seen. The spectrum of Figure 35 shows the result for a disordered ODS film. The corresponding sample was prepared by OTS deposition above the critical temperature  $T_C^{47,35,91}$  for ordered self-assembly. The film thickness obtained by ellipsometry was  $1,3 \pm 0,1\text{ nm}$ . Broad, down pointing absorption bands at about  $2860\text{ cm}^{-1}$  ( $\nu_s$  ( $\text{CH}_2$ )) and  $2930\text{ cm}^{-1}$  ( $\nu_{as}$  ( $\text{CH}_2$ )) are visible. The inversion of the absorption bands and the shift towards slightly

higher wavenumbers can be used for a very sensitive detection of structural order-disorder transitions, e.g. caused by a change in the surface coverage. A detailed explanation for this band inversion can be found elsewhere<sup>52,92</sup>.

The spectra shown in Figure 36 and Figure 37 correspond to wafers, which were deactivated with TMCS for 30 min. After deactivation they were immersed into an OTS solution for 4 hours and 20 hours, respectively. The spectra represent a linear combination of the spectra shown in Figure 34 and Figure 35 indicating that both densely packed, highly ordered regions and disordered areas are present on these samples. The spectra shown in Figure 36 and Figure 37 differ only in the relative intensity ratios of the absorption bands indicating an increase of the portion of the disordered film, which is also confirmed by the ellipsometric data. The film thickness was measured to be about  $1,9 \pm 0,1$  nm for the sample presented in Figure 36 and  $2,3 \pm 0,1$  nm for the sample in Figure 37, respectively. Since the portion of the ordered areas is constant, this increase in layer thickness must be attributed to the disordered fraction of the film.

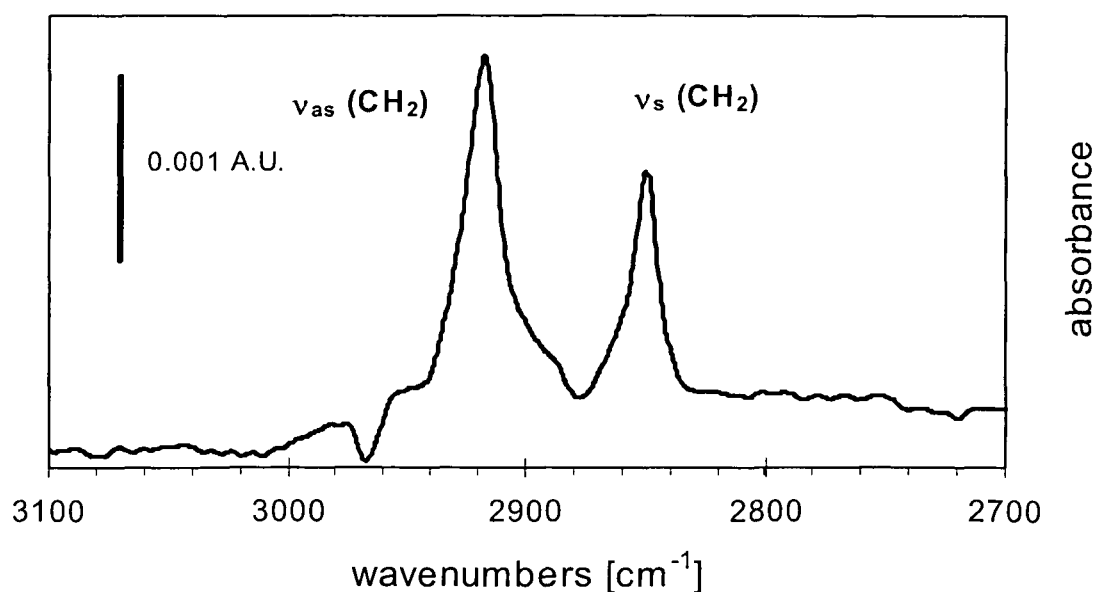


**Figure 34:** IR spectrum (region of CH-strech vibrations) of highly ordered ODS film.

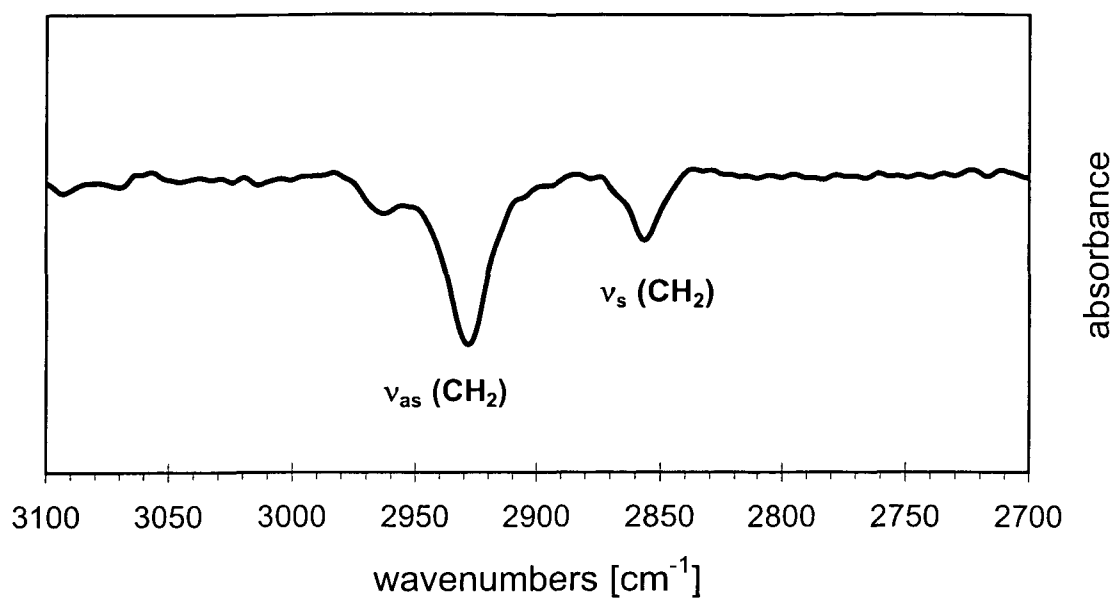


**Figure 35:** IR spectrum (region of CH-strech vibrations) of disordered ODS film grown at a temperature above  $T_C$ .

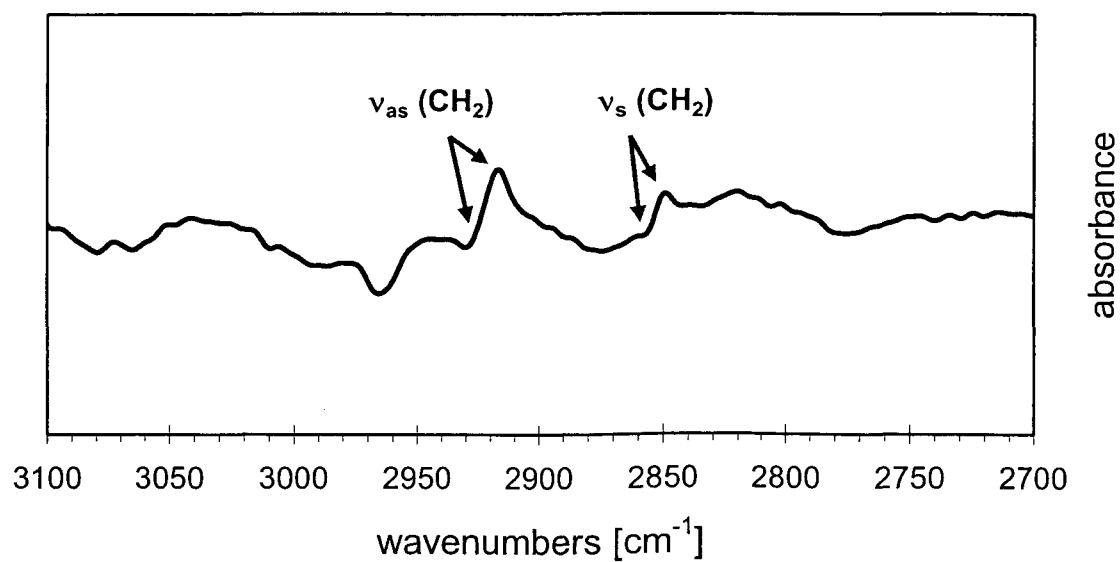


**Figure 36:** IR spectra of a film consisting of ordered and disordered regions => "hybrid" spectrum of Figure 34 and Figure 35 showing more ordered than disordered portions.



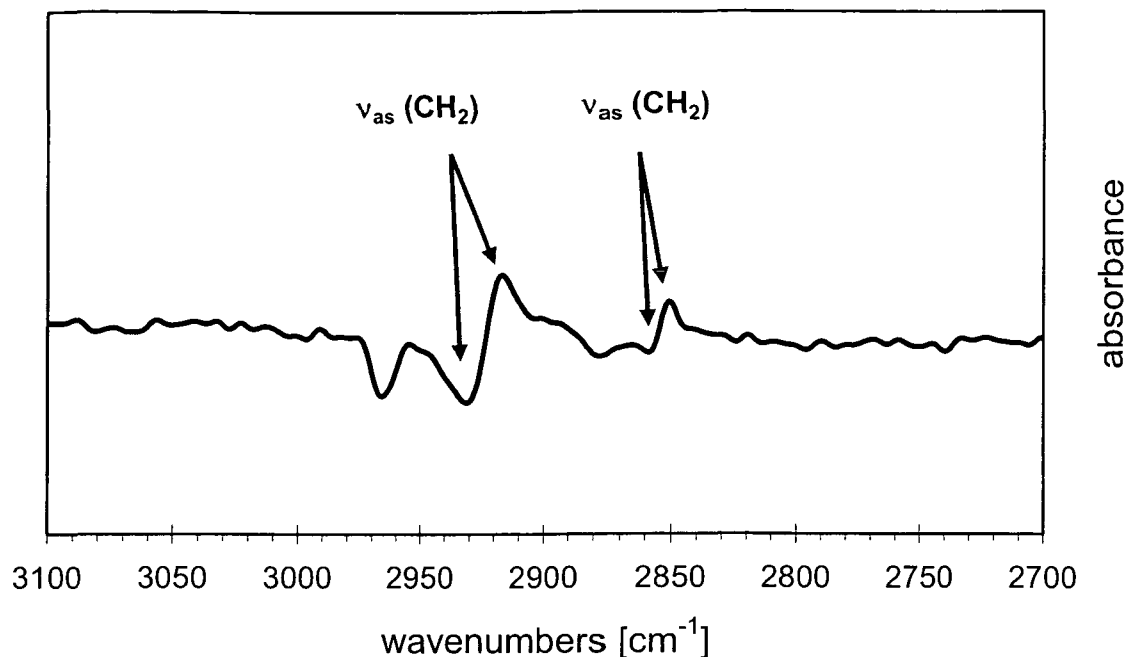


**Figure 37:** IR spectrum of a film consisting of ordered and disordered regions => "hybrid" spectrum of Figure 34 and Figure 35 showing almost equal parts of ordered and disordered contribution.

Considering the described results, a few aspects require further discussion. Surprisingly, the initial number of islands does not increase on the deactivated silicon surfaces during adsorption for a prolonged period of time. From that it could be concluded that adsorption of islands only takes place at preferred adsorption sites with a higher concentration of free silanol groups. A similar behavior is also known for defect distributions on adsorbing surfaces: the higher the local defect concentration, the more preferred an adsorption site would be. Furthermore, the size of the islands does not change significantly with increasing adsorption time. From that it can be concluded that particularly reactive groups at the border of the ordered regions are blocked. An explanation for such a blocking of reactive groups at the border of the ordered islands is shown in Figure 38. The OTS molecules are adjacent to TMCS molecules for a long time, thus TMCS can react with an island-terminating OTS molecule blocking its last freely available OH-group. Therefore, such terminal OTS molecules are no longer preferred sites for adsorption and island growth is stopped as observed by AFM.

In order to further confirm the exchange mechanism proposed in this thesis, an additional experiment with lower TMCS concentration and shorter deactivation time has been performed. Under these conditions the number of reactive sites should be higher and the



Increasing the adsorption time of OTS leads to a decrease of the height contrast of the islands. After 10 min only the outlines of the islands can be observed, whereas after 60 min the islands disappear completely and a closed monolayer film can be observed, which is also confirmed by the ellipsometric film thickness of  $2,6 \pm 0,1$  nm. This behavior can be explained by a decreased number of blocked silanol groups. This in turn increases the probability for adjacent OTS molecules to directly interact with each other via Van der Waals forces leading to a highly ordered film.

### *Conclusion*

The blockage of surface hydroxyl groups by a short chain molecule like TMCS opens up the opportunity to contribute to the study of the mechanism of alkylsiloxane self-assembly processes on silicon surfaces. We found that the growth behavior of self-assembled monolayers of alkylsiloxanes changes dramatically by a stepwise deactivation of active sites (surface OH-groups). Decreasing the number of binding groups results in a decrease in size and number of the islands. The island shape changes from fractal to a nearly circular geometry. Furthermore, it can be concluded that the size of the islands is influenced by the contiguity of the water film which in turn can be controlled through hydrophobization with TMCS. We found that the deactivation is reversible which can be explained by an exchange reaction, where OTS molecules replace the covalently bonded TMCS in the presence of water. In the case of longer deactivation times the monolayer consists of two different ODS regions with different state of order: ordered islands which are formed rather quickly in the beginning of the adsorption experiment and disordered regions formed during a comparatively slow exchange reaction.

### 6.3.3 TMCS hydrophobization of silicon substrates partially covered with ODS islands

In order to further support the proposed island termination reaction, a deactivation experiment using a substrate already covered with ODS islands (about 50 % coverage) has been performed. In this experiment the remaining active areas between the ODS islands were deactivated by immersion in 5 mmol/L-TMCS solution for 30 s. Then exposure to an OTS solution has been continued. Figure 40 shows that further island growth cannot be observed. However, the ellipsometric data clearly show an increase of the layer thickness after a prolonged period of time (Figure 41). Furthermore, the height contrast of the initial ODS island slightly decreases. This indicates again an exchange of TMCS by OTS as already discussed in the previous chapter. Moreover, it can be seen that blockage of further island growth can also be achieved for fractal ODS islands deposited on the active silicon surface prior to the deactivation step. A similar behaviour has also been found for prolonged exposure of the deactivated substrate in DTS as shown in Figure 42 and Figure 43.

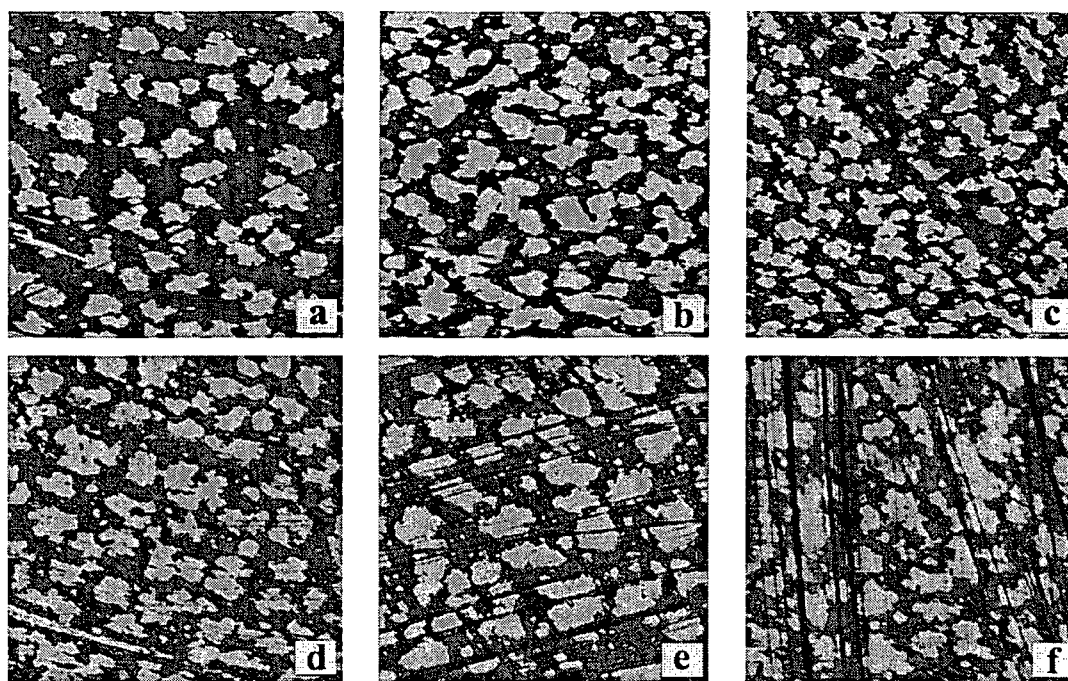


*Figure 40: AFM images of adsorption experiment consisting of three steps. i) Deposition of ODS (~50 % coverage), ii) Deactivation in 5 mmol/L TMCS for 30 min. iii) Immersion in a 1 mmol/L-OTS solution for a) 0, b) 5, c) 10, d) 30, e) 60, and f) 240 min.*

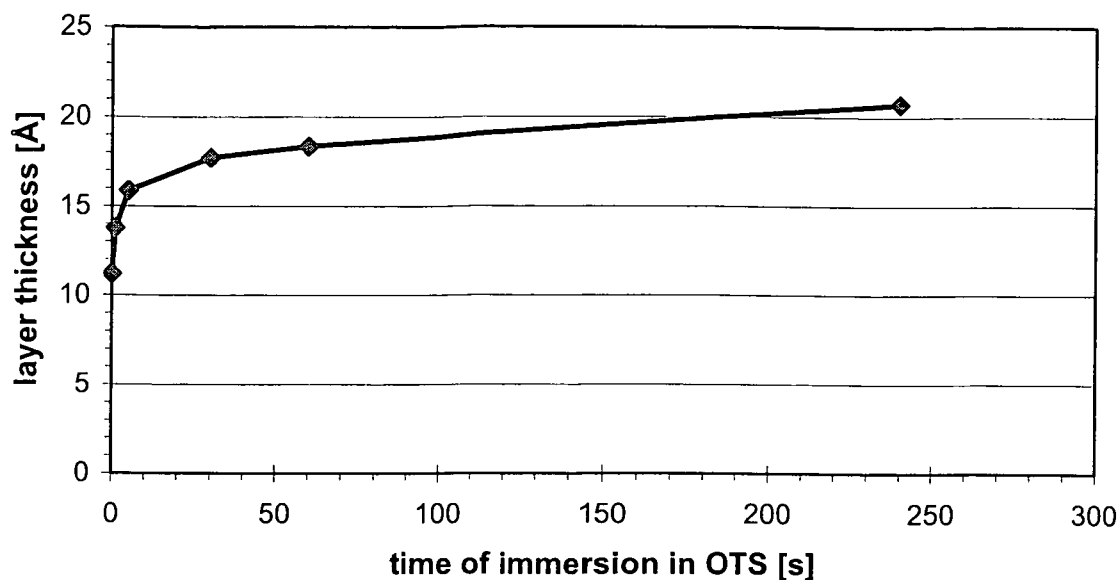


**Figure 41:** Ellipsometric layer thickness of ODS films on silicon (previously covered with ODS islands and deactivated with 5 mmol/L TMCS for 30 min) versus immersion time of the wafers in a 1 mmol/L OTS solution. The wafers were immersed for 5, 10, 30, 60, and 240 minutes.

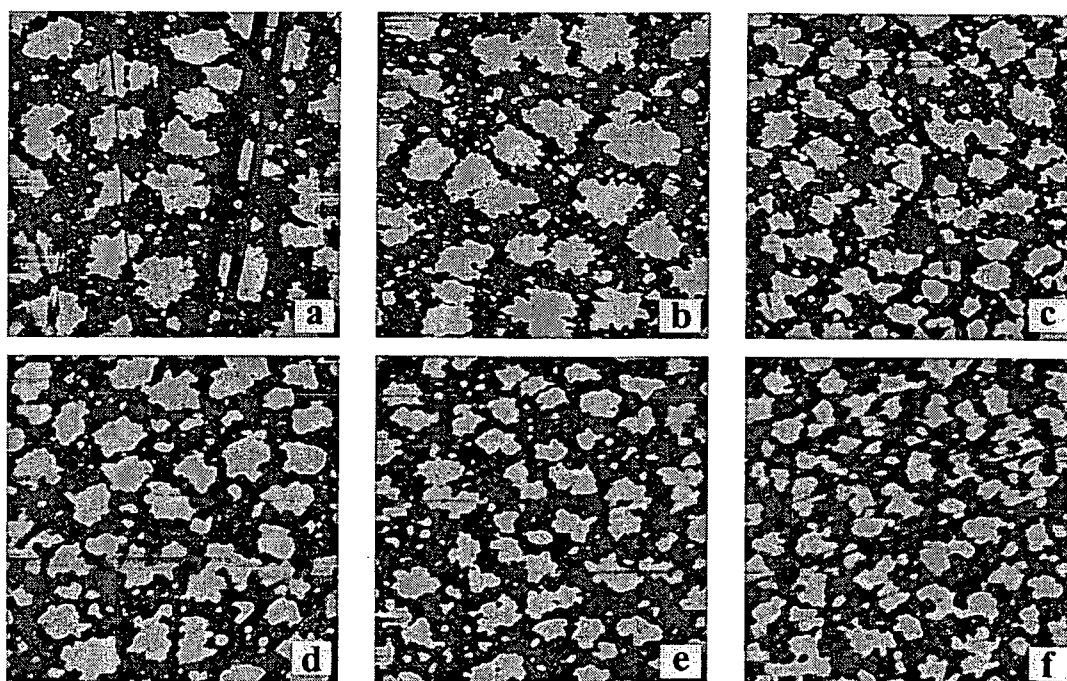


**Figure 42:** AFM images of adsorption experiment consisting of three steps. i) Deposition of ODS (~50 % coverage), ii) Deactivation in 5 mmol/L TMCS for 30 min. iii) Immersion in a 1 mmol/L-DTS solution for a) 0, b) 5, c) 10, d) 30, e) 60, and f) 240 min.

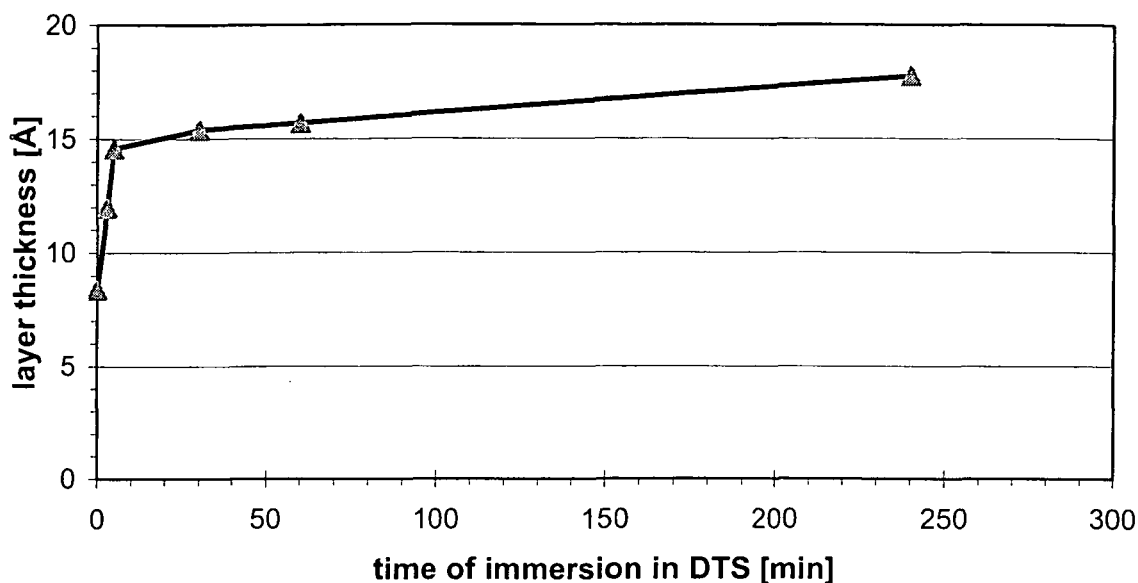


*Figure 43: Ellipsometric layer thickness of DTS films on silicon (previously covered with ODS islands and deactivated with 5 mmol/L TMCS for 30 min) versus immersion time of the wafers in a 1 mmol/L DTS solution. The wafers were immersed for 5, 10, 30, 60, and 240 minutes.*

#### 6.3.4 Simultaneous adsorption of TMCS and OTS

In addition to the experiments described in chapter 6.3.2 and 6.3.3 also simultaneous deposition of OTS and TMCS from one solution has been investigated. Figure 44 shows the growth behavior of the respective films for different mixing ratios between OTS and TMCS. It can be observed that the adsorption rate significantly decreases with increasing portions of TMCS which is particularly apparent within the first 300 s of adsorption. It is interesting to note, however, that in all cases a layer thickness of about 2,5 nm corresponding to a full monolayer of ODS can be achieved after 10 min.

This clearly shows that adsorption of OTS is preferred compared to TMCS. Furthermore, it should be mentioned that growth in case of simultaneous adsorption is much faster than on previously deactivated substrates. These results are a further argument for the exchange mechanisms described in the previous chapters.

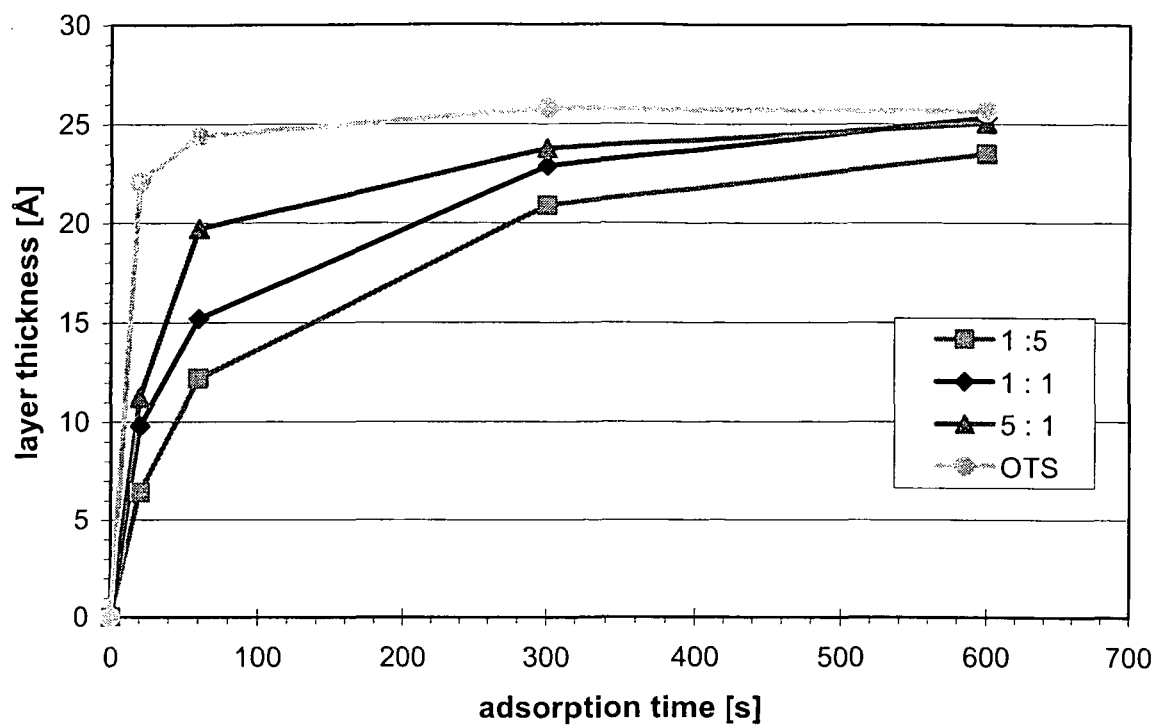


**Figure 44:** Ellipsometric layer thickness of ODS films on silicon versus immersion time of the wafers into mixtures of TMCS and OTS. The presence of TMCS decreases the growth rate in all cases. Surprisingly, the final film thickness achieved after ten minutes is  $2,5 \pm 0,1$  nm for all mixing ratios.

## 6.4 Adsorption of TSHME

The adsorption behavior of TSHME was investigated in order to obtain information about the influence of the terminal group on the growth of ester monolayers and in order to shed light on the growth mechanism of mixed monolayers of alkyltrichlorosilanes. A further motivation was the attempt to achieve nanostructured surfaces by the build-up of multilayer systems.

### 6.4.1 Adsorption of pure TSHME

The growth behavior of TSHME on silicon was studied and compared to the results obtained with OTS. These experiments were performed at  $15 \pm 1$  °C with a TSHME concentration of 1 mmol/L. The water content of the solvent was  $12 \pm 0,5$  mmol/L. Figure 45 shows that the growth rate of OTS is significantly higher than for TSHME. This leads to a deviation in layer thickness of about 0,5 nm within the first minute. After 5 min the TSHME monolayer reaches the same thickness as obtained for OTS. In fact similar layer thicknesses can be expected due to the almost identical chain length of the two molecules. However, given the fact that ellipsometric data rather reflect the density of films (see chapter 5.2) this surprisingly suggests that the packing density in both films is the same. Thus, it seems that the different terminal group does not have a pronounced influence on the degree of order in the monolayer. The corresponding AFM images are shown in Figure 46. It can be seen that under the given conditions island growth takes place as it is the case for ODS layers. The strong contamination and the bad image quality observed for longer adsorption times (Figure 46d) is due to a bad quality of the TSHME precursor. The bad quality has been caused by extended storage of the compound for several months leading to a gradual degradation due to polymerization of this water-sensitive molecule.



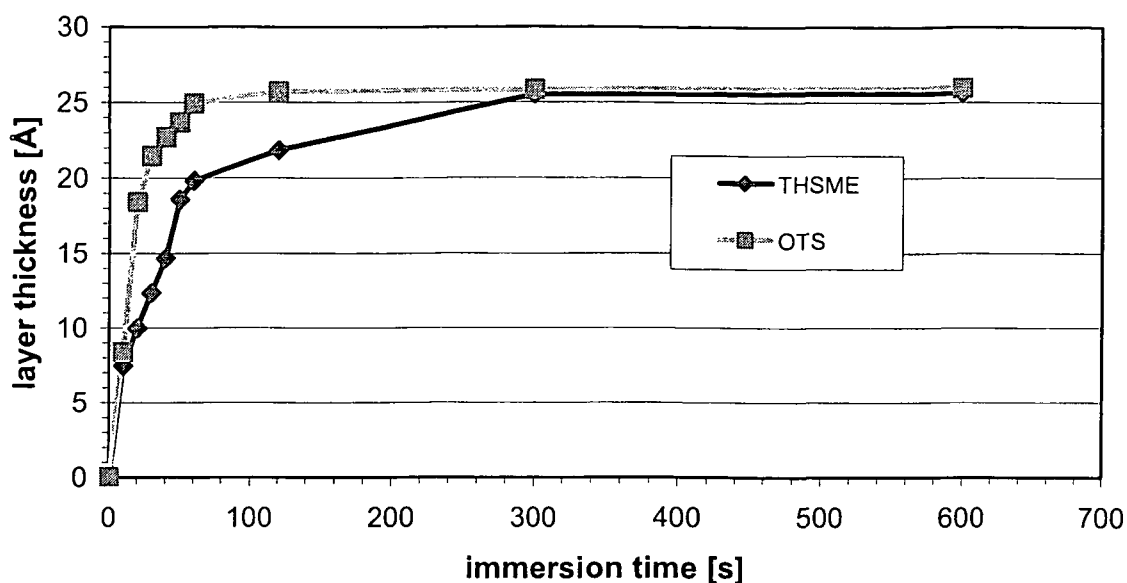


**Figure 45:** Comparison of ellipsometric layer thicknesses of ODS and TSHME films. The water content of the solvent was 12 mmol/L and the deposition temperature was 15 °C. Surprisingly, the final film thickness achieved after ten minutes is  $2,55 \pm 0,1\text{nm}$  for both compounds.

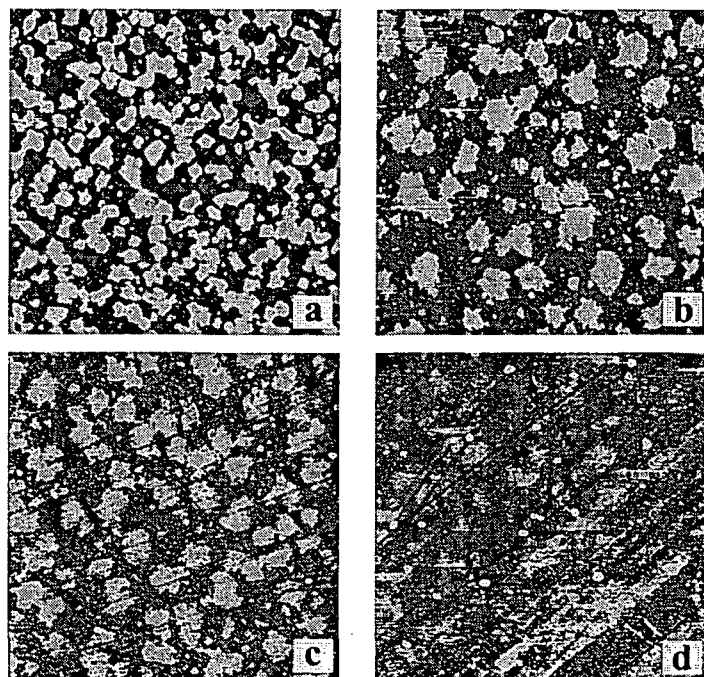


**Figure 46:** AFM images of TSHME films on silicon. The adsorption times were a) 20, b) 40, c) 60, and d) 120 s. Island growth can be observed and full monolayer coverage is achieved within 5 minutes (not shown). The bad quality of d) is due to degradation of the TSHME upon extended storage times for several months.

In order to shed more light on the unexpectedly high layer density of the TSHME films, ATR-IR measurements were performed. In Figure 47 IR spectra of an ODS monolayer and a TSHME film are compared. The main difference is the carboxylic band observed at  $1743\text{ cm}^{-1}$ , which is characteristic for an ester. In the region of the CH-stretch vibrations a significant difference cannot be observed, though the peaks of the ester are slightly shifted ( $\sim 2\text{ cm}^{-1}$ ) towards higher wavenumbers. By peak integration of the  $\text{CH}_2$ -stretch bands the packing density of the two films was calculated. The density of the TSHME film was about 80 % of the density obtained for the ODS monolayer, as expected. However, the discrepancy to ellipsometric data (see above) is not clear yet.

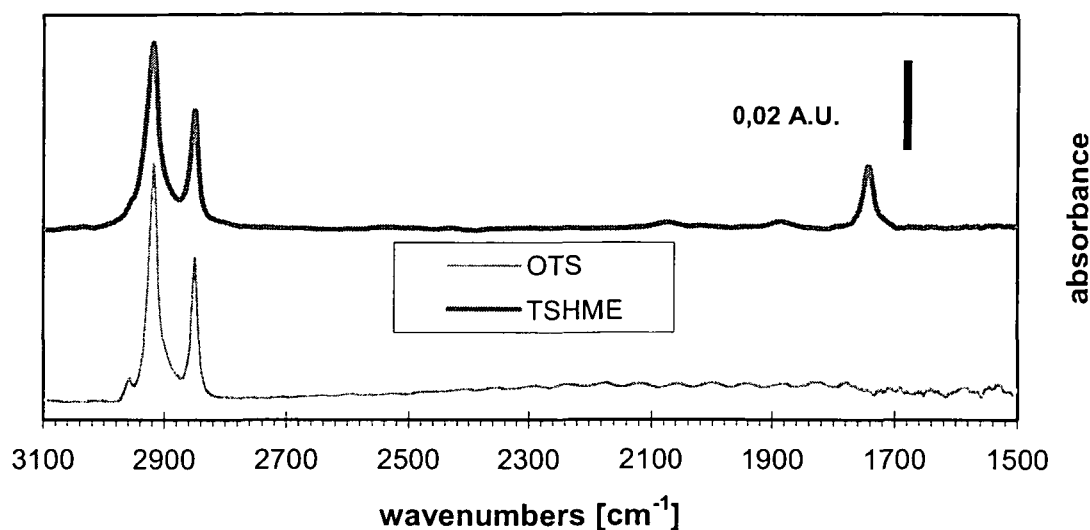


**Figure 47:** Comparison of ATR-IR spectra obtained from complete monolayers of ODS and TSHME. A slight shift ( $\sim 2\text{ cm}^{-1}$ ) of the  $\text{CH}_2$ -stretch vibrations towards higher wavenumbers was observed for the TSHME.

For the sake of completeness deactivation experiments were also performed with TSHME. Deactivation of the silicon oxide surface with TMCS led to a dramatical decrease of the subsequent TSHME adsorption as already reported for OTS (see chapter 6.3.2). Figure 48 shows the effect of deactivation in TMCS for immersion times from 0 up to 10 minutes. The immersion time in TSHME was 20 s in all cases. The surface coverage decreases from about  $1,9 \pm 0,1\text{ nm}$  to around  $0,8 \pm 0,1\text{ nm}$  for a deactivation time of only 40 s. A sharp decrease in adsorption within one minute of deactivation can clearly be seen. Then the layer thickness slowly decreases until a practically constant value is reached after 5 min. The layer thickness after 5 minutes of deactivation, followed by depositing the wafer into a 1-mmol/L TSHME solution for 20 s, is in the same range as observed for OTS.

The corresponding AFM images show circular islands already after a deactivation period of 40 s. A further increase of the deactivation time leads to a decrease in number of the islands until only a few larger islands are observed. Between these few large island (e.g. only two in the upper right of Figure 49b) a great number of smaller bright dots can be observed corresponding to contamination by polymerized TSHME aggregates.

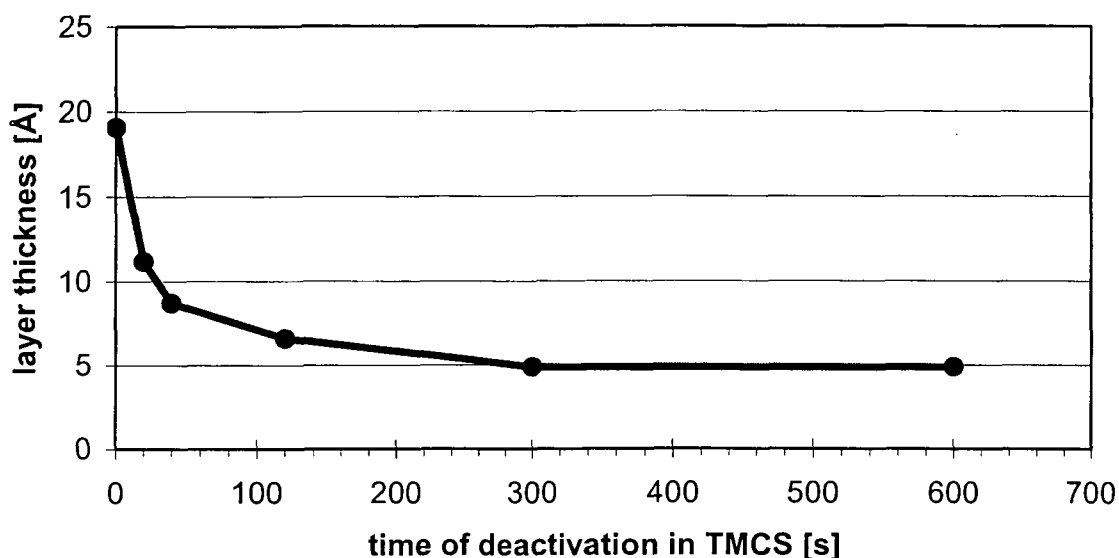


**Figure 48:** Layer thickness of TSHME layers versus deactivation time of the silicon substrate in TMCS. The adsorption time for TSHME was 20 s in all cases. A dramatic decrease of the coverage can be observed even for short deactivation times.

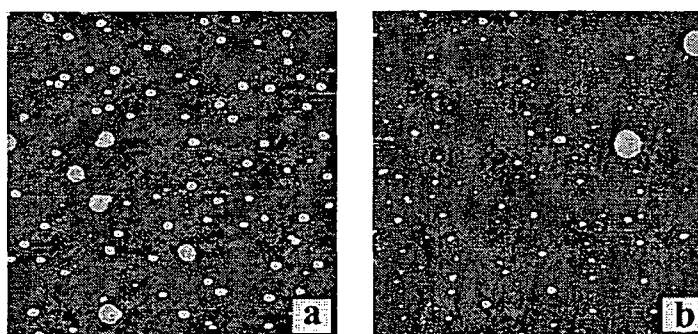


**Figure 49:** AFM images of TSHME films on silicon modified through increasing deactivation times of a) 40 and b) 120 s in TMCS ( $c = 5 \text{ mmol/L}$ ). The films were deposited through immersion in TSHME ( $c = 1 \text{ mmol/L}$ ) for 20 s. Circular islands appear after about 40 s of deactivation in TMCS.

The results shown in this chapter indicate that, apart from the lower packing density, the adsorption of TSHME is similar to that of OTS.

#### 6.4.2 Mixed films of ODS and TSHME

In addition to the experiments with single component monolayers, further experiments for fabrication of mixed films were performed. In a first experiment OTS was deposited onto silicon wafers up to a surface coverage of about 50 % by immersion into a 1 mmol/L OTS solution for 20 s. Subsequently, TSHME was adsorbed in order to fill up the remaining space between the ODS islands. Full monolayer coverage was reached within 5 minutes. The corresponding AFM images are shown in Figure 50. The height image (Figure 50a) does not show a pronounced contrast between the two regions. In Figure 50b the corresponding phase image is shown. Size and shape of the initial ODS islands are clearly visible.

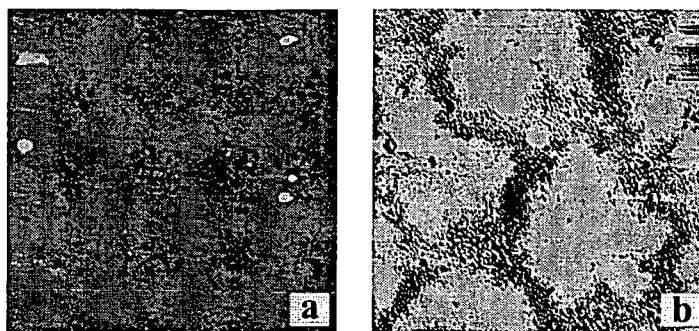


**Figure 50:** AFM images of mixed monolayers on silicon. The films were deposited through immersion in OTS ( $c = 1 \text{ mmol/L}$ ) for 20 s and subsequent deposition of TSHME ( $c = 1 \text{ mmol/L}$ ). **a)** height image, **b)** phase image.

In the next experiment the films were deposited by simultaneous deposition of OTS and TSHME from one solution. The concentration of both components was 1 mmol/L. The deposition solution was matured for 10 minutes with both components. Full monolayer coverage was reached within 5 minutes. Figure 51 shows AFM results for an adsorption time of 5 minutes. The size of the ODS islands is significantly smaller than for single component adsorption (see Figure 50). The material deposited between the islands seems to grow in a disordered manner. Thus, a significant height contrast is observed in Figure 51a, suggesting partial random mixing of the two components in these regions.

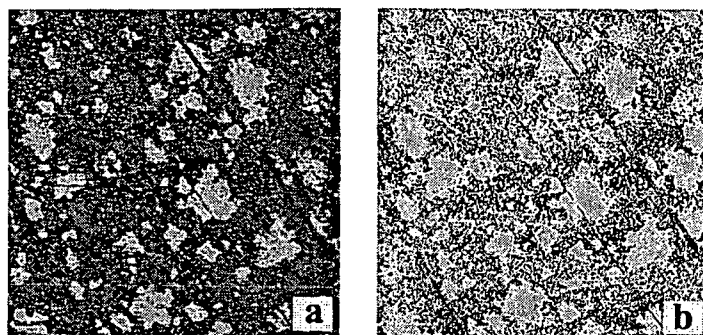


**Figure 51:** AFM images of mixed monolayers on silicon. The films were deposited through immersion in solution containing both OTS ( $c = 1 \text{ mmol/L}$ ) and TSHME ( $c = 1 \text{ mmol/L}$ ) and matured for 10 min. *a)* height image, *b)* phase image.

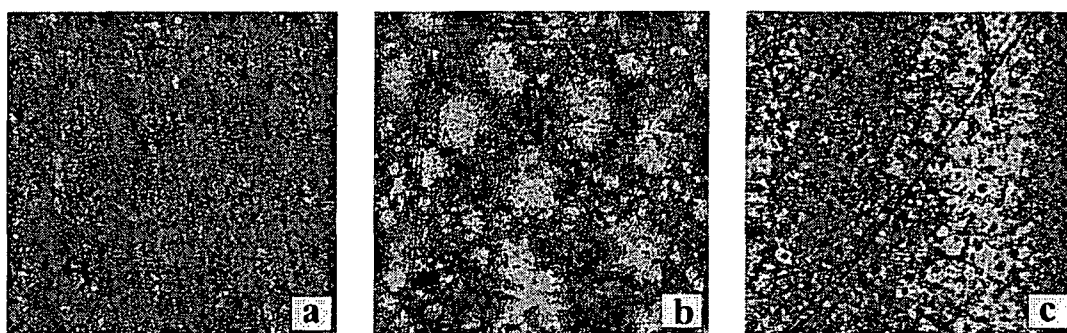


**Figure 52:** AFM images of mixed monolayers on silicon. The films were deposited through immersion in a freshly produced mixture of two separately matured solutions containing OTS ( $c = 1 \text{ mmol/L}$ ) and TSHME ( $c = 1 \text{ mmol/L}$ ). *a)* height image, *b)* phase image. The island sizes are slightly increased compared to the images of separately matured solutions. *c)* Image obtained by adsorption of one additional ODS layer after reduction of the ester group.

The last experiment was performed by immersing silicon wafers into a freshly prepared mixture of separately matured solutions of OTS and TSHME, respectively. The island size observed in Figure 52a is between the observed values for the other two experiments. As discussed in the introduction, OTS forms micelles in solution under the given conditions. Therefore, in the case of subsequent deposition of OTS and TSHME the island size is solely determined by undisturbed aggregation of OTS in solution. In the case of simultaneous maturation, TSHME molecules may inhibit the formation of larger aggregates in solution leading to smaller islands and random mixing in the regions between the islands. In the third case (separately matured solution freshly mixed prior to adsorption) the islands seem to be less densely packed and to exhibit a broad size distribution. This may be a result of the short homogenization time leading to both random mixing of individual molecules and smaller aggregates but also existence of larger undisturbed aggregates formed during maturation before mixing of the two precursor solutions. In order to obtain additional information on the state of mixing in these films a second layer of ODS has been deposited

after reduction of the ester groups. Pronounced islands of ODS cannot be observed on that sample (Figure 52c) indicating that the different terminal groups in the first layer are not present in a phase-separated manner. Thus, it can be concluded that the two components have largely mixed up in the precursor solution.

The described experiments indicate that the observed phase separation of OTS and TSHME for depositions from mixed solutions is caused by selective prearrangement of the precursor molecules in the solution.

### 6.4.3 Nanostructured surfaces

The formation of nanostructures is of great interest and provides the possibility for surface engineering on a molecular level. Thus, the know how on SAM growth achieved in this thesis has been applied for that purpose. In a first step OTS was deposited onto silicon wafers up to a surface coverage of about 50 % by immersion into a 1 mmol/L OTS solution for 20 s. Subsequently, TSHME was adsorbed to fill up the remaining space between the ODS islands. Full monolayer coverage was reached within 5 minutes. Afterwards, the ester was reduced in order to produce hydroxyl groups on the surface necessary for subsequent chemisorption of a further layer. Reduction was performed in a 0.1 mol/L solution of  $\text{LiAlH}_4$  in absolute toluene for 15 minutes, according to the procedure described in chapter 4.3.3. Multilayers can be produced by repeated adsorption and reduction cycles. Alternatively, growth can be stopped by a terminal layer of ODS on top of the ester regions. Figure 53 shows a series of AFM images for one, two, and three adsorption/ reduction cycles. The height contrast constantly increases with increasing number of deposition cycles with 1,4 nm per cycle. This corresponds to a surface fraction of about 65 % of the growing islands. This is somewhat higher than the coverage suggested by the initial coverage of ODS islands (~50 %). This could be explained by a slight “overgrowth” of the ODS islands in each cycle. In fact the  $5 \times 5\text{-}\mu\text{m}^2$  images (Figure 53d and e) suggest that such an “overgrowth” actually occurs.

Since it was not the primary goal of this thesis, this concept for nanostructuring has not been further pursued.

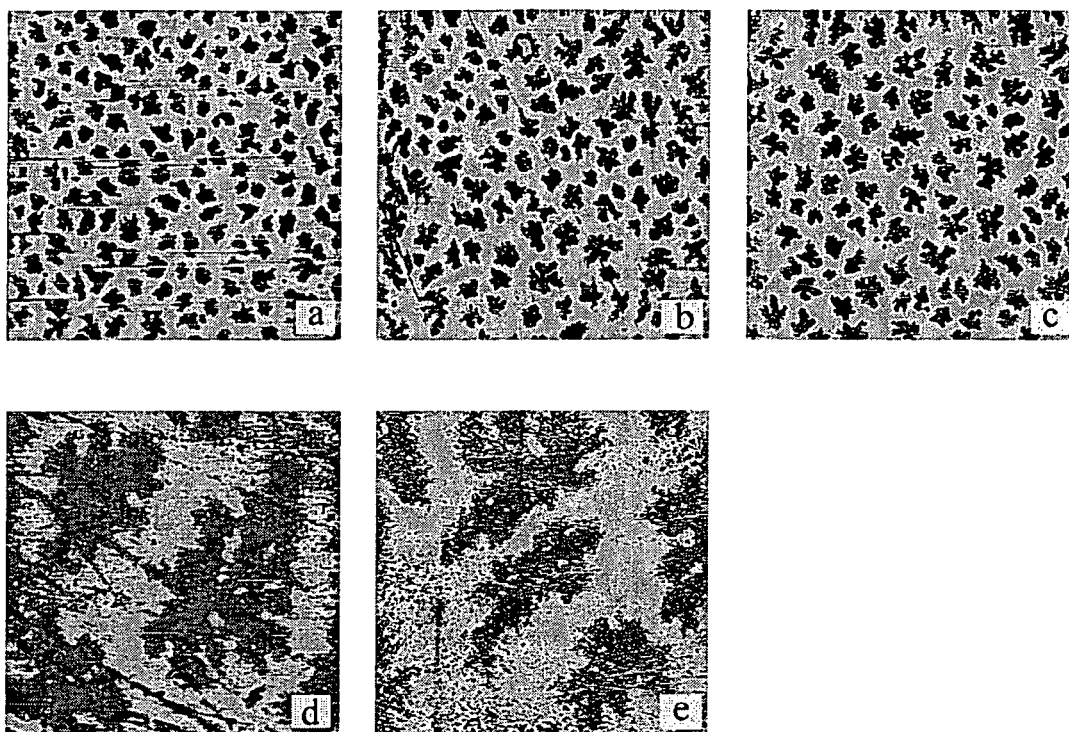


**Figure 53:** AFM images of nanostructured surfaces. The films were deposited through immersion in OTS ( $c = 1 \text{ mmol/L}$ ) for 20 s and subsequent deposition of TSHME ( $c = 1 \text{ mmol/L}$ ). Afterwards the ester was reduced as described in detail in chapter 4.3.3. Multiple layers in the TSHME region were produced by repeated reduction-adsorption cycles. **a, d)** one additional layer of ODS, **b, e)** one additional layer of TSHME and ODS, and **c)** two additional layers of TSHME and one layer of ODS. Image sizes: **a-c)**  $25 \times 25 \text{ } \mu\text{m}^2$ , **d, e)**  $5 \times 5 \text{ } \mu\text{m}^2$

## 7 Conclusion

The growth of self-assembled monolayers of alkylsiloxanes strongly depends on various deposition parameters. Therefore, an accurate control of these parameters is of outstanding importance for fabrication of thin films in a reproducible manner. Since the end of the 1980s several groups have investigated organosilane film formation on silicon. Most of them have focussed only on one or two adsorption parameters neglecting or even disregarding the existence of further influencing factors. In this work, it has been tried to study individual parameters while keeping several other parameters like water content of the solvent and deposition temperature constant.

The first parameter under investigation was the precursor concentration. A strong increase of the adsorption kinetics with increasing precursor concentration has been observed as expected. Moreover, experiments with highly concentrated solutions and alkylsilanes of different chain lengths opened up new insights into the ordering process in the precursor solution. The results have shown that the maturation time of the deposition solutions governs the concentration of preordered species (micelles or vesicles) in the solution. This in turn influences both adsorption kinetics and the degree of order in the obtained films. It is very interesting to note that a higher degree of order in the solution not only leads to higher film quality but also faster adsorption. Substantial film growth from freshly prepared "disordered solutions" can only be achieved, if precursor concentrations 1 to 2 orders of magnitude higher than usual concentrations for SAM formation are used. In view of these results it appears that the conditions in solution seem to be of superior importance compared to e.g. surface diffusion phenomena as mostly assumed in literature.

A further surprising result was the fact that a larger chain length of the precursor molecule requires a longer maturation time in order to achieve reasonable growth rates of flat ordered films. At the first glance this seems to be in contradiction with the known fact that longer chain lengths favour a higher degree of order due to Van der Waals stabilization between the individual molecules. Obviously, a dominance of a kinetic effect instead of a thermodynamical one is observed. Ordering of shorter molecules in solution proceeds at a higher pace even though the degree of order in the final state may be lower for thermodynamical reasons.

Certainly, also processes on the substrate surface are of high importance. This aspect has been addressed by experiments with chemically modified substrates. Short chain



molecules like TMCS open up the opportunity to control the number of freely accessible surface hydroxyl groups on silicon. In this way the number of active sites for subsequent chemisorption of OTS can be changed. Decreasing the number of these active sites leads to a dramatic decrease in the growth rate and the surface coverage. Furthermore, a lower number of active sites increases the mobility of the film molecules supporting reorganization processes on the surface which lead to thermodynamically favourable morphology of sub-monolayer structures, i.e. islands with nearly spherical shape and smooth edges.

At the same time blockage of active hydroxyl groups with TMCS leads to a hydrophobization of the substrate. As a consequence the contiguity of the adsorbed water film is disturbed. Since the presence of water on the surface is essential for migration of alkylsiloxanes<sup>90</sup>, long range transport of siloxane molecules across the surface is hindered on hydrophobic substrates. Thus, diffusion-supported island growth is largely limited which was actually observed in our experiments. These results are also consistent with the growth behaviour of alkylsiloxanes on mica<sup>46</sup>. Also in the case of mica the low number of active hydroxyl groups, and thus the high mobility of the film molecules, leads to formation of sub-monolayer structures with smooth edges. However, in contrast to hydrophobized silicon, mica is hydrophilic supporting long range transport of organic molecules. This is in fact observed as sub-monolayer islands on mica grow quickly and coalesce until a full monolayer film is formed.

A further aspect of island growth is the stable attachment of precursor molecules arriving at the edges of already existing islands. Island growth may also be hindered, if active OH-groups at the perimeter of the islands, which are necessary for chemical attachment of the approaching molecules, are blocked through reaction with TMCS. This is an indication that also crosslinking between the film molecules plays an important role in the growth of alkylsiloxane films.

Summarizing, it can be concluded that ordering processes taking place in solution are of dominating importance in the beginning of SAM adsorption. At this early stage large preordered species adsorb onto the surface right away leading to comparatively high surface coverages within a short period of time. Once space or active binding sites for such large preordered species in solution are not available anymore, further growth can only proceed through adsorption of smaller oligomers or individual molecules. Then, aspects of surface reactivity and surface diffusion are becoming dominant.

Although substantial insight into the growth mechanism of alkylsiloxane monolayers could be achieved in this thesis, the investigation of these systems will still remain an

interesting field of research. For instance, the influence of the terminal group in the alkyl chain has been only shortly tackled in this thesis. For ester-terminated precursors (TSHME) in principle a similar growth at a lower pace has been found. Implementation of infrared spectroscopy revealed a lower packing density in the corresponding films as expected. It has also been shown that simultaneous adsorption of two different precursors (OTS and TSHME) offers an exciting opportunity to study mutual influences on ordering in solution, phase separation phenomena, and competitive reactions and processes on the substrate surface. As already mentioned, these phenomena have only been shortly addressed at the end of this thesis and they require further investigation in future work.

Finally, it should be mentioned that apart from the aspects described in this thesis also further parameters as the water content of the deposition solution and the temperature, as well as their complex interplay are still a highly interesting field of research for the future.

## 8 Index of Figures

<b>Figure 1:</b> Langmuir-Blodgett transfer of amphiphilic molecules from a liquid/gaseous interface to a solid substrate .....	9
<b>Figure 2:</b> Various self-assembled structures of phospholipids for dimyristoyl phosphatidyl choline, DMPC .....	10
<b>Figure 3:</b> Scheme of self-assembly process .....	11
<b>Figure 4:</b> Scheme of tapping mode atomic force microscopy.....	22
<b>Figure 5:</b> Scheme of rotating angle ellipsometer <sup>15</sup> .....	23
<b>Figure 6:</b> Scheme of “glass tube experiment” .....	27
<b>Figure 7:</b> Scheme of temperature control unit with numbered positions for the reaction vessels.....	29
<b>Figure 8:</b> Photo of temperature control unit.....	30
<b>Figure 9:</b> Temperature versus time for positions 1-10 of the aluminum block. At I and II the set point temperature has been switched from 25 °C to 20 °C and from 20 °C to 25 °C, respectively. The line denoted with “control” represents the value displayed on the control unit of the instrument. ....	30
<b>Figure 10:</b> Ellipsometric layer thickness of ODS films on silicon versus distance from the drop-in position obtained in the “glass tube experiment” .....	31
<b>Figure 11:</b> AFM images of ODS films obtained in the “glass tube” experiment a) Drop-in position corresponding to region I in Figure 10. b) Closed ODS film observed in region II of Figure 10. The vertical stripes originate from cleaning the wafer with a tissue after the deposition experiment. c) – h) Island formation in region III of Figure 10. ....	33
<b>Figure 12:</b> AFM image of drop-in position after 45 min of oxidation. The size of the image is 5x5 $\mu\text{m}^2$ . The surface does not change qualitatively to the organic film shown in Figure 11 .....	34
<b>Figure 13:</b> UV-oxidation of ODS film found at the drop-in position. For explanation see text.....	34

<b>Figure 14:</b> Results of adsorption- oxidation cycles with UTS and OTS (see text for detail). The increase of the silicon oxide layer agrees well with literature values of 0,3 nm per cycle. ....	35
<b>Figure 15:</b> AFM-images of ODS films on silicon obtained for OTS concentrations of a) 0.5, b) 5, c) 10, d) 20, and e) 50 mmol/L. Both adsorption time and maturation time of the OTS solution was 20 s. ....	37
<b>Figure 16:</b> AFM-images of ODS films on silicon obtained for OTS concentrations of a) 0.5, b) 5, c) 10, d) 20, and e) 50 mmol/L. The maturation time of the OTS solution was 10 minutes. The adsorption time was 20 s.....	37
<b>Figure 17:</b> Layer thickness of alkylsiloxane films on silicon versus length of the alkylchain. The maturation time was 10 minutes (full line) and 20 s (dashed line), respectively. Deposition has been performed from a solution with an OTS concentration of 50 mmol/L. The adsorption time was 20 s in all cases.....	38
<b>Figure 18:</b> AFM images of alkylsiloxane films on silicon with an alkylchain length of a) 10, b) 12, c) 16, and d) 18 carbon atoms. Deposition has been performed for 20 s from a solution with an OTS concentration of 50 mmol/L. The maturation time of the deposition solution was 10 minutes. The stripes originate from cleaning of the wafer with a tissue.....	39
<b>Figure 19:</b> AFM images of alkylsiloxane films on silicon with an alkylchain length of a) 10, b) 12, c) 16, and d) 18 carbon atoms. Deposition has been performed for 20 s from a solution with an OTS concentration of 50 mmol/L. The maturation time of the deposition solution was 20 s. ....	40
<b>Figure 20:</b> Layer thickness of ODS layers versus deactivation time of the silicon substrate in BuTCS. The adsorption time for OTS was 20 s in all cases. After 1 min of deactivation the film thickness corresponds to a full monolayer of BuTCS (see Figure 22). ....	43
<b>Figure 21:</b> Layer thickness of ODS layers versus deactivation time of the silicon substrate in PhTCS. The adsorption time for OTS was 20 s in all cases. A dramatic decrease of the coverage can be observed even for short deactivation times.....	44

<b>Figure 22:</b> Layer thickness of BuTCS on silicon versus adsorption time The dashed line marks the theoretical maximum layer thickness <sup>32</sup> for BuTCS for an all-trans conformation of the chains. ....	45
<b>Figure 23:</b> AFM images of ODS films on silicon modified through increasing deactivation times of a) active, b) 30, and c) 300 s in BuTCS (c= 5 mmol/L). The films were deposited through immersion in OTS (c = 1 mmol/L) for 20 s. ...	45
<b>Figure 24:</b> AFM images obtained after deactivation of the silicon substrate with MTCS. No homogeneous film growth can be observed for a) 30 s, b) 300 s, and c) 600 s. Strong surface roughing due to three dimensional polymerization can be observed. ....	46
<b>Figure 25:</b> Layer thickness of ODS layers versus deactivation time of the silicon substrate in TMCS. The adsorption time for OTS was 20 s in all cases. A dramatic decrease of the coverage can be observed even for short deactivation times. ....	47
<b>Figure 26:</b> Layer thickness of HDS layers versus deactivation time of the silicon substrate in TMCS. The adsorption time for HTS was 20 s in all cases. ....	47
<b>Figure 27:</b> AFM images of ODS films on silicon modified through increasing deactivation times of a) 0, b) 30, c) 60, d) 120, and e) 300 s in TMCS (c = 5 mmol/L). The films were deposited through immersion in OTS (c = 1 mmol/L) for 20 s. Circular islands appear after about 60 s of TMCS deactivation. ....	48
<b>Figure 28:</b> AFM images of HDS films on silicon a) without deactivation, and b) after 120 s of deactivation in TMCS (c = 5 mmol/L). ....	49
<b>Figure 29:</b> Ellipsometric layer thickness of ODS films on silicon versus immersion time in a 1 mmol/L OTS solution. The wafers were immersed for 1, 5, 30, 60, and 240 minutes after a deactivation period of 30 min in a 5 mmol/L TMCS solution. ....	50
<b>Figure 30:</b> Mechanism for migration of chemisorbed siloxanes proposed by Wang et al. <sup>90</sup> ..	51
<b>Figure 31:</b> Proposed mechanism for exchange reaction of TMCS by OTS. ....	52

<b>Figure 32:</b> AFM images of ODS films on silicon obtained after deactivation with TMCS for 30 minutes. The wafers were deposited into an 1-mmol/L OTS solution for a) 5 min, b) 30 min, c) 60 min, d) 4 hours, and e) 20 hours. Circular islands can be observed in all cases. ....	52
<b>Figure 33:</b> Height of ODS islands versus immersion time of the wafers shown in Figure 32. The wafers were immersed for 5, 30, 60, and 240 minutes after a deactivation period of 30 min in a 5-mmol/L TMCS solution.....	53
<b>Figure 34:</b> IR spectrum (region of CH-strech vibrations) of highly ordered ODS film. ....	54
<b>Figure 35:</b> IR spectrum (region of CH-strech vibrations) of disordered ODS film grown at a temperature above $T_C$ . ....	55
<b>Figure 36:</b> IR spectra of a film consisting of ordered and disordered regions => “hybrid” spectrum of Figure 34 and Figure 37 showing more ordered than disordered portions. ....	55
<b>Figure 37:</b> IR spectrum of a film consisting of ordered and disordered regions => “hybrid” spectrum of Figure 34 and Figure 37 showing almost equal parts of ordered and disordered contribution. ....	56
<b>Figure 38:</b> Scheme of proposed island termination mechanism .....	57
<b>Figure 39:</b> AFM images of ODS films on silicon modified through deactivation in 1-mmol/L TMCS solution for 20 s. OTS adsorption times were a) 0, b) 20, c) 60, d) 300, e) 600, and f) 3600 s. Circular islands cannot be observed and full monolayer coverage is achieved after 1 hour.....	57
<b>Figure 40:</b> AFM images of adsorption experiment consisting of three steps. i) Deposition of ODS (~50 % coverage), ii) Deactivation in 5 mmol/L TMCS for 30 min. iii) Immersion in a 1 mmol/L-OTS solution for a) 0, b) 5, c) 10, d) 30, e) 60, and f) 240 min. ....	59
<b>Figure 41:</b> Ellipsometric layer thickness of ODS films on silicon previously covered with ODS islands and deactivated with 5 mmol/L TMCS for 30 min versus immersion time of the wafers in a 1 mmol/L DTS solution. The wafers were immersed for 5, 10, 30, 60, and 240 minutes. ....	60

- Figure 42:** AFM images of adsorption experiment consisting of three steps.  
 i) Deposition of ODS (~50 % coverage), ii) Deactivation in 5 mmol/L TMCS for 30 min. iii) Immersion in a 1 mmol/L-DTS solution for a) 0, b) 5, c) 10, d) 30, e) 60, and f) 240 min. .... 60
- Figure 43:** Ellipsometric layer thickness of DTS films on silicon (previously covered with ODS islands and deactivated with 5 mmol/L TMCS for 30 min) versus immersion time of the wafers in a 1 mmol/L DTS solution. The wafers were immersed for 5, 10, 30, 60, and 240 minutes. .... 61
- Figure 44:** Ellipsometric layer thickness of ODS films on silicon versus immersion time of the wafers into mixtures of TMCS and OTS. The presence of TMCS decreases the growth rate in all cases. Surprisingly, the final film thickness achieved after ten minutes is for all mixing ratios  $2,5 \pm 0,1$  nm. .... 62
- Figure 45:** Comparison of ellipsometric layer thicknesses of ODS and TSHME films. The water content of the solvent was 12 mmol/L and the deposition temperature was 15 °C. Surprisingly, the final film thickness achieved after ten minutes is  $2,55 \pm 0,1$  nm for both compounds. .... 64
- Figure 46:** AFM images of TSHME films on silicon. The adsorption times were a) 20, b) 40, c) 60, and d) 120 s. Island growth can be observed and full monolayer coverage is achieved within 5 minutes (not shown). The bad quality of d) is due to degradation of the TSHME upon extended storage times for several months. .... 64
- Figure 47:** Comparison of ATR-IR spectra obtained from complete monolayers of ODS and THSME. A slight shift ( $\sim 2 \text{ cm}^{-1}$ ) of the  $\text{CH}_2$ -stretch vibrations towards higher wavenumbers was observed for the TSHME. .... 65
- Figure 48:** Layer thickness of TSHME layers versus deactivation time of the silicon substrate in TMCS. The adsorption time for TSHME was 20 s in all cases. A dramatic decrease of the coverage can be observed even for short deactivation times. .... 66
- Figure 49:** AFM images of TSHME films on silicon modified through increasing deactivation times of a) 40, and b) 120s in TMCS ( $c = 5 \text{ mmol/L}$ ). The films were deposited through immersion in TSHME ( $c = 1 \text{ mmol/L}$ ) for 20 s. Circular islands appear after about 40 s of deactivation in TMCS. .... 66

- Figure 50:** AFM images of mixed monolayers on silicon. The films were deposited through immersion in OTS ( $c = 1 \text{ mmol/L}$ ) for 20 s and subsequent deposition of TSHME ( $c = 1 \text{ mmol/L}$ ). a) height image, b) phase image..... 67
- Figure 51:** AFM images of mixed monolayers on silicon. The films were deposited through immersion in solution containing both OTS ( $c = 1 \text{ mmol/L}$ ) and TSHME ( $c = 1 \text{ mmol/L}$ ) and matured for 10 min. a) height image, b) phase image..... 68
- Figure 52:** AFM images of mixed monolayers on silicon. The films were deposited through immersion in a freshly produced mixture of two separately matured solutions containing OTS ( $c = 1 \text{ mmol/L}$ ) and TSHME ( $c = 1 \text{ mmol/L}$ ). a) height image, b) phase image. The island size has slightly increased compared to AFM images of separately matured solutions. c) image obtained by adsorption of one additional ODS layer after reduction of the ester group. .... 68
- Figure 53:** AFM images of nanostructured surfaces. The films were deposited through immersion in OTS ( $c = 1 \text{ mmol/L}$ ) for 20 s and subsequent deposition of TSHME ( $c = 1 \text{ mmol/L}$ ). Afterwards the ester was reduced as described in detail in chapter 4.3.3. Multiple layers in the TSHME region were produced by repeated reduction-adsorption cycles. a, d) one additional layer of ODS, b, e) one additional layer of TSHME and ODS, and c) two additional layers of TSHME and one layer of ODS. Image sizes: a-c)  $25 \times 25 \text{ } \mu\text{m}^2$ , d, e)  $5 \times 5 \text{ } \mu\text{m}^2$  ..... 70



## 9 References

- <sup>1</sup> Bowden, F. P.; Tabor, D. *The Friction and Lubricant of Solids*;  
Clarendon Press: Oxford, **1986**
- <sup>2</sup> Miyamoto, T.; Sato, I.; Ando, Y. *Tmechanics of Magnetic Storage Devices*,  
2<sup>nd</sup> edition; Bhushan, B.; Eiss, N. S.,Eds.; Springer-Verlag: New York, **1990**
- <sup>3</sup> Zarrad, H.; Clechet, P.; Belin, M.; Martelet, C.; Jaffrezic-Renault, N. J.  
*Micromech. Microeng.* **1993**, 3,222
- <sup>4</sup> Schwartzman, M.; Sidorov, V.; Ritter, D.; Paz, Y. J. *Vac. Sci. Technol. B* **2003**, 1, 148
- <sup>5</sup> Haneda, R.; Aramaki, K. *J. Electrochem. Soc.* **1998**, 145, 1856
- <sup>6</sup> Ulman, A. *Chem. Rev.* **1996**, 96, 1533
- <sup>7</sup> Schreiber, F. *Progr. Surf. Sci.* **2000**, 65, 151
- <sup>8</sup> Boussad, S.; Tao, N. J. *J. Am. Chem. Soc.* **1999**,121, 4510
- <sup>9</sup> Chaki, N. K.; Vijayamohanan, K. *Biosensors & Bioelectronics* **2002**, 17, 1
- <sup>10</sup> Forrest, S. R. *Chem. Rev.* **1997**,97, 1793
- <sup>11</sup> KSV Instruments, USA, Homepage: <http://www.ksvinc.com/index.html>
- <sup>12</sup> Schnur, J. *Science* **1993**, 262, 1670
- <sup>13</sup> Bigelow, W. C.; Pickett, D. L.; Zisman, W. A. *J. Colloid Interface Sci.* **1946**, 1, 513
- <sup>14</sup> Huie, J. C. *Smart Mater. Struct.* **2003**, 12,,264
- <sup>15</sup> Thomas Leitner, Diplomarbeit, TU Wien, **1998**
- <sup>16</sup> Allara, D. L.; Nuzzo, R. G. *Langmuir* **1985**, 1, 52
- <sup>17</sup> Woodward, J. T.; Doudevski, I.; Sikes, H. D.; Schwartz, D. K.  
*J. Phys. Chem. B* **1997**, 38, 7535
- <sup>18</sup> Linford, M. R.; Chidsey, C. E. D. *J. Am. Chem. Soc.* **1993**, 115, 12631
- <sup>19</sup> Van Alsten, J. G. *Langmuir* **1999**, 22, 7605
- <sup>20</sup> Lercel, M.; Tiberio, R. C.; Chapman, P. F.; Craighead, H. G.; Sheen, C. W.;  
Parikh, A. N.; Allara, D. L. *J. Vac. Sci. Technol. B* **1993**, 11, 2823

- 
- 21 Huang, J.; Hemminger, J. C. *J. Am. Chem. Soc.* **1993**, 115, 5305
- 22 Ross, C. B.; Sun, L.; Crooks, R. M. *Langmuir* **1993**, 9, 632
- 23 Xia, Y.; Zhao, X.-M.; Whitesides, G. M. *Microelectronic Engineering* **1996**, 32, 255
- 24 Jeon, N. L.; Finnie, K.; Branshaw, K.; Nuzzo, R. G. *Langmuir* **1997**, 13, 3382
- 25 Jeon, N. L.; Nuzzo, R. G.; Xia, Y.; Mrksich, M.; Whitesides, G. M.  
*Langmuir* **1995**, 11, 3024
- 26 Jeon, N. L.; Clem, P. G.; Payne, D. A.; Nuzzo, R. G. *J. Mater. Res.* **1995** 10, 2996
- 27 Tarlov, M. J. *US Patent 5,514,501*, May 7 1996
- 28 Maoz, R.; Sagiv, J. *J. Colloid Interface Sci.* **1984**, 100, 465
- 29 Allara, D. L.; Parikh, A. N.; Rondelez, F. *Langmuir* **1995**, 11, 2357
- 30 Vallant, T.; Brunner, H.; Mayer, U.; Hoffmann, H.; Leitner, T.; Resch, R.;  
Friedbacher, G. *J. Phys. Chem. B* **1998**, 102, 7190
- 31 Parikh, A. N.; Schivley, M. A.; Koo, E.; Aurentz, D.; Mueller, K.; Allara, D. L.  
*J. Am. Chem. Soc.* **1997**, 119, 3135
- 32 Wassermann, S. R.; Whitesides, G. M.; Tidswell, I. M.; Ocko, B.M.; Pershan, P. S.;  
Axe, J. D. *J. Am. Chem. Soc.* **1989**, 111, 5852
- 33 Tidswell, I. M.; Rabedeau, T. A.; Pershan, P. S.; Kosowsky, S. D.; Folkers, J. P.;  
Whitesides, G. M. *J. Chem. Phys.* **1991**, 95 (4), 2854
- 34 Brunner, H.; Vallant, T.; Mayer, U.; Hoffmann, H.  
*J. Colloid Interface Sci.* **1999**, 212, 545
- 35 Carraro, C.; Yauw, O. W.; Sung, M. M.; Maboudian, R.  
*J. Phys. Chem. B* **1998**, 102 (23), 4441
- 36 Resch, R.; Grasserbauer, M.; Friedbacher, G.; Vallant, T.; Brunner, H.; Mayer, U.;  
Hoffmann, H. *Appl. Surf. Sci.* **1999**, 140, 168
- 37 Ho, M.; Pemberton, J. E. *Anal. Chem.* **1998**, 70, 4915
- 38 Kluth, G. J.; Carraro, C.; Maboudian, R. *Phys. Rev. B* **1999**, 59, R10449

- 39 Vilar, M. R.; Bouali, Y.; Kitakatsu, N.; Lang, Ph.; Michalitsch, R.; Garnier, F.;  
Dubot, P. *Thin Solid Films* **1998**, 327-329, 236
- 40 Houssiau, L.; Bertrand, P. *Appl. Surf. Sci.* **2001**, 175-176, 351
- 41 Wolf, K. V.; Cole, D. A.; Bernasek, S. L. *Anal. Chem.* **2002**, 74, 5009
- 42 Ye, S.; Nihonyanagi, S.; Uosaki, K. *Phys. Chem. Chem. Phys.* **2001**, 3, 3463
- 43 Kluth, G. J.; Sung, M. M.; Maboudian, R. *Langmuir* **1997**, 13, 3775
- 44 Ulmann, A. Introduction to Ultrathin Organic Films, Academic Press: London, **1991**
- 45 Leitner, T.; Friedbacher, G.; Vallant, T.; Brunner, H.; Mayer, U.; Hoffmann, H.  
*Mikrochim. Acta* **2000**, 133, 331
- 46 Brunner, H.; Vallant, T.; Mayer, U.; Hoffmann, H.; Basnar, B.; Vallant, M.;  
Friedbacher, G. *Langmuir* **1999**, 15, 1899
- 47 Parikh, A. N.; Allara, D. L.; Azuz, I. B.; Rondelez, F. *J. Phys. Chem.* **1994**, 98, 7577
- 48 Iimura, K.-I.; Nakajima, Y.; Kato, T. *Thin Solid Films* **2000**, 379, 230
- 49 Rye, R. R. *Langmuir* **1997**, 13, 2588
- 50 Goldmann, M.; Davidovits, J. V.; Silberzan, P. *Thin Solid Films* **1998**, 327-329, 166
- 51 Bierbaum, K.; Grunze, M.; Baski, A. A.; Chi, L. F.; Schrepp, W.; Fuchs, H.  
*Langmuir* **1995**, 11, 2143
- 52 Vallant, T.; Kattner, J.; Brunner, H.; Mayer, U.; Hoffmann, H.  
*Langmuir* **1999**, 15, 5339
- 53 Hoffmann, H.; Mayer, U.; Krischanitz, A. *Langmuir* **1995**, 11, 1304
- 54 Lio, A.; Charych, D. H.; Salmeron, M. *J. Phys. Chem. B* **1997**, 101, 3800
- 55 Jennings, G. K.; Munro, J. C.; Yong, T.-H.; Laibinis, P. E. *Langmuir* **1998**, 14, 6130
- 56 Zamborini, F. P.; Crooks, R. M. *Langmuir* **1998**, 14, 3279
- 57 Angst, D. L.; Simmons, G. W. *J. Langmuir* **1991**, 7, 2236
- 58 Le Grange, J. D.; Markham, J. L.; Kurkjian, C. R. *Langmuir* **1993**, 9, 1749
- 59 Terrill, R. H.; Tanzer, T. A.; Bohn, P. W. *Langmuir*, **1998**, 14, 845

- 
- 60 Rozlosnik, N.; Gerstenberg, M. C.; Larsen, N. B: *Langmuir*, **2003**, 19, 1182
- 61 Glaser, A.; Foisner, J.; Müllner, C.; Hoffmann, H.; Friedbacher, G.  
manuscript in preparation
- 62 Pomerantz, M.; Segmuller, A.; Netzer, L.; Sagiv, J. *Thin Solid films* **1985**, 132, 153
- 63 Tillmann, N.; Ullman, A.; Penner, T. L. *Langmuir* **1989**, 5, 101
- 64 Wassermann, S. R.; Tao, Y.-T.; Whitesides, J. M: *Langmuir* **1989**, 5, 1074
- 65 Offord, D. A.; Griffin, J. H. *Langmuir* **1993**, 9, 3015
- 66 Lagutchev, A. S.; Song, K. J.; Huang, J. Y.; Yang, P. K.; Chuang, T. J.  
*Chem. Phys.* **1998**, 226, 337
- 67 Mathauer, K; Frank, C. W. *Langmuir* **1993**, 9, 3446
- 68 Kropman, B. L.; Blank, D. H. A.; Rogalla, H. *Langmuir* **2000**, 16, 1469
- 69 Stranick, S. J.; Atre, S. V.; Parikh, A. N.; Wood, M. C.; Allara, D. L.; Winograd, N.;  
Weiss, P. S. *Nanotechnology* **1996**, 7, 438
- 70 Atre, S. V.; Liedberg, B.; Allara, D. L. *Langmuir* **1995**, 11, 3882
- 71 Folkers, J. P.; Laibinis, P. E. ; Whitesides, G. M. *Langmuir* **1992**, 8, 1330
- 72 Wirth, M. J.; Fairbank, R. W. P.; Fatunmbi, H. O. *Science* **1997**, 275, 44
- 73 Fang, J.; Knobler, C. M. *Langmuir* **1996**, 12, 1368
- 74 Jürgen Kattner, Dissertation, TU Wien, **2002**
- 75 Tripp, C. P.; Hair, M. L. *Langmuir* **1995**, 11, 149
- 76 Tripp, C. P.; Hair, M. L. *Langmuir* **1991**, 7, 923
- 77 Garbassi, F.; Balducci, L.; Chiurlo, P.; Deiana, L.  
*Applied Surface Science* **1995**, 84, 45
- 78 Zhao, X. S.; Lu, G. Q. *J. Phys. Chem. B* **1998**, 102, 1556
- 79 Fuji, M.; Fujimori, H.; Takei, T.; Watanabe, T.; Chikazawa, M.  
*J. Phys. Chem. B* **1998**, 102, 10498
- 80 Bernhard Basnar, Dissertation, TU Wien, **2002**

- 
- <sup>81</sup> Ingo Schmitz, Dissertation, TU Wien, **1996**
- <sup>82</sup> McCrackin, F.; Passaglia, E.; Stromberg, R.; Steinberg, H.  
*J. Res. Natl. Bur. Stand. Sect. A*, **1963**, 67, 363
- <sup>83</sup> Palik, E. D. Handbook of Optical Constants of Solids, Academic, New York, 1985
- <sup>84</sup> Vallant, T.; Brunner, H.; Kattner, J.; Mayer, U.; Hoffmann, H.; Leitner, T.;  
Friedbacher, G.; Schügerl, G.; Svagera, R.; Ebel, M. *J. Phys. Chem. B* **2000**, 104, 5309
- <sup>85</sup> Bunker, B. C.; Carpick, R. W.; Assink, R. A.; Thomas, M. L.; Hankins, M. G.;  
Voigt, J. A.; Sipola, D.; de Boer, M. P.; Gulley, G. L. *Langmuir* **2000**, 16, 7742
- <sup>86</sup> Israelachvili, J. *Intermolecular and surface forces*,  
Second Edition; Academic Press: New York, **1991**
- <sup>87</sup> Biebuyck, H. A.; Bain, C. D.; Whitesides, G. M. *Langmuir* **1994**, 10, 1825
- <sup>88</sup> Chung, C.; Lee, M. *J. Electroanal. Chem.* 468, **1999**, 91
- <sup>89</sup> Kajikawa, K.; Hara, M.; Sasabe, H.; Knoll, W. *Jpn. J. Appl. Phys.* 36, **1997**, L 1116
- <sup>90</sup> Wang, H.; Harris, J. M. *J. Am. Chem. Soc.* **1994**, 116, 5754
- <sup>91</sup> Rye, R. R. *Langmuir* **1997**, 13, 2588
- <sup>92</sup> Hoffmann, H.; Mayer, U.; Krischanitz, A. *Langmuir* **1995**, 11, 1304

# Lebenslauf

<b>Persönliche Daten:</b>	
Name:	Johann Foisner
Anschrift:	Pernerstorfergasse 3/18 A-1100 Wien
Telefon:	0699/19410664
e-Mail:	jfoisner@iac.tuwien.ac.at
Geburtsdatum:	23. April 1971
Geburtsort:	Linz
Familienstand:	ledig
Staatsbürgerschaft:	Österreich
<b>Schulbildung:</b>	
1977-1990	Volksschule Schenkenfelden Bundesrealgymnasium Freistadt
19. Juni 1990	Matura
<b>Studium:</b>	
1995 - 2001	Diplomstudium der Technischen Chemie an der TU Wien, Studienzweig Analytisch-Physikalische Chemie. Diplomarbeit in der Arbeitsgruppe Physikalische Analyse: „SIMS investigations of ion implantations in semiconductors“ bei Prof. H. Hutter
15.10.2001	Diplomprüfung
2001 - 2003	Dissertation in der Arbeitsgruppe Mikro- und Nanoanalytik: „Investigations of the growth mechanism of alkylsiloxane films by atomic force microscopy, ellipsometry, and infrared spectroscopy“ Betreuer : Prof. G. Friedbacher

<b>Berufserfahrung:</b>	
07/90 – 09/90	Büroangestellter Fa. Panalpina Wels
06/91 – 05/97	Zeitsoldat beim Österreichischen Bundesheer im Anschluß an Präsenzdienst (10/90-05/91)
7/98 – 9/98	Studentenjob bei Fa. LGV
02/99 – 09/00	durchgehend diverse „full-time“ Jobs bei OMV, PTS, Manner, ....
08/01-09/01	Studentenjob bei Fa. TecWings
<b>Weitere Informationen :</b>	
<b>Computerkenntnisse</b>	Windows NT, Microsoft Office, Chemiesoftware (Datenbanken, Zeichenprogramme), Delphi, .....
<b>Sprachkenntnisse</b>	Deutsch : Muttersprache Englisch : in Wort und Schrift
<b>Führerschein</b>	B
<b>Interessen</b>	Lesen, Sport, Musik, Computer, Freunde,
<b>Besonderheiten</b>	„Mühlviertler“